

Faculty of Engineering



Development of thermal network to simulate light structured buildings and comparison with heavy structured buildings

Master Thesis

Miguel Solchaga Erneta
Master in Industrial Engineering

Under the supervision of:

Prof. V. Feldheim

M. A. Bagheri and Dr. J. Quinten

Prof. L. Van Wunnik

June 2018

(supervisor UMONS)

(co-supervisors UMONS)

(Home inst. supervisor UPC)

THANKS

I would like to thank Professor Véronique FELDHEIM, the supervisor of this master thesis, for giving me the chance to participate in this research. I will also like to express my gratitude to her for always taking time to answer my questions and for giving me useful feedback.

Additionally, I would also like to show my gratitude to Mr Ali BAGHERI for introducing me the subject and for the given advices and feedback during the realization of the present master thesis.

I would like to thank Doctor Julien QUINTEN for introducing me to the TRNSYS software and for giving me helpful feedback on the present report.

Furthermore, I would like to express my gratitude to UPC-ETSEIB for giving me the opportunity of having an international exchange in Belgium.

Finally, I would like to thank UMONS for receiving me at its university.

ABSTRACT

In the past years there have been numerous researches centred in the optimization of the simplified thermal network models, in order to simulate the thermal behaviour of buildings. The present master thesis has been done within the frame of the RESIZED project – a multidisciplinary project on energy savings funded by the European Union – at the Department of Thermal Engineering and Combustion at the Faculty of Engineering of the University of Mons; the thesis forms part of a bigger research whose main objective consist in simulating the energy consumption and the thermal behaviour of a whole district composed by different typologies of buildings. The latter might be a complex and difficult task to carry out. Hence, in order to make it easier, the simplified models (which reduce the heating problems into few parameters) will be employed.

This dissertation is focused on a specific simplified RC model: 4R3C model. The mentioned model is composed by a thermal network that connects together two 2R1C branches: the first one represents the envelope of the building that is in contact with the outside air and the second one means to represent the building's floor. There is an extra capacitor that is attached to the connection point of the two branches, which represents the internal temperature of the building and, consequently, its internal capacitance. Therefore, the goal of this master thesis consists in studying the evolution of the model's components - resistances and capacitors - on the light structured buildings and comparing them with the ones achieved on the heavy structured buildings.

The data for both light and heavy structured buildings will be obtained in TRNSYS, a simulation software that uses measuring "real" data to calculate the building's internal temperature and the actuating heat fluxes. Then, the obtained outcome is ran with an optimization process (by using Matlab software) that determines the most suitable values for the 4R3C model's components in order to give the maximum fitting proportion on the same output variables (temperatures and heat fluxes) that TRNSYS gives.

In order to carry out the study, two different parameters have been observed. On the one hand, the fitting proportion on the building's internal temperature between the data provided by TRNSYS and the data provided by the Matlab model. On the other hand, the relation of the 4R3C model's components determined with Matlab and the ones calculated theoretically with the buildings properties.

As for the structure of the thesis, three studies can be distinguished. The first research has been focused on analysing the impact of different heating loads and indoor conditions on the model's components; both on light and heavy structured buildings. As the study reveals, the use of heating systems on the buildings brings the most precise results.

The second and most relevant study has been centred on analysing how the components of light and heavy structured buildings are influenced by variations on four different characteristics of each type of building: the building's floor surface, its width-to-depth ratio, its windows-to-floor surface ratio and its orientation angle. As it has been proven, the fitting proportion of the internal temperature has been higher than 80% in both types of buildings. Moreover, the resistances have obtained more accurate results than capacitances in both cases compared to the "real" values. In addition, the capacitances results of the light structured buildings have been more precise than the ones acquired for the heavy structured buildings.

The third and last main study of this master thesis has consisted on verifying the employed model by making a simulation of a whole year duration. This has revealed that the used model is correct.

Key words: simulation - energy and building - grey-box model - RC thermal network.

TABLE OF CONTENTS

Table of Figures	6 -
Table of Tables	9 -
Nomenclature	11 -
Introduction	12 -
1. State of the art	14 -
1.1. Existing modelling approaches	14 -
1.2. Modelling techniques	15 -
1.3. RC Models	16 -
1.4. Contextualisation	17 -
2. Theoretical considerations	18 -
2.1. The RC model	18 -
2.2. Governing equations of the 4R3C model	19 -
2.3. Construction of the grey-box model	20 -
2.4. Methodology.....	21 -
3. The light structured building	26 -
3.1. Concept of a light structured building	26 -
3.2. The used light structured building model	26 -
3.3. Heavy structured buildings	27 -
4. Study of the impact of different heating loads and indoor conditions on the accuracy of the internal state and on the RC parameters.....	28 -
4.1. Impact on heavy structured buildings.....	28 -
4.2. Impact on light structured buildings	34 -
5. Study of the impact of changes on the buildings geometry and structure on the identified parameters of the 4R3C model	40 -
5.1. Changing the floor surface (FS).....	40 -
5.2. Changing the width-to-depth ratio (WD).....	43 -
5.3. Changing the windows-to-floor surface ratio (WF)	46 -
5.4. Changing the orientation angle (OA)	49 -
5.5. Combining the changes.....	51 -
5.5.1. Resistance of the outside envelope ($R_{outside}=R_o+R_{io}$).....	52 -
5.5.2. Resistance of the floor ($R_{floor}=R_{if}+R_f$).....	55 -

5.5.3.	Capacitance of the outside envelope (Co)	57 -
5.5.4.	Internal capacitance (Ci)	59 -
5.5.5.	Capacitance of the floor (Cf)	61 -
6.	Simulation verification	64 -
	Conclusions	65 -
	Bibliography	67 -
	Table of Appendixes	68 -
	Appendix A – Physical characteristics of basic light structured building	69 -
	Appendix B – Physical characteristics of basic heavy structured building	70 -
	Appendix C – Modelling hypothesis used in TRNSYS modelling	71 -
	Appendix D - Evolution of Routside’s DTP in light structured buildings for different FS, WD, WF and OA	72 -
	Appendix E - Evolution of Rfloor’s DTP in light structured buildings for different FS, WD, WF and OA	73 -
	Appendix F - Evolution of Co’s DTP in light structured buildings for different FS, WD, WF and OA	74 -
	Appendix G - Evolution of Ci’s DTP in light structured buildings for different FS, WD, WF and OA	75 -
	Appendix H - Evolution of Cf’s DTP in light structured buildings for different FS, WD, WF and OA	76 -
	Appendix I - Evolution of Routside’s DTP in heavy structured buildings for different FS, WD, WF and OA	77 -
	Appendix J - Evolution of Rfloor’s DTP in heavy structured buildings for different FS, WD, WF and OA	78 -
	Appendix K - Evolution of Co’s DTP in heavy structured buildings for different FS, WD, WF and OA	79 -
	Appendix L - Evolution of Ci’s DTP in heavy structured buildings for different FS, WD, WF and OA	80 -
	Appendix M - Evolution of Cf’s DTP in heavy structured buildings for different FS, WD, WF and OA	81 -

TABLE OF FIGURES

Figure 1: Black box, white box and grey box behaviour [3].	15 -
Figure 2 : 4R3C model schematic representation [7].	18 -
Figure 3: Visual aspects of a 100_2_15_0 building [7].	23 -
Figure 4: Ti (inside) and To (outside) temperature data for 75 hours from the TRNSYS simulation on 100_2_30_0 light structured building.	23 -
Figure 5: Qrad1, Qrad2, Qvent, Qin and Qheat heat flux data for 75 hours obtained in TRNSYS for a 100_2_30_0 light structured building.	23 -
Figure 6: Comparison between the obtained Ti data in Matlab with the one obtained in the TRNSYS simulation including the value of the fitting proportion for a 100_2_30_0 light structured building.	24 -
Figure 7: Ro+Rio and Rif+Rf values for a 50_1_5_0 heavy structured building in different heating situations.	30 -
Figure 8: Co and Cf values for a 50_1_5_0 heavy structured building in the different heating situations.	30 -
Figure 9: Ci value for a 50_1_5_0 heavy structured building in the different heating situations.	31 -
Figure 10: Ro+Rio and Rif+Rf values for a 100_1_5_0 heavy structured building in the different heating situations.	32 -
Figure 11: Co and Cf values for a 100_1_5_0 heavy structured building in the different heating situations.	33 -
Figure 12: Ci value for a 50_1_5_0 heavy structured building in the different heating situations.	33 -
Figure 13: Ro+Rio and Rif+Rf values for a 50_1_5_0 light structured building in different heating situations.	35 -
Figure 14: Co and Ci values for a 50_1_5_0 light structured building in the different heating situations.	36 -
Figure 15: Cf values for a 50_1_5_0 light structured building in the different heating situations.	36 -
Figure 16: Ro+Rio and Rif+Rf values for a 100_1_5_0 light structured building in different heating situations.	37 -
Figure 17: Cf values for a 100_1_5_0 light structured building in the different heating situations.	38 -
Figure 18: Co and Ci values for a 100_1_5_0 light structured building in the different heating situations.	38 -
Figure 19: DTP of resistances for different FS in X_2_15_0 light structured buildings.	41 -
Figure 20: DTP of resistances for different FS in X_2_15_0 heavy structured buildings.	41 -

Figure 21: DTP of capacitances for different FS in X_2_15_0 light structured buildings. - 42 -

Figure 22: DTP of capacitances for different FS in X_2_15_0 heavy structured buildings. .. - 42 -

Figure 23: DTP of resistances for different WD in 100_X_15_0 light structured buildings. . - 44 -

Figure 24: DTP of resistances for different WD in 100_X_15_0 heavy structured buildings. - 44 -

Figure 25: DTP of capacitances for different WD in 100_X_15_0 light structured buildings. - 45 -

Figure 26: DTP of capacitances for different WD in 100_X_15_0 heavy structured buildings..... - 45 -

Figure 27: DTP of resistances for different WF in 100_2_X_0 light structured buildings..... - 47 -

Figure 28: DTP of resistances for different WF in 100_2_X_0 heavy structured buildings... - 47 -

Figure 29: DTP of capacitances for different WF in 100_2_X_0 light structured buildings... - 48 -

Figure 30: DTP of capacitances for different WF in 100_2_X_0 heavy structured buildings. - 48 -

Figure 31: DTP of resistances for different OA in 100_2_15_X light structured buildings. .. - 49 -

Figure 32: DTP of resistances for different OA in 100_2_15_X heavy structured buildings. - 50 -

Figure 33: DTP of capacitances for different OA in 100_2_15_X light structured buildings. - 50 -

Figure 34: DTP of capacitances for different OA in 100_2_15_X heavy structured buildings..... - 51 -

Figure 35: R² for linear regressions for Routside’s DTP for light structured buildings with FS between 50m² and 100m² with a WD ratio of two for several WF ratios while the OA varies. - 53 -

Figure 36: R² for linear regressions for Routside’s DTP for light structured buildings with FS between 50m² and 100m² with a WF ratio of 15% for several WD ratios while the OA varies. - 53 -

Figure 37: R² for linear regressions for Routside’s DTP for heavy structured buildings with FS between 50m² and 100m² with a WD ratio of two for several WF ratios while the OA varies. - 53 -

Figure 38: R² for linear regressions for Routside’s DTP for heavy structured buildings with FS between 50m² and 100m² with a WF ratio of 15% for several WD ratios while the OA varies. - 53 -

Figure 39: Routside’s DTP evolution for 75_2_X_Y light structured building..... - 54 -

Figure 40: Routside’s DTP evolution for 75_2_X_Y heavy structured building. - 54 -

Figure 41: Routside’s DTP evolution for 75_X_15_180 light structured building. - 54 -

Figure 42: Routside’s DTP evolution for X_Y_15_0 light structured building..... - 55 -

Figure 43: Routside’s DTP evolution for X_Y_15_0 heavy structured building. - 55 -

Figure 44: Rfloor’s DTP evolution for 100_2_X_Y light structured building..... - 56 -

Figure 45: Rfloor’s DTP evolution for 100_2_X_Y heavy structured building. - 56 -

Figure 46: Rfloor’s DTP evolution for 100_X_15_Y light structured building..... - 56 -

Figure 47: Rfloor’s DTP evolution for 100_X_15_Y heavy structured building..... - 56 -

Figure 48: Rfloor’s DTP evolution for X_Y_15_0 light structured building. - 57 -

Figure 49: Rfloor’s DTP evolution for X_Y_15_0 heavy structured building. - 57 -

Figure 50: Co’s DTP evolution for 100_2_X_Y light structured building. - 58 -

Figure 51: Co’s DTP evolution for 100_2_X_Y heavy structured building..... - 58 -

Figure 52: Co’s DTP evolution for 100_X_15_Y light structured building. - 58 -

Figure 53: Co’s DTP evolution for 100_X_15_Y heavy structured building. - 58 -

Figure 54: Co’s DTP evolution for X_Y_15_0 light structured building..... - 59 -

Figure 55: Co’s DTP evolution for X_Y_15_0 heavy structured building..... - 59 -

Figure 56: Ci’s DTP evolution for 50_2_X_Y light structured building..... - 60 -

Figure 57: Ci’s DTP evolution for 75_2_X_Y heavy structured building..... - 60 -

Figure 58: Ci’s DTP evolution for 100_X_15_Y light structured building. - 60 -

Figure 59: Ci’s DTP evolution for 100_X_15_Y heavy structured building. - 60 -

Figure 60: Ci’s DTP evolution for X_Y_15_0 light structured building..... - 61 -

Figure 61: Ci’s DTP evolution for X_Y_15_0 heavy structured building..... - 61 -

Figure 62: Cf’s DTP evolution for 50_1_X_Y light structured building..... - 62 -

Figure 63: Cf’s DTP evolution for 75_2_X_Y heavy structured building. - 62 -

Figure 64: Cf’s DTP evolution for 100_X_15_Y light structured building. - 62 -

Figure 65: Cf’s DTP evolution for 100_X_15_Y heavy structured building..... - 62 -

Figure 66: Cf’s DTP evolution for X_Y_15_0 light structured building..... - 63 -

Figure 67: Cf’s DTP evolution for X_Y_15_0 heavy structured building. - 63 -

TABLE OF TABLES

Table 1: Equations and schemes for the thermal model and its electrical equivalent. - 16 -	
Table 2: Initial values given to Ro, Rio, Rif, Rf, Co, Ci and Cf in the Matlab programme.	- 24 -
Table 3 : Percentage of fitting on the internal state T_i between the 4R3C model approximation (Matlab) and the real data (TRNSYS) for different heating situations in 50_1_5_0 and 100_1_5_0 heavy structured buildings.	- 31 -
Table 4: Comparison of the reduction/increase of the error obtained for the 50_1_5_0 light structured building when the obtained error percentage values are compared (in absolute percentage terms) with the ones obtained for the 50_1_5_0 heavy structured building. The green values represent an error reduction while the red and negative ones represent an error increase.....	- 36 -
Table 5: Percentage of fitting on the internal state T_i between the 4R3C model approximation (Matlab) and the real data (TRNSYS) for different heating situations in 50_1_5_0 and 100_1_5_0 light structured buildings.	- 37 -
Table 6: Comparison of the reduction/increase of the error obtained for the 100_1_5_0 light structured building when the obtained error percentage values are compared (in absolute percentage terms) with the ones obtained for the 100_1_5_0 heavy structured building. The green values represent an error reduction while the red and negative ones represent an error increase.....	- 38 -
Table 7: Percentage of fitting on the internal state T_i between the 4R3C model approximation (Matlab) and the real data (TRNSYS) for different FS values in X_2_15_0 light and heavy structured buildings.....	- 40 -
Table 8: Windows surfaces on each wall for different WD ratios in 100_X_15_0 light and heavy structured buildings.....	- 43 -
Table 9: Percentage of fitting on the internal state T_i between the 4R3C model approximation (Matlab) and the real data (TRNSYS) for different WD values in 100_X_15_0 light and heavy structured buildings.	- 43 -
Table 10: Windows surfaces on each wall for different WF ratios in 100_2_X_0 light and heavy structured buildings.....	- 46 -
Table 11: Percentage of fitting on the internal state T_i between the 4R3C model approximation (Matlab) and the real data (TRNSYS) for different WF values in 100_2_X_0 light and heavy structured buildings.....	- 46 -
Table 12: Percentage of fitting on the internal state T_i between the 4R3C model approximation (Matlab) and the real data (TRNSYS) for different OA values in 100_2_15_X light and heavy structured buildings.	- 49 -
Table 13: Representation of the buildings configurations (for light and heavy structured buildings) that have been studied. It has to take into account that the OA has not been represented in the table. However, all the displayed building configurations have been tested for all the OA (0° , 45° , 90° , 135° and 180°).....	- 51 -
Table 14: Obtained results for 100_2_15_0 light and heavy structured buildings in an 8760 hours simulation.	- 64 -
Table 15: Physical properties of the light structured building.	- 69 -

Table 16: Values of the thermal surface resistances used for the calculation of the building's thermal resistances.	- 69 -
Table 17: Physical properties of the heavy structured building.	- 70 -

NOMENCLATURE

DTP	Proportion between the values of the 4R3C model's parameters determined by Matlab, which provides the best-fitting 4R3C model, and the theoretically obtained ones according to the building's physical characteristics.
FS	Floor surface of the building
WD	Building's width-to-depth ratio
WF	Building's windows-to-floor surface ratio
OA	Building's orientation angle
Ro	Outside part of the thermal resistance of the envelope in contact with the outside air
Rio	Inside part of the thermal resistance of the envelope in contact with the outside air
Rif	Inside part of the thermal resistance of the floor
Rf	Outside part of the thermal resistance of the floor
Routside	Thermal resistance of the envelope in contact with the outside air (Routside=Ro+Rio)
Rfloor	Thermal resistance of the floor (Rfloor=Rif+Rf)
Co	Thermal capacitance of the envelope in contact with the outside air
Ci	Internal thermal capacitance: inside walls, furniture and air
Cf	Floor's thermal capacitance in contact with the ground
To	Temperature of the air outside the building
Tio	Fictive temperature describing the state of the envelope in contact with the outside air
Ti	Temperature of the air inside the building
Tif	Fictive temperature describing the state of the floor
Tg	Temperature of the ground
Qheat	Heat flux provided by heating devices to the inside air in the building
Qvent	Heat flux due to the air renewal through ventilation
Qinf	Heat flux due to air uncontrolled air renewal through infiltration
Qrad1	Radiative flux on the opaque envelope (takes into account the absorbance coefficient of the elements)
Qrad2	Radiative flux through the windows (takes into account the glazing characteristics)

INTRODUCTION

As time passes, the importance of saving and optimizing the energy consumption in the residential sector has increased. The amount of unrenovable energy resources have decreased notoriously. Due to these problems, the governments and national and international institutions have decided to promote new policies in order to deal with the issue. Policies have been mainly centred in the following aspects: limiting the consumption of non-renewable resources, enhancing the efficiency of the consuming systems and fostering the substitution of them with renewable resources.

In order to take the best solution, the evaluation and simulation of the energy consumption in buildings, districts and even regions has great relevancy.

As the state of the art shows, several and different techniques exist in order to analyse and simulate the thermal behaviour of the buildings. The first chapter of this master thesis exposes the existing options with their strengths and drawbacks.

In this context, the UMONS – Energy Institute with the funding of the EU has proposed the RESIZED project, which has been created with the aim of setting multidisciplinary teams in order to develop and implement tools and methodologies that make possible the development of net zero energy districts. Within the frame of this project, the Department of Thermal Engineering and Combustion of the Faculty of Engineering of University of Mons is carrying out a study to which this master thesis is linked; the thesis forms part of a bigger research that is centred on developing a system that will be able to simulate the energy consumption and the thermal behaviour of a whole district. Those districts are composed by building groups of different typologies with different characteristics. Carrying out a simulation of a whole district is thought and complex task due to the fact that many different parameters have to be taken into account at the same time. Therefore, in order to make it easier, the simplified models will be utilized. Those models describes the building's behaviour by gathering the required information in a small number of parameters. This simplifies the problem and facilitates the evaluation.

This master thesis is focused on a specific simplified RC model: the four resistances and three capacitors (4R3C) thermal network model (Figure 2). This model simplifies the simulation of the building's thermal behaviour by establishing an analogy with an electrical system. Its behaviour is represented on a simple thermal network which is composed by resistances and capacitors that represent the building's elements (walls, windows, roof, etc.). The 4R3C model is formed by two 2R1C branches that join together at a common node which represents the interior of the building. The first 2R1C branch represents the envelope of the building that is in contact with the outside air and is connected to the outside air conditions. The second one represents the floor of the building and it is linked to the ground. There is an extra capacitor that is attached to the connection point of the two branches, which represents the internal temperature of the building and, consequently, its internal capacitance.

Based on a previous research done by Ms. Y. Touly [7], where the 4R3C model has been analysed for the heavy structured buildings typology by testing it in different conditions, the present master thesis will be focused on studying the 4R3C model with the light structured buildings. Therefore, the goal of this master thesis will consist in studying the evolution of the model's components - resistances and capacitors - on the light structured buildings and comparing them with the ones achieved on the heavy structured buildings.

The data for both types of buildings (light and heavy structured) will be acquired in TRNSYS, a simulation software that employs measuring "real" data in order to calculate

the building's internal temperature and the actuating heat fluxes. Then, the obtained outcome will be ran with an optimization process (by utilizing Matlab software) that determines the most suitable values for the 4R3C model's components in order to give the maximum fitting proportion on the same output variables (temperatures and heat fluxes) that TRNSYS gives.

The core of this master thesis will be focused on studying the evolution of the 4R3C model's components on the light structured buildings and comparing them with the ones acquired on the heavy structured buildings. The model's components behaviour will be analysed in both types of buildings by simulating them with different indoor conditions and by changing their geometry and structure.

Finally, the employed model will be verified by simulating both types of buildings; making use of different simulation period. The thesis will end with a compilation of the most relevant conclusions that will be extracted from the research.

1. STATE OF THE ART

In this chapter a literature review of the state of the art addressed to the studied subject will be carried out. In this review different articles will be analysed. Those will serve to introduce the existing modelling approaches and techniques in order to calculate the energy consumption profile or the internal temperature evolution for a single or a group of buildings.

1.1. EXISTING MODELLING APPROACHES

In order to generate a model that describes the energy consumption some input data will be needed, such as the building's physical characteristics, the appliances, the climatic conditions or the historical consumption between others.

Therefore, depending on the hierarchical position of the input data two ways of facing the buildings energy consumption exist: the "Top-down" approach and the "Bottom-up" approach [1].

In the "Top-down" approach data is collected from a large scale resources (districts, regions, countries, etc.) to understand the buildings energy consumptions on this big scale. It has a big reliance on the historical data that also provides an inertia to the model. This approach treats the buildings sector as an energy sink without taking care about the final use of the energy [1]. The gathered data is studied by analysing large scale variables such as macroeconomic indicators (GDP, employment rate, etc.) or climatic conditions among others. This model is commonly utilized to determine the impact of long term changes in the energy consumption. It also serves to clarify the reasons that explain people's energy consumption behaviour [1]. One of its strengths resides on its simplicity that is combined with the fact that it only needs aggregated data (which is widely available). However, this approach is unable to provide reliable results when a major change happens. For instance, if there is a big economic crisis in a region, the top-down approach would not be useful to deduce this new situation and consequently, it would not provide trustworthy results.

The top-down approach has two different types of models [1]: the "econometric" models and the "technological" models. The first one considers factors that are associated with the economy, income and prices. The second one is related with physical parameters; for instance, the characteristic of the housing stock or the developments on air conditioning technology among others.

The "Bottom-up" approach uses a hierarchical structure [1]. It has basic data that comes from a local level (a single building or a small group of them) as an input and, by getting those buildings together it can represent large scale aspects; such as neighbourhoods, regions or even countries. The input data includes diverse parameters such as indoor temperatures, occupancy schedules or equipment uses. One of its strengths is the high level of detail [1]. This fact enables the possibility of taking into account different technological options or even the determination of each end-use consumption [1]. Moreover, it can simulate the energy consumption of different areas just by weighting the consumption based on few typical buildings.

As it has happened in the previous approach, the bottom-up approach has also two different types of methods to calculate the energy consumption [1]: the "statistical" method and the "engineering" method.

The statistical method collects historical consumption data and makes a regression to determine the building's energy consumption. The consumption data usually comes from billing and it is complemented with surveys, which is helpful to relate the energy consumption with the behaviour of the occupants [1].

The other method of the bottom-up approach is the engineering method. This method employs data coming from the building's physical characteristics (such as the size and composition of the walls, the total windows surface or the consumption of the appliances) in order to calculate the energy consumption. As it determines the consumption without relying in historical data [1], it can be used to calibrate the models. Furthermore, this characteristic enables the possibility of evaluating the influence of new technologies [1]. Its main drawback is that the behaviour of the occupants must be assumed.

As the study of Lukas G. Swan [1] reveals, all the modelling approaches are useful. The top-down approaches are the best options in terms of energy supplying due to their relation with the historical consumption data. The bottom-up statistical models are the most accurate ones in order to take into account the occupants' behaviour. Finally, the bottom-up engineering models are the most useful models to identify the influence of new technologies.

1.2. MODELLING TECHNIQUES

The simplified building models are classified in three types of models: the "black box" models (or neural network models), the "white box" models (or lumped capacitance models) and the "grey box" models (or linear parametric models) [2-3], which are obtained by combining the previous two types. These three types of models are represented in the Figure 1.

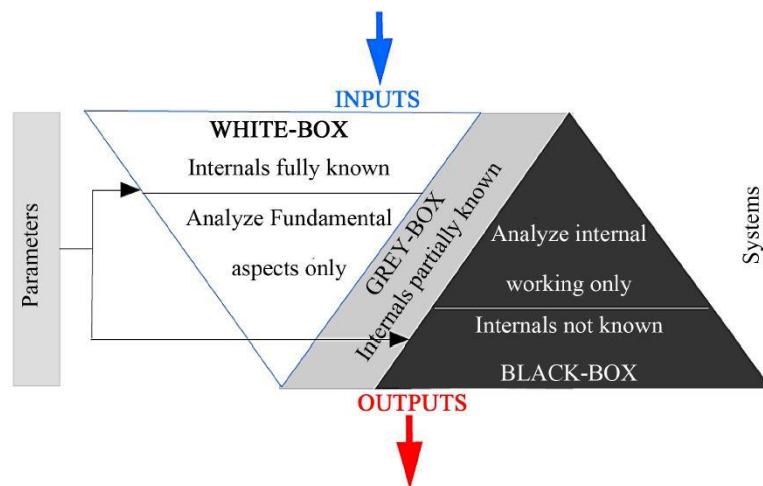


Figure 1: Black box, white box and grey box behaviour [3].

The black box models do not need any kind of knowledge about the physical properties of the building. Therefore, when the model's parameters have been acquired by computing a large amount of data and they do not have a physical meaning, it is indicating that it is a black box model. This lack of information has the disadvantage of been unable of being characterised by its parameters. These models can be employed with the goal of removing unimportant inputs [2] and also for error detections [3].

In the case of the white box models, their parameters have a clear physical meaning [3]. The equations that govern the building's thermal behaviour are also known as well as its physical characteristics (for example, the building's walls composition or the inclination degree of the roof). Then, with the equations and the physical characteristics the model is constructed.

The grey box modelling is used when a set of data is necessary to estimate the model's parameters [4]. It is a combination between the white box and the black box model. The grey box model's parameters have a physical meaning (as it occurs in the white box models) and they use training data (like the black box models) in order to optimize it.

1.3. RC MODELS

The present master thesis is based on a specific RC model; therefore, these types of models must be presented.

The RC models consist in a grey box model that is employed to describe the thermal behaviour of a building providing a robust and accurate estimation of the heat loads based on measured data [5]. The RC model represents the building by connecting capacitors and resistances in a network that will be used to simulate the thermal dynamic behaviour.

The parameters of the RC models have a clear physical meaning and they are complemented by using some training data. The models have been based on an analogy with electrical networks [2] that makes them very intuitive. As it has been said, the models are generated by creating a network composed by resistances and capacitors. In this network each node represents a certain temperature. Each resistance represent a particular thermal resistance of the building, that depending on the employed level of precision, could represent a layer of a wall or even the whole building's envelope. The same thing happens with the capacitors. Those represent the thermal capacitances of the building and as it has occurred in the case of the resistances, the corresponding element will vary depending on the used level of detail.

The following table (Table 1) shows the equations and schemes for the thermal model with its electrical equivalent.

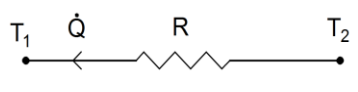
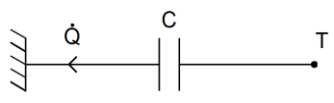
Thermal network scheme	Governing thermal equations	Electrical equivalent
	$(\Delta T) = R \times \dot{Q}$ <p>Where</p> <ul style="list-style-type: none"> • ΔT is the temperature difference [°C] or [K] • R is the thermal resistance [°C/W] or [K/W] • \dot{Q} is the heat flux [W] 	$U = R_{elec} \times I$ <p>Where</p> <ul style="list-style-type: none"> • U is the voltage [V] • R_{elec} is the electric resistance [Ω] • I is the current [A]
	$\dot{Q} = C \times \frac{d(T)}{dt}$ <p>Where</p> <ul style="list-style-type: none"> • \dot{Q} is the thermal capacitance [J/°C] or [J/K] • C is the thermal capacitance [J/°C] or [J/K] • T is the temperature [°C] or [K] • t is the time [S] 	$I = C \times \frac{dV}{dt}$ <p>Where</p> <ul style="list-style-type: none"> • I is the current [A] • C is the electric capacitance [F] • V is the potential [V] • t is the time [S]

Table 1: Equations and schemes for the thermal model and its electrical equivalent.

The RC models have the advantages of being easy to use and practical to simulate the energy consumption of buildings. Therefore, multiple researches exist in order to find the most accurate RC model for each application.

One of these researches has been done by G. Fraisse [6]. On his work he made a comparison between three different RC models: 3R2C, 3R4C and 1R2C. He analysed the performance of each model by simulating the thermal behaviour of a multilayer wall. On his research he observed that it is possible to obtain good results when several walls are aggregated into a single branch when those walls have similar characteristics. In order to do the comparison, he made use of TRNSYS software.

1.4. CONTEXTUALISATION

Y. Touly [7] has worked on a 4R3C simplified RC model in the frame of a master thesis at the Faculty of Engineering of the University of Mons. On her research she has studied the impacts that changes on the building's geometry and envelope generate over the 4R3C model's components. Her work has been centred in the heavy structured buildings. For her study, she has used TRNSYS software to obtain training data for the buildings and she has developed a Matlab code in order to compare the results.

The RESIZED project is a project written and proposed by M. Frère (Institute of Energy) and funded by the European Union. Its main objective is to create multidisciplinary teams to develop and implement methodologies and tools in order to make available Net Zero Energy Districts.

In this context, the present master thesis will use the 4R3C simplified thermal network to try to find if there is a link between the characteristics of a real light structured building and the parameters found by the optimisation process. In addition, the results of the light structured buildings will be compared with the ones obtained from the heavy structured building in order to see if there is any type of relation between them.

2. THEORETICAL CONSIDERATIONS

The previous chapter has shown the importance of the RC models in order to simplify the calculations and the problems of studying the thermal behaviour of buildings. This master thesis has its focus on investigating and analysing the precision, characteristics and correlations that exist between the simulations executed with a simplified model and the ones obtained with traditional thermal simulating programmes, TRNSYS in this occasion (which employs "real" measuring data as an input and brings the building's internal temperature and internal temperature and the actuating heat fluxes as an output). Thus, in order to proceed on this research the utilised simplified model must be explicated.

In the present chapter the used 4R3C simplified model will be presented, describing and showing all its characteristics. Simultaneously, the supposed theoretical considerations will be illustrated. Moreover, the used methodology for simulating and obtaining all the results along this master thesis will be elucidated.

2.1. THE RC MODEL

In this master thesis the 4R3C (four resistances and three capacitors) thermal network model will be studied. In Figure 2, the schematic representation of the 4R3C model can be appreciated.

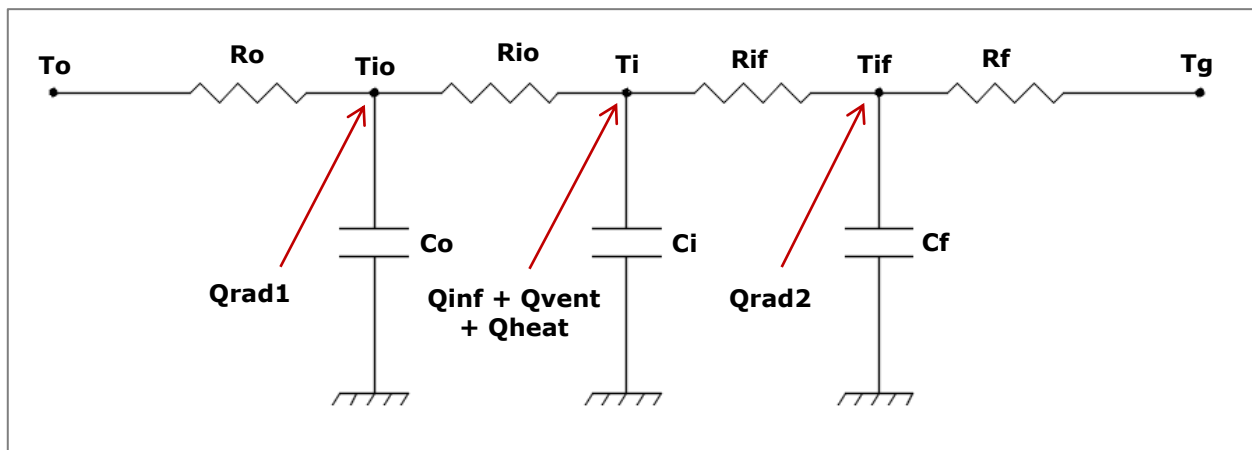


Figure 2 : 4R3C model schematic representation [7].

The 4R3C model has been used as a result of Mr A. Bagheri's work on the RESIZED project [4-8-9]. It also has been used by Ms Y. Touly during her master thesis [7], the referent work on which the present master thesis has been based. This model is composed of two 2R1C branches that join together in a node that represents the internal state of the building, in this case the internal temperature (T_i), with an additional capacitor connected to this node.

The first 2R1C branch goes from node T_o to node T_i . It represents the walls, windows and roof that form the exterior envelope of the building that is in contact with the outside air. It is composed by R_o and R_{io} resistances and its sum is equal to $R_{outside}$ (the global thermal resistance of the envelope in contact with the air), and a C_o capacitor. The node T_{io} formed between the two resistances, represents the inside state of the elements that compose the outside envelope, but it does not correspond to any particular surface temperature.

In this first branch, the value for the $R_{outside}$ resistance provided by Matlab (by using an optimization process that brings the best fitting with the TRNSYS output) will be

compared with its corresponding theoretical value (calculated through the building's characteristics). At the same time, the simplified model's Co capacitor's capacitance value will be compared with the theoretical value of the thermal capacitance of the building's outside envelope (formed by walls, windows and roof).

The second 2R1C branch is located between T_i and T_g nodes, where T_g represents the ground temperature. This temperature has been considered as constant with a value of 10°C . Due to the thermal inertia of the ground, the floor temperature remains constant over the year without any significant affectation from the outside climate conditions. This branch represents the building's floor that connects the interior state of the building with the ground. As it happens in the first branch, it is composed by two resistances (R_f and R_{if}), of which sum is equal to R_{floor} , and a C_f capacitor. Moreover, there is an intermediate node (T_{if}) that is located between the two resistances. This node represents the interior state of the elements that form the floor. Nevertheless, as it has happened in the first 2R1C branch, this intermediate node does not correspond to any specific surface temperature.

For this second branch, as it has occurred in the first branch, the values of the R_{floor} thermal resistance and the values of the C_o thermal capacitance acquired by the optimization process with Matlab will be compared with its corresponding theoretical values.

In the middle node (which represents the internal state of the building (T_i)) where the two 2R1C branches connect together, there is an additional capacitor connected to it. This element represents the internal capacitance of the building and it is symbolised by the C_i capacitor. This capacitance takes into account the influence caused by the internal furniture, walls and the inside air.

In addition, in Figure 2 three red arrows can be observed which are pointing T_{io} , T_i and T_{if} nodes. Those arrows represent different heat flux inputs that fall upon each surfaces. On T_{io} node the input heat flux is Q_{rad1} , which symbolises the radiative heat flux that goes through the exterior walls, taking into account the absorbance coefficients of the elements that compose those walls. For the case of the T_{if} node, Q_{rad2} is the one that heats it. In this case, Q_{rad2} is referred to the solar heating flux that passes through the windows and hits the building floor. Finally, in the middle node (T_i) three different heat fluxes arrive simultaneously (Q_{inf} , Q_{vent} and Q_{heat}). Q_{inf} represents the heat flux due to the uncontrolled air infiltrations, while, Q_{vent} symbolised the heat flux caused by the building air ventilation. The last remaining one (Q_{heat}), is referred to heat provided by the heating system of the building.

2.2. GOVERNING EQUATIONS OF THE 4R3C MODEL

In this section the equations that govern the previously presented 4R3C model will be deduced.

As it has been seen previously in the present master thesis, the simplified RC models presents simple thermal networks that are composed by resistances R and capacitances C . Those circuits describe the heat transfer between the formed nodes. Each node corresponds to a specific isothermal surface temperature. One of the advantages of those simplified models is the existing analogy between those thermal systems and the electrical ones. Due to this fact, simple laws that govern the electric systems, such as the Ohm's law, can be applied in thermal networks. Those relations can be appreciated in Table 1 (located in the first chapter).

This analogy brings a very intuitive approach that gives the chance to simplify the formulation of complex thermal systems. Thanks to this fact, complex thermal systems can be easily represented with uncomplicated thermal networks that are commanded by simple equations.

When those concepts are applied in the used 4R3C model, the following equations can be extracted for the three nodes (T_{io} , T_i and T_{if}) that compose the unknown states of the model:

➤ Node T_{io} :

$$\frac{T_o - T_{io}}{R_o} - C_o \times \frac{dT_{io}}{dt} + \frac{T_i - T_{io}}{R_{io}} + Q_{rad1} = 0 \quad (1)$$

$$T_{io}(t + \Delta t) = \left(1 - \frac{\Delta t}{C_o \times R_o} - \frac{\Delta t}{C_o \times R_{io}}\right) \times T_{io}(t) + \frac{\Delta t}{C_o \times R_o} \times T_o(t) + \frac{\Delta t}{C_o \times R_{io}} \times T_i(t) + \frac{\Delta t}{C_o} \times Q_{rad1}(t) \quad (2)$$

➤ Node T_i :

$$\frac{T_{io} - T_i}{R_{io}} - C_i \times \frac{dT_i}{dt} + \frac{T_{if} - T_i}{R_{if}} + Q_{inf} + Q_{vent} + Q_{heat} = 0 \quad (3)$$

$$T_i(t + \Delta t) = \left(1 - \frac{\Delta t}{C_i \times R_{io}} - \frac{\Delta t}{C_i \times R_{if}}\right) \times T_i(t) + \frac{\Delta t}{C_i \times R_{io}} \times T_{io}(t) + \frac{\Delta t}{C_i \times R_{if}} \times T_{if}(t) + \frac{\Delta t}{C_i} \times [Q_{inf}(t) + Q_{vent}(t) + Q_{heat}(t)] \quad (4)$$

➤ Node T_{if} :

$$\frac{T_i - T_{if}}{R_{if}} - C_f \times \frac{dT_{if}}{dt} + \frac{T_g - T_{if}}{R_f} + Q_{rad2} = 0 \quad (5)$$

$$T_{if}(t + \Delta t) = \left(1 - \frac{\Delta t}{C_f \times R_{if}} - \frac{\Delta t}{C_f \times R_f}\right) \times T_{if}(t) + \frac{\Delta t}{C_f \times R_{if}} \times T_i(t) + \frac{\Delta t}{C_f \times R_f} \times T_g(t) + \frac{\Delta t}{C_f} \times Q_{rad2}(t) \quad (6)$$

2.3. CONSTRUCTION OF THE GREY-BOX MODEL

Once having deduced the governing equations of the model, the required conditions to proceed with the construction of a Grey-box model must be clarified. In this Grey-box model, a set of data provided by the TRNSYS software will be employed to estimate the parameters of the 4R3C models by an optimisation process.

Based on the deduced equations, it will be suitable to write them in a systematic way. For doing this rewriting, the most convenient representation is the one obtained with state space illustration. This representation helps with the understanding of the things that occur inside the system. Nevertheless, the most useful property that the state space brings, is the possibility of dealing with the problem by utilizing matrices. This gives the chance to implement a programme in Matlab. The programme will be able to determine the optimized values of the components of the model that brings the best fitting with the output results obtained in TRNSYS.

After having commented those aspects, a discrete Grey-box model can be obtained. By using the following equations (7 and 8) the target system can be completely described:

$$\mathbf{x}(t + \Delta t) = \mathbf{A} \times \mathbf{x}(t) + \mathbf{B} \times \mathbf{u}(t) \quad (7)$$

$$\mathbf{y}(t) = \mathbf{C} \times \mathbf{x}(t) + \mathbf{D} \times \mathbf{u}(t) \quad (8)$$

where

$\mathbf{x}(t)$ represents the model states.

$\mathbf{u}(t)$ corresponds to the input vector.

$\mathbf{y}(t)$ is the output vector.

Δt is the sample time.

\mathbf{A} , \mathbf{B} , \mathbf{C} and \mathbf{D} are the matrices that describe the Grey-box model.

Based on the previous equations (7 and 8), each parameter can be described. Therefore, if the systems equations are written down in the matrix form, the $x(t)$ and $u(t)$ vectors are obtained in expression 9 and in equation 10 the A , B , C and D matrices are represented:

$$x(t) = \begin{bmatrix} T_{io}(t) \\ T_i(t) \\ T_{if}(t) \end{bmatrix} ; \quad u(t) = \begin{bmatrix} T_o(t) \\ T_g(t) \\ Q_{rad1}(t) \\ Q_{rad2}(t) \\ Q_{heat}(t) \\ Q_{inf}(t) \\ Q_{vent}(t) \end{bmatrix} \quad (9)$$

$$A = \begin{bmatrix} 1 - \frac{\Delta t}{C_o R_o} - \frac{\Delta t}{C_o R_{io}} & \frac{\Delta t}{C_o R_{io}} & 0 \\ \frac{\Delta t}{C_i R_{io}} & 1 - \frac{\Delta t}{C_i R_{io}} - \frac{\Delta t}{C_i R_{if}} & \frac{\Delta t}{C_i R_{if}} \\ 0 & \frac{\Delta t}{C_f R_{if}} & 1 - \frac{\Delta t}{C_f R_{if}} - \frac{\Delta t}{C_f R_f} \end{bmatrix}$$

$$B = \begin{bmatrix} \frac{\Delta t}{C_o R_o} & 0 & \frac{\Delta t}{C_o} & 0 & 0 & 0 & 0 & 0 \\ 0 & 0 & 0 & 0 & \frac{\Delta t}{C_i} & \frac{\Delta t}{C_i} & \frac{\Delta t}{C_i} & \frac{\Delta t}{C_i} \\ 0 & \frac{\Delta t}{C_f R_f} & 0 & \frac{\Delta t}{C_f} & 0 & 0 & 0 & 0 \end{bmatrix} \quad (10)$$

$$C = [0 \quad 1 \quad 0]$$

$$D = [0 \quad 0 \quad 0 \quad 0 \quad 0 \quad 0 \quad 0 \quad 0]$$

Once written down the equations that govern the 4R3C system, they can be easily introduced in a Matlab programme. Matlab can work with matrices without any complication. When those equations are properly introduced in the Matlab code, the input vector ($u(t)$) and the output one ($y(t)$) will be generated in Matlab. Matlab will utilize the output files provided by the simulations in TRNSYS for this proposal.

2.4. METHODOLOGY

The goal of the present master thesis is to study the influence that changes of different buildings parameters have on the relationship between the real light structured building and its simplified 4R3C model. The achieved results for the light building will be compared with the ones reached for the heavy structured buildings.

TRNSYS software will be employed to compile the required data for the "real" light building. On this software, different models of this type of building will be simulated. The results that TRNSYS provides are quite realistic and they match in a generous proportion with the ones that are obtained in an in-situ measurement [11-12]. This way of recovering data permits time- and cost-savings while the results are enough precise. The 4R3C simplified model has been presented in the previous sections.

When the changes in the building's characteristics are done, the 4R3C model components (resistances and capacitors) behaviour will be the analysed parameters. In order to carry out this study, two different parameters will be observed. On the one hand, the fitting proportion on the building's internal temperature between the data provided by TRNSYS and the data provided by the Matlab model. On the other hand, the relation of the 4R3C model's components determined with Matlab (Matlab will provide the most suitable values for the 4R3C model's components by an optimization process in order to have the maximum fitting on the internal temperature with the output of TRNSYS) and the ones calculated theoretically with the buildings properties.

As it has been explained before, the 4R3C model represented in Figure 2 shows two 2R1C branches. The first one represents the outside envelope of the building while the other describes the building's floor. As it can be appreciated, the outside resistance ($R_{outside}$) and the floor resistance (R_{floor}) are composed by two partial resistances; R_o and R_{io} for the first one and R_{if} and R_f for the second one. Those partial resistances do not have any relation with building's physical characteristic. Therefore, for the present analysis the total resistances ($R_{outside}=R_o+R_{io}$ and $R_{floor}=R_{if}+R_f$) will be the only ones to take into account.

In order to simplify the analysis, the thesis will be focused on the first 1000¹ hours of simulation that correspond with winter's days.

After having explained the functioning and goals of this thesis, in the following lines the employed methodology will be presented (this methodology will be also used for calculating the heavy structured buildings):

FIRST STEP:

The first stage begins with the utilization of TRNSYS software. This software will provide the needed data of the real light structured buildings that will be necessary for the posterior Matlab simulation.

For analysing the light structured buildings, four different building's parameters will be varied. Furthermore, those parameters will be used to reference each building with the purpose of facilitating the study. Therefore, each light structured building will be referenced by the stencil A_B_C_D, where:

- A corresponds to the building's floor surface [m^2].
- B corresponds to the building's width-to-depth ratio [-].
- C corresponds to the building's window-to-floor surface ratio [%].
- D corresponds to the building's orientation angle [$^\circ$].

The used light building, for all the studied cases, has a 3m high flat roof with a single floor and a rectangle base form. Additionally, it has three windows, that for the initial south orientation, the windows will be located in the south, east and west walls. There is not any window in north wall due to the fact that the sun proportion that will enter through that window will be very small and architecturally are not very used. The Appendix A and Appendix C² provide further information about the light structured building. The first one presents detailed data about the building's physical composition while the second one gives details about the used modelling characteristics in TRNSYS.

In order to have a clearer idea of the building's geometry, the Figure 3 shows the visual aspects of a 100m² with a width-to-depth ratio of two, a windows-to-floor surface ratio of 15% and an orientation angle of 0° (south orientation of the front wall).

¹ The viability of this time period will be verified in chapter 6.

² The Appendix C also includes details that have been used for the heavy structured building. There is also an Appendix B which has the physical composition of the heavy structured building.

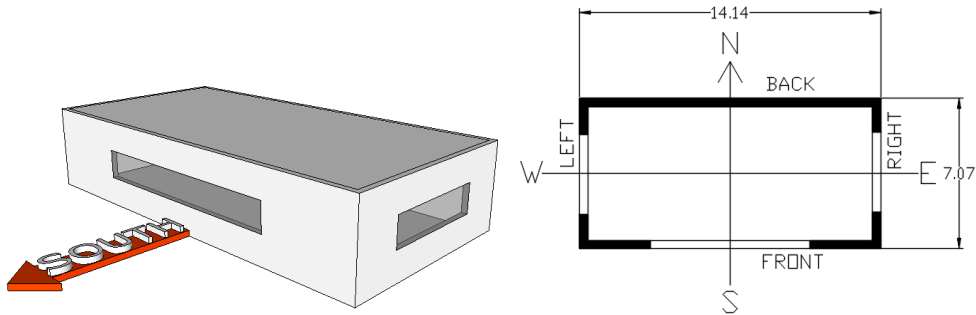


Figure 3: Visual aspects of a 100_2_15_0 building [7].

In order to analyse each building, a TRNSYS file with a model of a basic building will be used. This basic file will be adapted to all the studied situations by changing the proper parameters. For that reason, the basic building model includes all the investigated characteristics of the light structured building (floor surface, orientation, width-to-depth ratio, windows-to-floor ratio, envelope's composition...). When the desired parameters are correctly set, a 1000 hour simulation will be run generating a text file with all the results. This file will include data about the inside and outside air temperature, the heating load, the heat gains/losses caused by the ventilation and infiltrations as well as the solar radiation that hits each of the building's surfaces that are in communication with the outside air.

In order to provide a clearer vision, the following figures illustrate the obtained data in TRNSYS for a 100m² light building with a heating model that emulates an office-like occupancy (described on Appendix C). This building has a width-to-depth ratio of two, with a windows-to-floor ratio of 30% and south orientation (100_2_30_0). The Figure 4 shows the buildings inside (Ti) and outside (To) temperatures while Figure 5 presents the heat flux fluctuations.

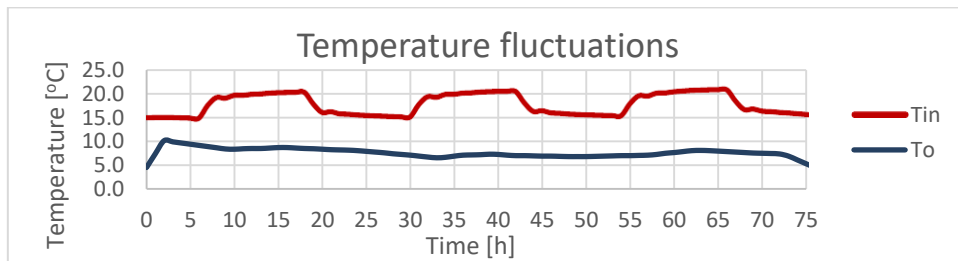


Figure 4: Ti (inside) and To (outside) temperature data for 75 hours from the TRNSYS simulation on 100_2_30_0 light structured building.

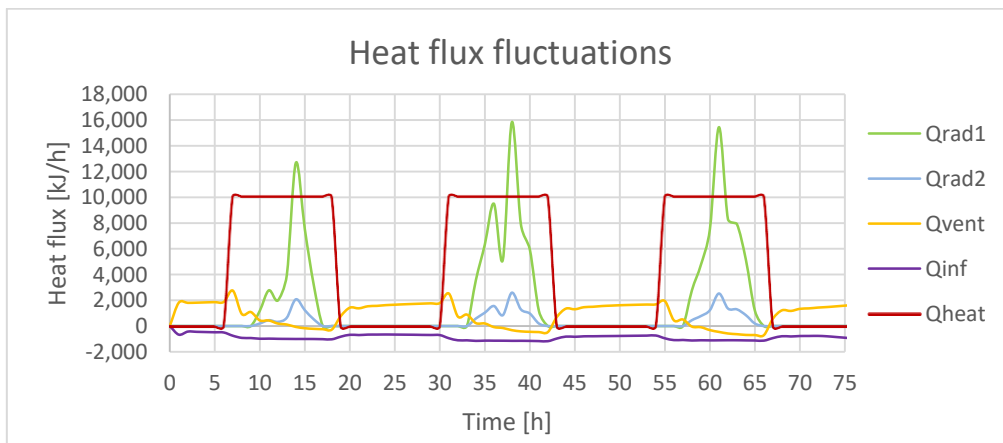


Figure 5: Qrad1, Qrad2, Qvent, Qin and Qheat heat flux data for 75 hours obtained in TRNSYS for a 100_2_30_0 light structured building.

SECOND STEP:

In this second step the Matlab software comes into play. With the building characteristics and the obtained TRNSYS data a Matlab programme will be run. This program has been done by modifying the one that Ms Y. Touly developed on her master thesis [7] based on Mr A. Bagheri’s work [4-8-9-10].

The program uses Matlab System Identification Toolbox which permit the calculations of a Grey-box model. The previously presented Grey-box has T_o , T_g , Q_{rad1} , Q_{rad2} , Q_{vent} , Q_{inf} and Q_{heat} as input parameters and the internal temperature (T_i) as the only output. Matlab will import the obtained data in the TRNSYS simulation and the buildings physical characteristics (such as the floor and roof surfaces or the walls and glazing surface with their orientation among others) to do the calculations. When all the data are imported, the Matlab System Identification Toolbox will find the best values for the 4R3C model’s parameters (R_o , R_{io} , R_{if} , R_f , C_o , C_i and C_f) in order to have the highest fitting proportion between the output T_i obtained with Matlab and the one acquired on the TRNSYS simulation. Figure 6 displays the results that Matlab brings in this respect for a 100_2_30_0 building (the one used previously), that simultaneously serves as an example.

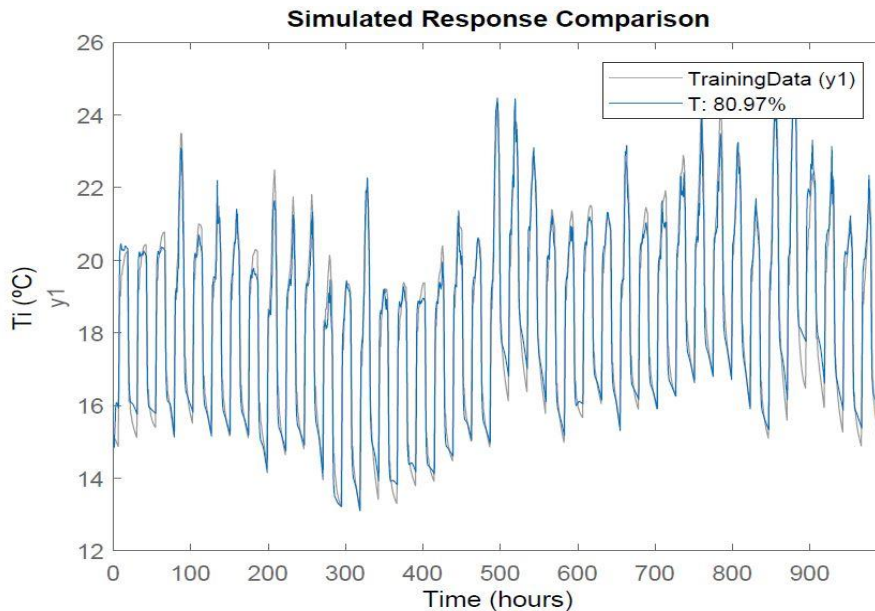


Figure 6: Comparison between the obtained T_i data in Matlab with the one obtained in the TRNSYS simulation including the value of the fitting proportion for a 100_2_30_0 light structured building.

When the simulation is done in Matlab, the importance of the initial value for the 4R3C model’s components has to be taken into account. In the used identification algorithm, the initial values of the components have an impact on the Matlab’s ability to find the most accurate values for the models parameters (R_o , R_{io} , R_{if} , R_f , C_o , C_i and C_f). This problem is beyond the scope of the present master thesis and it will not be studied. For the Matlab simulations, the used initial values for the components will be the ones that are proposed in Table 2. In the cases where the accomplished precision on the Matlab results is low (in this case when the values are far from 80% of fitting), small changes will be applied on the internal capacitance (C_i). This variations will permit to maintain the accuracy close to 80% of fitting.

	R_o [K/W]	R_{io} [K/W]	R_{if} [K/W]	R_f [K/W]	C_o [W·h/K]	C_i [W·h/K]	C_f [W·h/K]
Initial value	0.05	0.05	0.05	0.05	1000	100	1000

Table 2: Initial values given to R_o , R_{io} , R_{if} , R_f , C_o , C_i and C_f in the Matlab programme.

THIRD STEP:

The third step is the last one of the employed methodology. In this step the reached values for the 4R3C model's components provided by the optimisation process will be compared with the theoretically calculated ones.

First of all, the theoretical values of the 4R3C model's components (R_o , R_{io} , R_{if} , R_f , C_o , C_i and C_f) will be calculated in an Excel file by using the buildings physical characteristics. Then, those results will be compared with the ones achieved with Matlab. In chapter 4, where the impact of different heating loads and indoor conditions are analysed for heavy and light buildings, the comparison will be done in terms of the obtained deviation error percentage, because, from the point of view of the author it is the clearest way to analyse the obtained precision. Nevertheless, in the case of the chapter 5 the obtained results, for heavy and light structured buildings, will be compared in terms of a coefficient that is equal to the proportion accomplished by dividing the Matlab values with the theoretical ones. This coefficient gives an idea of how deviated the theoretical results are from the Matlab ones. In addition, this coefficient serves to calculate the 4R3C model's parameters that Matlab will bring from the theoretically calculated ones (by multiplying each coefficient with their respective theoretical parameters value). Moreover, to be more practical the coefficient will receive the acronym of DTP (Determined/Theoretical Proportion), which is essentially the same that Ms Y. Touly employed on her research [7].

ADDITIONAL INFORMATION:

As it has been explained, the methodology consists in applying the previously presented three steps. In this section, additional information referred to the employed methodology will be explained.

The study will analyse the buildings by changing the previously mentioned four characteristics (A_B_C_D). The first characteristic (A) is the building's surface. In the present thesis 50m², 75m², 100m², 150m² and 200m² surface sizes will be studied. The second characteristic (B) is the width-to-depth ratio and the investigated values will be 0.25, 0.5, 1, 2 and 4. In the case of the third characteristic (C), it is referred to window-to-floor surface ratio and values of 5%, 10%, 15%, 20% and 30% will be considered. Finally, the fourth characteristic (D) corresponds to the orientation angle and the building will be turned an angle of 0° (south orientation), 45°, 90°, 135° and 180°. All those modifications will be furtherly studied in the chapter 5.

Another interesting point is the way in which the TRNSYS, Matlab and Excel files are constructed. Based on Ms Y. Touly's works [7], the files have been improved. In the Excel "BC" files, where the buildings physical properties and the theoretical calculations can be found, some small nomenclature errors have been corrected. Moreover, there have been added all the units of the written variables. In addition, some useless calculations have been eliminated. Finally, an additional sheet has been incorporated (4R3CResults) where the Matlab results and the theoretical results are compared, including the reached T_i fitting proportion and its graph. In the case of the Matlab files, some additional comments have been added in order to clarify the code comprehension. Furthermore, the title of the vertical axis of the T_i fitting proportion graph has been changed. Besides, the sum of the resistances ($R_{outside}=R_o+R_{io}$ and $R_{floor}=R_f+R_{if}$) and the acquired fitting proportion have been included on the code. Those files are easy to manage and intuitive. They bring the chance to change diverse building characteristics for further building analyses without any significant problems.

3. THE LIGHT STRUCTURED BUILDING

In the present chapter, the studied light structured building will be presented by explaining all its major characteristics and particularities. Moreover, due to the fact that the results from the light structured building will be compared with the ones achieved on the heavy structured one, defined on Ms Y. Touly's master thesis [7], a few concepts and notions about this last building will be described.

3.1. CONCEPT OF A LIGHT STRUCTURED BUILDING

The present master thesis is focused on light structured buildings. As the name itself indicates, this types of buildings are the ones that compared to the others have a lighter structure and in consequence, they have a smaller thermal capacity. Their total weight is smaller due to the properties of the used building materials. They use to be constructed by employing different types of light materials, such as aluminium or wood. Those materials have very good constructive properties. In the case of the aluminium, it has a density that is approximately three times smaller than the steel. It also has an excellent resistance to the corrosion, with good mechanical properties and easily formable. In the case of the wood, it is even less weight than the aluminium (its density is around three times smaller than the aluminium one). It also has good mechanical properties and it has a good behaviour when it works as a thermal insulation.

The present thesis will be focused on the ones that use wood as the major construction material. In this type of constructions, another remarkable aspect is that they use to have insulation within the structure thickness.

3.2. THE USED LIGHT STRUCTURED BUILDING MODEL

Having explained the concept of a light structured building, in the present section the utilized light structured buildings model will be described.

As it has been said before, the used model have been developed from the one designed by Ms Y. Touly on her master thesis [7]. In this case, the walls are made with composite wood, covered by a plasterboard and insulated with glass wool. The physical characteristics of walls, windows and roof are described in Appendix A.

In order to consider the internal walls of the building, it has been taken the same decision as the one that was chosen by Ms. Y. Touly [7]. Therefore, as she selected for her buildings, the internal walls of the light structured buildings will have a surface that is equal to the half of the total floor surface. This decision makes sense from an architectural point of view and also brings stability to the results.

So as to maintain the same insulation levels on the construction materials, the structural and insulation thicknesses have to be adapted. Due to this fact and as the values displayed on Appendix A reflect, the obtained material thicknesses do not have a standardized value.

Another relevant fact is that the model has been developed under the hypothesis that all the solar radiation that passes through the window heats the floor. In order to consider this hypothesis on TRNSYS simulations, a coefficient called "Geosurf" has been used. This coefficient establishes the fraction of the entire entering direct solar radiation that hits a specific surface. So, for imposing this hypothesis, the floor has been given a Geosurf value of 1 while the rest of the internal surfaces have obtained a value of 0.

In the developed light structured model, the interior thermal capacitance has been taken into account. This parameter emulates the thermal capacitance composed by the sum of the capacitances of the interior furniture and the inside air. This parameter has

been introduced into TRNSYS through the “air capacitance” entry. For this occasion, in order to take into consideration both elements (interior air and furniture), it has been decided to give a value to the capacitance that is equal to 2.4 times the building’s inside air volume. For instance, if a building of 100m^2 (which has an inside air volume of 300m^3) is considered, the interior capacitance will have a value of $720[\text{kJ}/\text{K}]$. In addition, the capacitance of the previously commented internal walls must be considered.

Finally, there are the convective heat transfer coefficients used on the model. In this case, it has been used the default values that TRNSYS brings. For the components that are in contact with the inside air, the convective coefficient has a value of $3.06[\text{W}/\text{m}^2\cdot\text{K}]$ ($11[\text{kJ}/\text{h}\cdot\text{m}^2\cdot\text{K}]$ in TRNSYS units). In the case of components that are in contact with the outside air, this convective coefficient is higher with a value of $17.78[\text{W}/\text{m}^2\cdot\text{K}]$ ($64[\text{kJ}/\text{h}\cdot\text{m}^2\cdot\text{K}]$ in TRNSYS units).

3.3. HEAVY STRUCTURED BUILDINGS

As their name itself indicates, those buildings are the ones that have a heavier structure which involves a bigger thermal capacitance. They use heavier construction materials, so, as it can be noticed, the major difference between the heavy and light buildings will be in the walls composition. In this occasion, the analyse will be centred in the heavy structured buildings where the walls are made of concrete and insulated from the exterior side.

For its simulation, as it has happened in the case of the light structured building, the employed models will be based on the ones that Ms Y. Touly developed on her master thesis [7]. Basically, the only difference between those two models will be the composition of the exterior walls. These walls have the characteristics that are described in Appendix B. The rest of the elements (the interior walls, the solar radiation hypothesis, the interior thermal capacitance and the convective heat transfer coefficients) are the same that the ones employed for the light structured buildings.

4. STUDY OF THE IMPACT OF DIFFERENT HEATING LOADS AND INDOOR CONDITIONS ON THE ACCURACY OF THE INTERNAL STATE AND ON THE RC PARAMETERS

This chapter presents a study on the impact of different heating loads and indoor conditions on the accuracy of the internal state T_i and on the 4R3C model's parameters of the designed buildings. In order to make this research, for the first aspect, the fitting proportion between the internal states (T_i) obtained with the simulation of the simplified 4R3C model on Matlab and the ones obtained with TRNSYS will be analysed. For the second feature, the proportion of fitting between the RC parameters determined by Matlab and those calculated theoretically using the physical characteristics of the building will be studied.

Firstly, the study will analyse this impact on heavy structured buildings. For this analyse, the heavy structured buildings designed in Ms Y. Touly's master thesis [7] will be used. Finally, the same study will be done with light structured building, the core case of study of this master thesis.

For this analyse, the behaviour of two different buildings will be studied for both building models (heavy and light structured). The first building will be a building of 50m² with a width-to-depth ratio of one, a window-to-floor surface ratio of 5% and south orientation (50_1_5_0). The second building will be 100m² with a width-to-depth ratio of one, a window-to-floor ratio of 5% and south oriented (100_1_5_0).

In order to consider diverse heating situations, five different heating models will be studied. In the first two, the building thermostat temperature will be fixed with a different schedule for each case. The next will approximate a situation where there is not any heating system on the building. In this case, the interior temperature (T_i) will strongly depend on the outside weather conditions. For the last two models, the heating system behaviour will be fixed with two different schedules that control the heating system activation.

The principal goal of this chapter is to see if there is any correlation on the accuracy of the obtained model with the different heating loads and interior conditions. The study will also be used to see the relations and similarities between the heavy structured and the light structured buildings on this aspect. Finally, the heating model that brings the best accuracy on the results on each type of building (light and heavy structured buildings) will be used for the rest of simulations and analysis of the present master thesis.

4.1. IMPACT ON HEAVY STRUCTURED BUILDINGS

In this first part of the chapter, the focus will be centred on the heavy structured buildings. Two sizes of buildings will be simulated in five different heating situations.

The first simulation (*Set temperature 0_1_0*) will suppose a situation where the thermostat temperature will be fixed. In this case, the heating system will have a simple schedule that will be the same for every day of the week: from 06:00 till 18:00 the thermostat temperature will be set at 22°C, while the rest of the day it will be fixed at 15°C. In this situation, the heating system will deliver enough heating power in order to obtain the fixed temperature (there is no limitation on the power of the heating system).

For the second situation (*Set temperature Room1*), as it occurs in the first one, the thermostat temperature will be set, but, with a different schedule that varies during the week. Monday, Tuesday, Friday and Saturday will follow the same characteristic as the first simulation. For the rest of the days, the only difference will be that from 06:00 to

18:00 the temperature instead of being 22°C it will be 20.25°C. This value is obtained by fixing the thermostat temperature increase (ΔT) with a value that correspond to the 75% of the one used in the previous heating situation, where the ΔT value was 7°C.

In the third situation (*No heating*), a state where there isn't any heating system will be simulated. Without any heating system, the inside temperature of the building (T_i) will be strongly influenced by the weather conditions.

The fourth situation (*Set heating 0_1_0*) will represent a state where the heating power will be the fixed parameter. In this case, the heating system will get on from 06:00 to 18:00, with a fixed heating power of 2777.78[W] (10000[kJ/h] in TRNSYS units), while the rest of the time will be turned off. Moreover, in this heating situation the thermostat temperature will not have any limitation, it will be set with an infinite value. Due to this fact, the heating system will deliver its maximum heating power while it is functioning.

Finally, the fifth simulation (*Set heating Room1*) will consider, as it occurs in the fourth one, a situation in which the heating system will be set by fixing the heating power while the thermostat temperature set with an infinite value. As it happens in the second simulation, on Monday, Tuesday, Friday and Saturday the heating system will follow the same schedule and behaviour as in the fourth simulation. Then, for the remaining days, the only variation will be that from 06:00 to 18:00 the heating power instead of being 2777.78[W] it will be of 2083.33[W] (7500[kJ/h] in TRNSYS units).

As it has been previously presented, the first analysis will be done with a small squared building of 50m² with 2.5m² of its walls covered by windows and with south orientation.

Taking into account the accuracy on the proportion of fitting between the internal states (T_i), determined by the simulated 4R3C model in Matlab and those calculated with TRNSYS, it can be observed that in general the fitting has been quite good. This accuracy has a value that approaches the 80% of fitting in almost every situation. There has been an exception in the third simulation, the one without a heating system. In this condition, the fitting has only reached 63.9%, which is notorious comparing with other situations. In the other hand, there is the fourth situation (*Set heating 0_1_0*) in which the accuracy has achieved 81.85%. But in general, the accuracy in the first, second, fourth and fifth have been almost the same, with a maximum variation of approximately 2%. Those values are displayed in the Table 3.

When the focus is centred on the obtained values of resistances and capacitances, interesting results have been obtained from the simulations and calculations. The accomplished results show that there are two separated groups depending on the reached precision: resistances and capacitances.

As it has been explained in the chapter 2, the four resistances that compose the 4R3C simplified model have been analysed in groups of two, R_o+R_{io} and $R_{if}+R_f$. The first sum (R_o+R_{io}) represents the resistance that simulates the envelope of the building that is in contact with the outside air. The second sum defines the buildings floor resistance that links the building with the ground. The achieved resistance values have been very accurate in comparison with capacitance ones. As it can be appreciated in the Figure 7, the R_o+R_{io} values obtained with Matlab simulation have been almost the same as the theoretical ones in all the heating situations. The major error has been 9.4%, while the most accurate situation has had an error of 6.32%. So, there have been observed very similar error values in all the studied situations. In the case of the values for the $R_{if}+R_f$ resistance, they have also been quite similar, but, compared to the ones achieved in the R_o+R_{io} resistance, their variations have been more astounding. Surprisingly, the most precise value for the R_o+R_{io} resistance has been reached in the third heating situation (*No heating*) with an error of 19.13%. The rest of the heating situations have brought

errors that are inside the interval of 41% to 56%, where the first heating situation has been the most precise one and the fifth situation the less accurate.

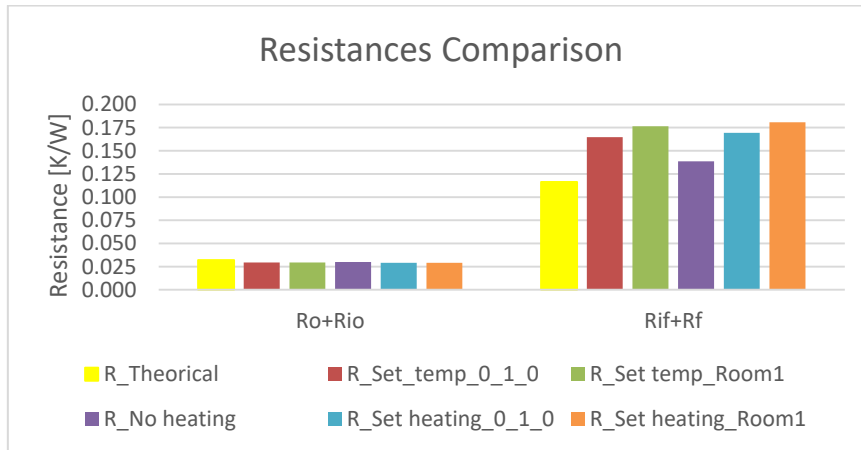


Figure 7: Ro+Rio and Rif+Rf values for a 50_1_5_0 heavy structured building in different heating situations.

When the capacitances are analysed, it can be observed that the reached results have been less accurate than in the resistance case. The 4R3C model’s capacitances values obtained with Matlab simulation have been dispersed from the ones calculated theoretically by using the buildings properties. In general, the diversion from both values have been more noticeable. As Figure 8 and Figure 9 shows, the difference between those values is remarkable for all the capacitances in all the heating situations. If the obtained error is evaluated, it can be appreciated that the Ci and Cf capacitances have been the most precise ones. The error in both capacitances has been located in a similar range, between 34% and 40% for the Ci capacitance and between 30% and 46% the Cf capacitance. The most accurate result has been achieved for the Cf capacitance in the fourth heating situation where the error reached a value of 30.18%. The worst results, in errors terms, have been the ones obtained for the Co capacitance, where the error have been moving between values of 56.76% in the best case, and 78.73% in the worst case. Notwithstanding the differences between the theoretical and simulated results, the obtained values in the simulations have been close between each other.

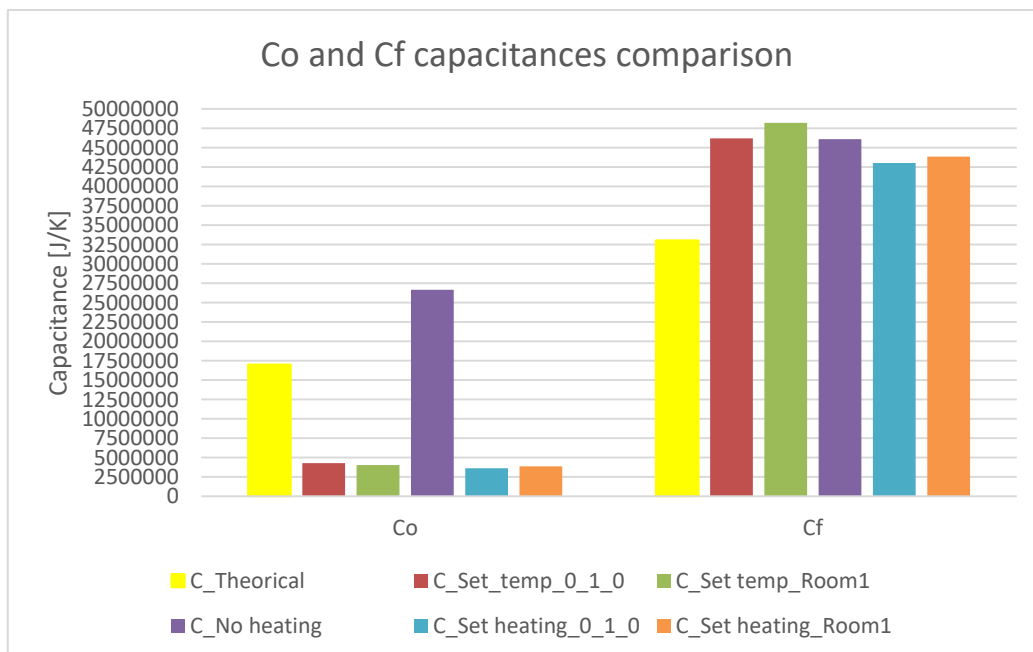


Figure 8: Co and Cf values for a 50_1_5_0 heavy structured building in the different heating situations.

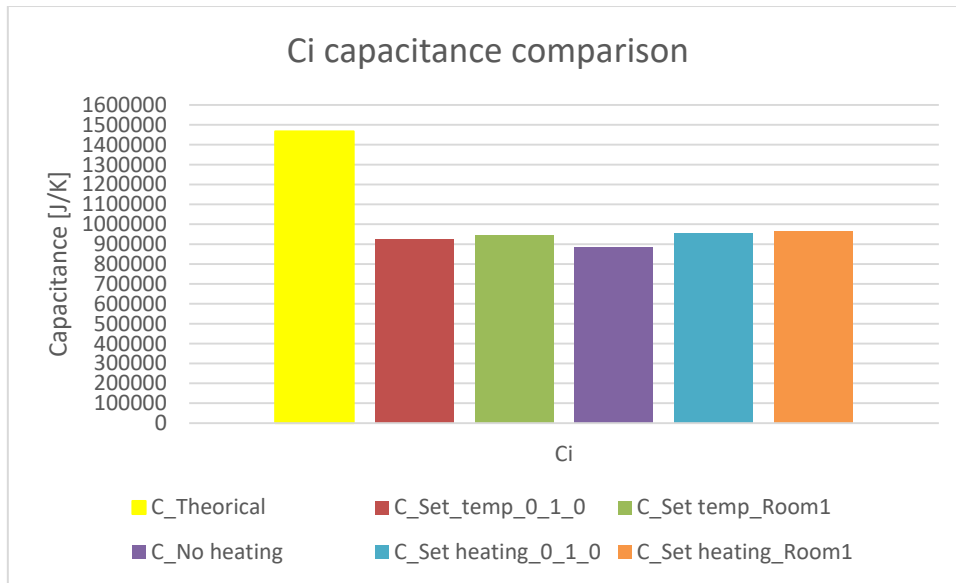


Figure 9: Ci value for a 50_1_5_0 heavy structured building in the different heating situations.

After having analysed the 50_1_5_0 building, the next step consists in studying a 100m² with a width-to-depth ratio of one, a window-to-floor ratio of 5% and south oriented (100_1_5_0) heavy structured building. In this building the behaviour tendency has been really similar to the one observed in the smaller building.

As it has happened in the smaller building, the obtained accuracy on the interior temperature (Ti), in almost every heating situation, has been around the 80%. Practically in every heating situation, the achieved accuracy has been higher compared to the results obtained in the previous building. The major precision gain has been noticed in the no heating situation, where the obtained precision has been increased (77.63% instead of 63.9%). In this case, the most accurate value has been obtained in the first heating situation (*Set temperature 0_1_0*). It has reached almost 83% of fitting between the values acquired on the 4R3C model simulation and the ones recovered with TRNSYS. The accomplished accuracies on the fourth and fifth situations, where the heating power is set, have been the most constant ones in both building sizes. The acquired values have been higher than 80% while they have experimented a very small variation. Those results are represented in the following table, Table 3.

Type of building	Heating situation on heavy structured buildings				
	Set temperature 0_1_0	Set temperature Room1	No heating	Set heating 0_1_0	Set heating Room1
50_1_5_0	79.69%	79.56%	63.90%	81.85%	81.30%
100_1_5_0	82.94%	82.77%	77.63%	81.85%	81.54%

Table 3 : Percentage of fitting on the internal state Ti between the 4R3C model approximation (Matlab) and the real data (TRNSYS) for different heating situations in 50_1_5_0 and 100_1_5_0 heavy structured buildings.

When the precision on the obtained values of resistances and capacitances are analysed, it has been seen that the behaviour of the results have been essentially the same as the one observed in the case of the smaller heavy structured building.

As it has happened with the resistances of the smaller building, in the case of the bigger building the obtained values of the resistances in the simulated 4R3C model have been closer to the theoretically calculated ones than the capacitances. When the values

of Ro+Rio resistance are examined, those have been quite accurate in every heating situation. However, if they are compared with the ones of the smaller building, the bigger building's results are less precise. For all the heating situations excluding the no heating one, the increase on the error has not reached the 4%. The circumstances of the third heating situation has been less good for both resistances (Ro+Rio and Rif+Rf), specially for the second one. For the first pair of resistances the achieved error has risen till 17.76%, while for the second pair, the increase has reached an enormous 345.14%. Excepting the third heating situation, the acquired results for the Rif+Rf resistance have been improved in a remarkable way. The reduction on the error has been higher than 23.59% for the four situations. The greater error reduction has been perceived for the second heating situation, where the decrease on the error has been of almost 43%. The accomplished results for both resistances are displayed on Figure 10.

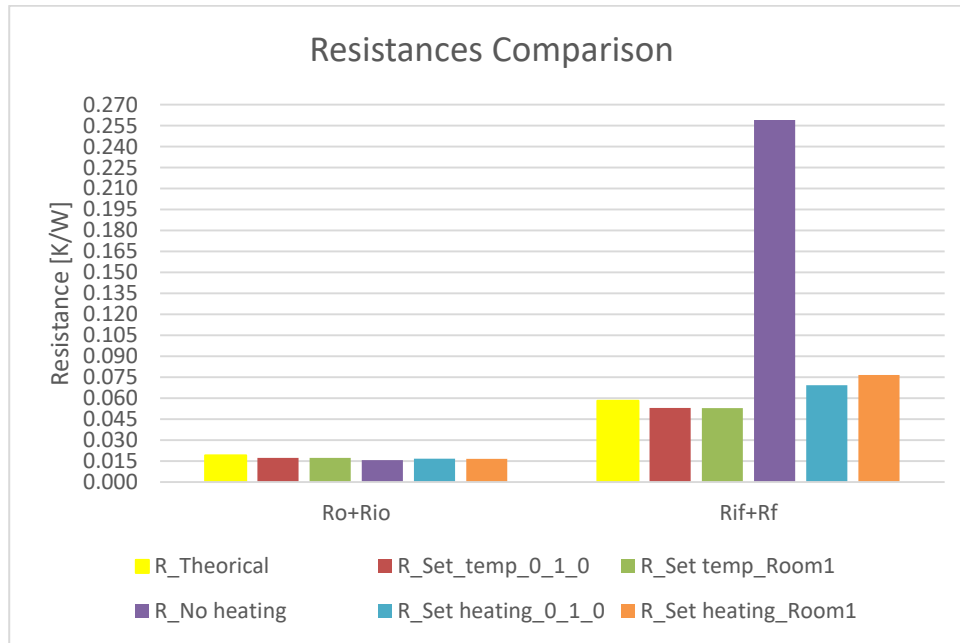


Figure 10: Ro+Rio and Rif+Rf values for a 100_1_5_0 heavy structured building in the different heating situations.

The capacitances values have followed the same tendency that has been seen in the 50m² heavy building. As the Figure 11 and Figure 12 reflect, the results of the capacitances have been more dispersed than the resistances ones. The results for the Cf capacitance have been the most accurate ones, followed very close by the Ci capacitance ones and then by the ones achieved for the Co capacitance. From a general point of view, the fitting proportion between the acquired results in the Matlab simulation and the ones attained theoretically have been higher in the bigger building than in the smaller one. When the results of both buildings are compared, it has been noticed that the bigger error reduction has been for the Co capacitance, which coincides with the one that has the worst accuracy between the simulation and the theoretical value. For this capacitance, the highest error reduction has been 22.38% for the first heating situation, while the third heating situation has been the worst one. In this heating situation, the error has been increased by 5.5%. In the case of the Co capacitance, all the heating situation, with the exception of the third one, have suffered an error augmentation. The bigger increase has happened in the second heating situation, with an error increase of 7.4%. In contrast to what have happened with the previous capacitance, the third heating situation has suffered an error reduction, in this case with a decrease of 5.51%. Finally, when the Cf capacitance is studied, the most astounding characteristic is that in every heating situation the error has been reduced. The second heating situation has the major reduction (16.84%) while the third one has the smaller one (1.65%).

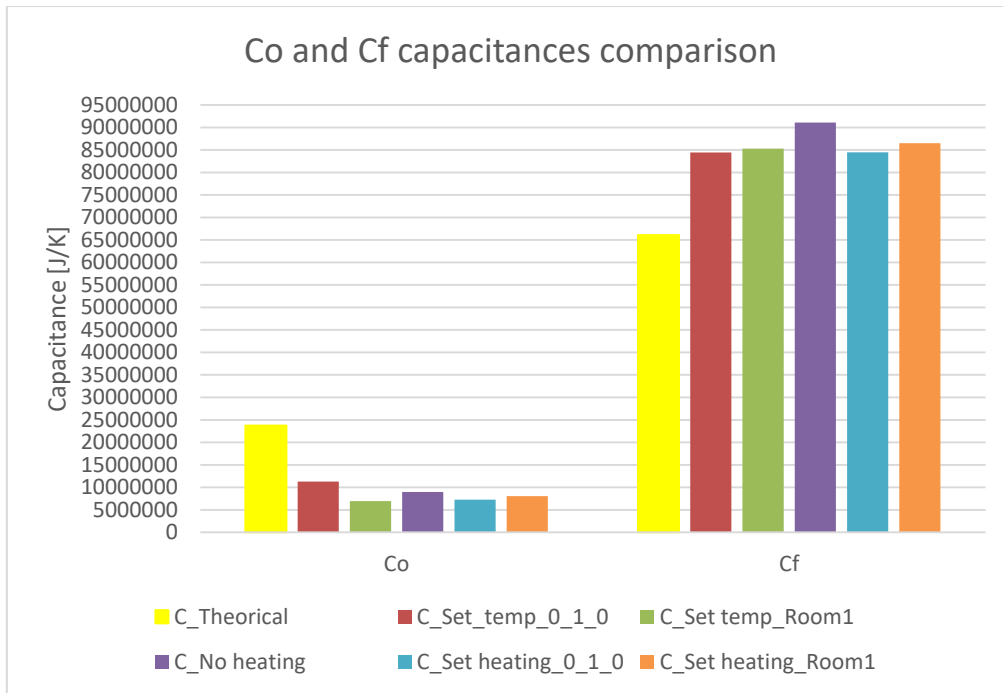


Figure 11: Co and Cf values for a 100_1_5_0 heavy structured building in the different heating situations.

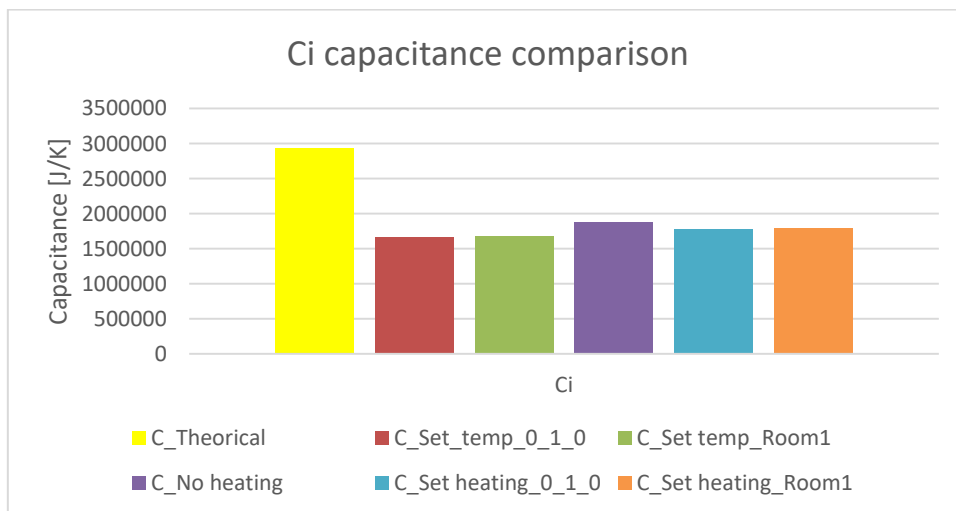


Figure 12: Ci value for a 50_1_5_0 heavy structured building in the different heating situations.

After having analysed the two buildings, some interesting conclusions can be extracted.

In the first place, it has been proved that the 4R3C model for heavy structured buildings has some sensitivity on its accuracy depending on the heating situation. The simulated values for the internal temperature (T_i) and for the model's elements have been different from the real and theoretically calculated ones. In theory, the values of resistances and capacitances only depend on the building characteristics and the heating situation has no influence on them. Nevertheless, as it has been seen in previous analysis, the simplified model has been influenced by the heating situation.

In second place, after proving the influence of the heating situation on the model's precision, it has been appreciated that the worst results on accuracy of the value of the internal temperature (T_i) have been achieved in the third heating situation, the one that doesn't have any heating system. The other heating models (the models that use a heating system) provide similar results that have reached 80% on the accuracy.

However, inside this group the ones that have a constant heating power (the fourth and fifth heating situations) have brought the most stable results, always providing values for the accuracy that have been over the barrier of the 80%.

In third place, it has been observed that the heavy buildings in both sizes behave in a similar way in the analysed heating situations. The resistances values have been more accurate than the capacitances ones in both cases. But, those values have not been the same. If they are analysed from a general perspective, the ones acquired in the bigger building have been more precise. In addition, as it has been commented before, in the situations where the building has a heating system, the obtained accuracy on the internal temperature (T_i) in both building sizes did not vary significantly. The case without any heating system has been different because the reached results were notoriously distinct.

Finally, compiling all the studies, it has been seen that the best option, in order to analyse the behaviour of a heavy structured building, is the one that uses a heating model in which the building has a heating system. In side this group, the situations with a constant heating power have brought more constant and stable results. But in general, the characteristics of the heating system do not have a big influence on the result. If the acquired knowledge is applied in Ms Y. Touly's master thesis [7], it can be concluded that the heating model that she has used was suitable. This is due to the fact that she has analysed a heavy structured buildings and, in order to do that, she has used a heating system with a specific schedule for her simulations, that as it has been seen, brings the best results. In order to obtain better results, she could improve her models by changing her heating system with one that uses a constant heating power.

4.2. IMPACT ON LIGHT STRUCTURED BUILDINGS

In the present section, the same study done in the section 4.1 for heavy structured buildings will be performed for the light structured ones.

As it has been done in the previous section, five distinct heating situations, that encompasses the typical thermal conditions, will be simulated for light structured buildings. Moreover, in order to have a global view of the impact on this type of buildings, two different sizes (50m^2 and 100m^2) of this building will be studied.

One of the most notorious aspect watched on those simulations has been the sensitivity of the 4R3C model to the initial conditions viewed on the achieved results. The initial conditions of the models, especially the initial values of the capacitances, have been a crucial issue on this study. In some of the simulations, the change of the initial condition has supposed a variation of a 20% on the accuracy of the proportion of fitting of the internal state (T_i). For instance, in the 100m^2 light structured building, when the first heating condition (*Set temperature 0_1_0*), which has a heating system with a fixed temperature schedule on its thermostat, has been simulated with the predefined values for the capacitances ($C_o=1000[\text{W}\cdot\text{h}/\text{K}]$, $C_i=100[\text{W}\cdot\text{h}/\text{K}]$ and $C_f=1000[\text{W}\cdot\text{h}/\text{K}]$), the accuracy has only reached a scarce 59.64%. When the conditions of C_o and C_f were changed to $10000[\text{W}\cdot\text{h}/\text{K}]$ in both cases, the accuracy has been improved up to 81.21%, that is remarkably more precise.

The south oriented 50m^2 squared building with 2.5m^2 of its walls covered by windows (*50_1_5_0*) will be the first to study. As it has happened in the heavy structured building, the obtained results have many common points.

When the accuracy on the fitting proportion of the results obtained for the interior temperature of the building (T_i) with the simplified model and the "real" ones, obtained with TRNSYS, is studied, it can be observed that the tendency is the same as it happened for the heavy structured building. For the first two simulations where the thermostat temperature was fixed and for the fourth and fifth ones where the controlled parameter was the activation of the heating system, the achieved accuracy has been close to 80%.

In the other hand, for the case without any heating system, the fitting proportion has been less precise with an accuracy of 68.45%. This situation has been the same for the heavy structured building, where the simulation without any heating system has been the less precise while the other cases, also, have a fitting that rounds the 80%. Getting back to the light structured building and giving a look to the simulations where the results were precise, as it can be noticed in the Table 5, the fourth and fifth heating situations give better results than the first two, which have an accuracy near 76%.

If the focus is changed to the values of the simplified model parameters (resistances and capacitances), the tendency is quite similar to the one seen in the heavy structured buildings: the values of resistances theoretically calculated and the ones obtained with Matlab are closer between them while the values of some of the capacitances are more unlike.

In the case of the resistances, when the achieved results described in Figure 13 are compared with the same size heavy building's ones, it can be noticed that they have had a different tendency depending on the analysed resistance. While for the R_{o+Rio} resistance the results are less precise, for the case of the R_{if+Rf} resistances are more accurate except for the third heating situation. The R_{o+Rio} resistances have had similar fitting error between the theoretical and the simulation values in all the studied heating situations. This error has had a value that has been between 16.38% for the case with no heating and 19.87% for the first heating situation. As the Table 4 shows, the reached results have been around 10% less precise than the ones accomplished in the heavy building. In the other hand, the R_{if+Rf} resistance has had a more unlike accuracy between the different heating situations when the error between the theoretical and simulation values are compared. The heating situation where the temperature has been the set parameter (first and second situations) have acquired the smaller error (16.44% for the first heating situation and 27.31% for the second one). The next ones on the precision scale are the fourth and fifth heating situations (with a constant heating power) which have accomplished 31.63% and 38.08% of error respectively. The third heating situation has obtained extremely bad results. It has reached the enormous value of an error of 763.72%. When those results are compared with the heavy structured building ones, it can be appreciated that in the majority of the analysed heating situations the attained results have been more accurate. There have been a clear decrease on the error. In the first two situations the error have been reduced by approximately 25% while the last two have dismissed it by 15%. Due to the bad results of the third heating situation, the error has drastically increase its value instead of decreasing.

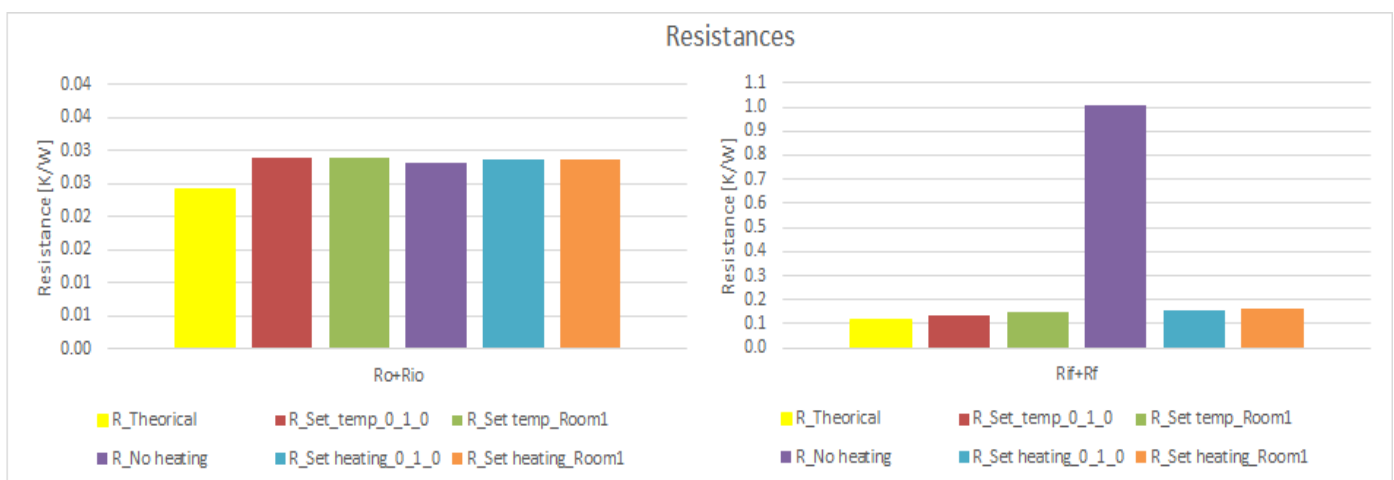


Figure 13: R_{o+Rio} and R_{if+Rf} values for a 50_1_5_0 light structured building in different heating situations.

	Set temperature_0_1_0	Set temperature_Room1	No heating	Set heating_0_1_0	Set heating_Room1
Ro+Rio [%]	-11.76	-11.23	-10.06	-9.13	-9.44
Rif+Rf [%]	25.05	24.35	-744.59	13.90	17.23
Co [%]	-240.14	-287.66	-99.70	-34.32	-81.62
Ci [%]	19.57	22.20	39.49	16.88	17.81
Cf [%]	33.57	39.20	39.39	19.18	24.67

Table 4: Comparison of the reduction/increase of the error obtained for the 50_1_5_0 light structured building when the obtained error percentage values are compared (in absolute percentage terms) with the ones obtained for the 50_1_5_0 heavy structured building. The green values represent an error reduction while the red and negative ones represent an error increase.

From a general perspective, the achieved results for the capacitances have been notably more precise than in the heavy structured buildings, as the Table 4 reflects. There is an exception with the Co capacitance (Figure 14) which has reached very bad results. The error between the theoretical value and the simulated one in this capacitance has been very big in all the heating situations reaching error values of 363.96%. Moreover, the Co capacitance has been the only capacitance that has worsen its results compared to the heavy structured building. The obtained results for the other two capacitances (Ci and Cf) that are represented in Figure 14 and Figure 15 respectively, have been very good. The error between the simulated value and the theoretically calculated one has been very small. For the Ci capacitance, the smallest error has been obtained in the third heating situation with a value of 0.41%. At the same time, its higher error has reached a value of 18.08 which is quite accurate. The results for the Cf capacitance have been even better than the previous capacitance's ones. Its smaller error has a value of 0.13% while the bigger one has a value of 11%. Furthermore, the error value of those capacitances (Ci and Cf) has been reduced in comparison with the acquired results in heavy structured building.

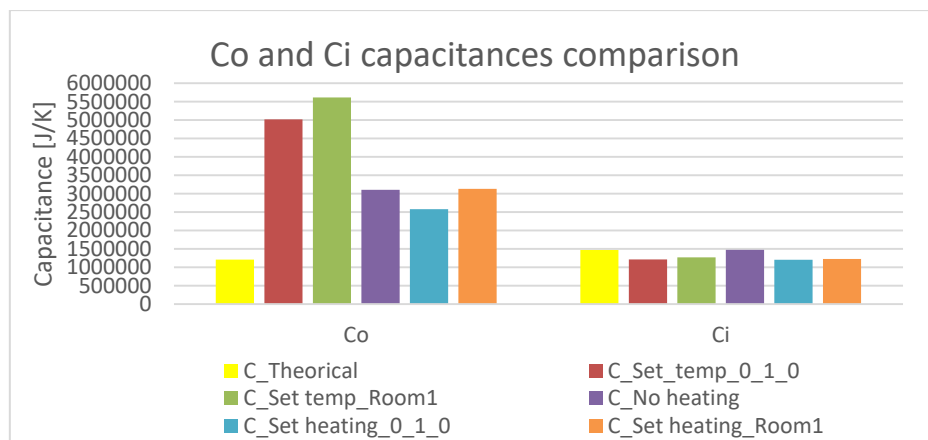


Figure 14: Co and Ci values for a 50_1_5_0 light structured building in the different heating situations.

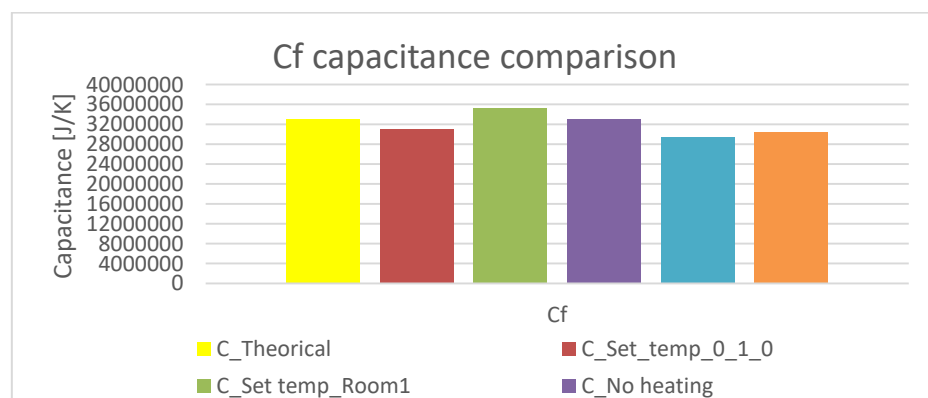


Figure 15: Cf values for a 50_1_5_0 light structured building in the different heating situations.

After having analysed the behaviour of a light structured building of 50m², the following step will be the study of a bigger light structured building of 100m² with a width-to-depth ratio of one, a window-to-floor ratio of 5% and south oriented (100_1_5_0).

The achieved results for the case of a bigger light structured building have had similarities with the behaviour seen on the previous case of 100m² heavy structured building. The obtained accuracy on the internal state has been considerably good while the precision of the resistances has been greater than the capacitances one.

In the Table 5 the obtained results on the fitting proportion of the interior temperature (Ti) are presented. As it has happened in case of the heavy structured building, the results of the bigger building have been more precise than in the smaller building. In this occasion, all the heating situations present values that are around 80% of fitting. The third heating situation, the one where the building has no heating system, has been the one with the bigger accuracy improve with almost 10% increase. The first two situations present the second bigger progress by acquiring a gain of 5%. The third situation has been the only one that is under the 80% with an accuracy of 78.38%. The rest of situation are above the 80% of fitting.

Type of building	Heating situation on light structured buildings				
	Set temperature 0_1_0	Set temperature Room1	No heating	Set heating 0_1_0	Set heating Room1
50_1_5_0	76.56%	76.25%	68.45%	81.20%	80.75%
100_1_5_0	81.21%	81.00%	78.38%	82.34%	82.14%

Table 5: Percentage of fitting on the internal state Ti between the 4R3C model approximation (Matlab) and the real data (TRNSYS) for different heating situations in 50_1_5_0 and 100_1_5_0 light structured buildings.

When the values of the 4R3C model are analysed, the discrepancy in the achieved accuracy between the resistances and the capacitances is still astounding. The resistances have obtained values that are very accurate in comparison with the capacitances ones. When the obtained results (Figure 16) are compared with the smaller light building (Figure 13), it can be seen that the ones for the bigger building have been more precise. As seen on Table 6, when the results are compared with the big heavy building, it can be noticed that for the last three heating situations the accuracy has increased while for the first two it has suffered a reduction. The Ro+Rio resistance has had good precision results. The third situation has been the most precise with an error between the theoretical and the simulate value of 4.83%, while the rest of situations have given errors between the 10% and 14%. The Rif+Rf resistance has provided different values depending on the heating situation. In this case, the situations with a constant thermal power have had the most accurate values (2.89% of error for the fourth situation and 3.71% for the fifth one).

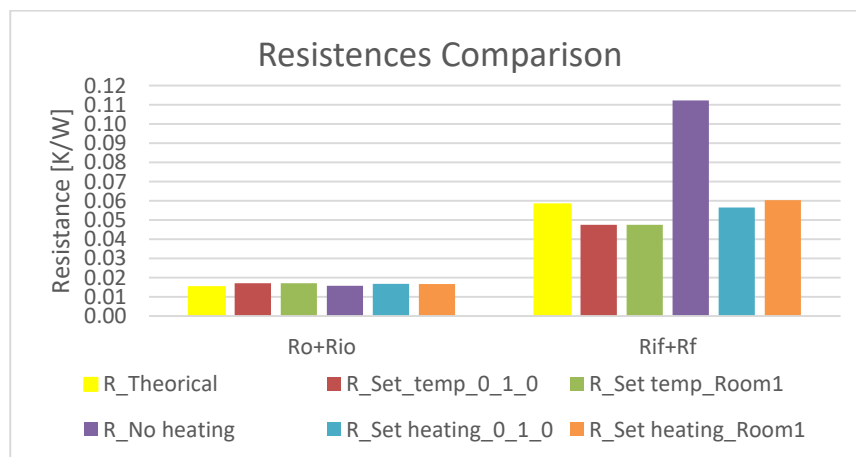


Figure 16: Ro+Rio and Rif+Rf values for a 100_1_5_0 light structured building in different heating situations.

	Set temperature_0_1_0	Set temperature_Room1	No heating	Set heating_0_1_0	Set heating_Room1
Ro+Rio [%]	-4.20	-4.42	12.92	0.90	2.55
Rif+Rf [%]	-9.56	-9.35	252.26	16.13	28.01
Co [%]	-349.52	-389.33	-241.86	-221.00	-253.54
Ci [%]	10.25	11.20	20.53	11.95	12.72
Cf [%]	18.87	24.34	29.61	22.89	29.19

Table 6: Comparison of the reduction/increase of the error obtained for the 100_1_5_0 light structured building when the obtained error percentage values are compared (in absolute percentage terms) with the ones obtained for the 100_1_5_0 heavy structured building. The green values represent an error reduction while the red and negative ones represent an error increase.

As it has taken place in all the studied cases, for heavy and light structured buildings of all sizes, the accuracy of the capacitances has been lower in general. As it has happened before for the smaller light structured building, the Ci and Cf capacitances have reached better results than in the heavy structured building. Nonetheless, the other capacitance (Co) has had very bad results. The case of the Cf capacitance (Figure 17) has been surprisingly very precise. All the obtained errors between the simulated values and the theoretically calculated ones have been under the 10%. The most accurate result has been acquired in the fifth heating situation where the error has had a value of 1.72%. The case of the Ci capacitance is also quite accurate. In all the heating situation the value of the error has been under the 34%. For this capacitance, the best result has been obtained in the third heating situation with an error of 15.49%. The Co capacitance (Figure 18) has obtained remarkably bad results. As it has happened for the smaller light building, it has lost precision compared to the heavy buildings. For this capacitance, all the error values have been above 250%.

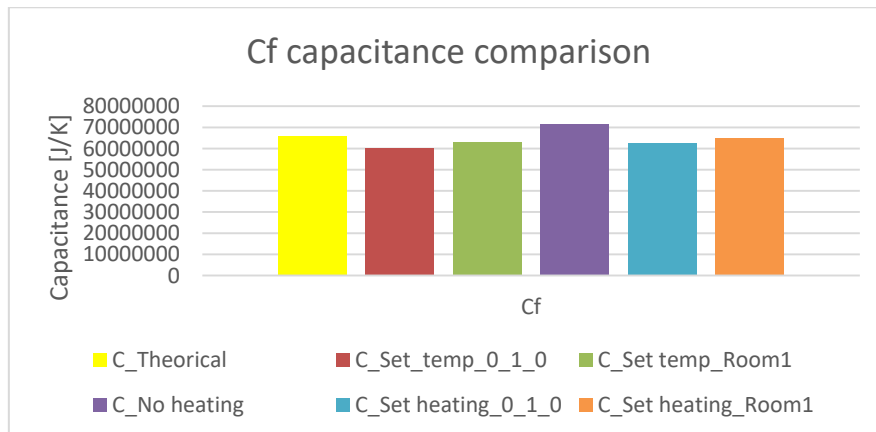


Figure 17: Cf values for a 100_1_5_0 light structured building in the different heating situations.

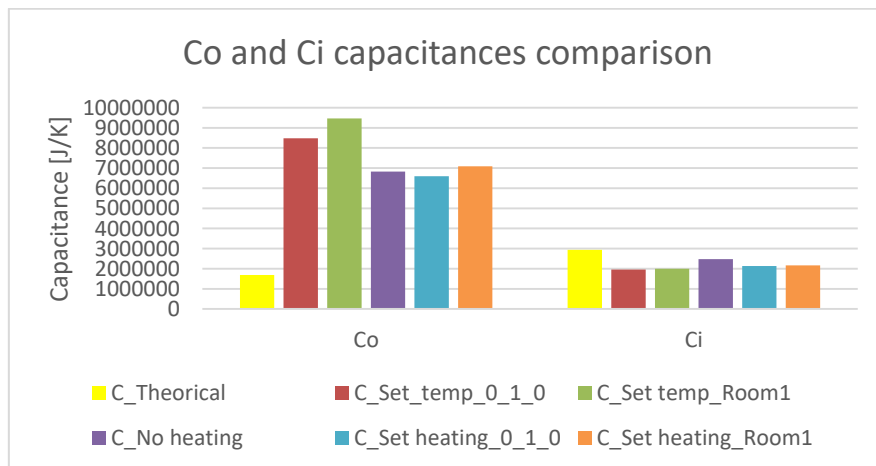


Figure 18: Co and Ci values for a 100_1_5_0 light structured building in the different heating situations.

Once having studied all the heating cases for heavy and light structured buildings of difference sizes, some conclusions can be extracted from the research.

The first characteristic that can be extracted from the present research, is that the behaviour of the buildings has had some similarities on the response in the tested heating situations in both types of buildings (heavy and light). The obtained results on the fitting proportion of the internal state have been practically the same and the heating situations with a heating system have brought the best results in both buildings.

Another remarkable point is the noticed sensitivity of the 4R3C model on the light buildings to the initial parameters values. As it has been explained previously in the present chapter, the light structured buildings have a clear susceptibility on the achieved results precision associated to the initial values of the parameters, especially to the capacitances ones. This sensitivity is less notorious in the heavy structured building.

As it has occurred in the heavy structured building, in the light structured buildings the values of the resistances have been more precise than the capacitances ones. In the case of the resistances, some values have improved their accuracy compared to the results of the heavy building, but, others have decreased it. So, there haven't been a clear tendency. The case of the capacitances have been noticeable different. The light buildings have visibly given better results on the C_i and C_f capacitances than the heavy ones. Although, the other capacitance (C_o) has had much more imprecise values.

Moreover, it has been proved for both types of buildings that the heating situations with a thermal heating system brought the best results in terms of accuracy on the obtained internal temperature (T_i). The simulations where the building has a heating system (first, second, fourth and fifth simulations) bring values of fitting that are approximately around 80%. This precision has been maintained with very small fluctuations when the size of the building was changed. The case where the building does not have any kind of heating system brings the worst results. Those did not reach the barrier of 80% of fitting and they have changed their value drastically when the building size was variated.

After having analysed all those aspects, it can be concluded that in order to make the following simulations on light structured buildings on the present master thesis, the building must include in its characteristics a heating system. Between the five studied heating models, the fourth one, the one that has the heating power fixed and has its schedule programme to be activated from 06:00 to 18:00, is the chosen option. This model has provided results that are beyond the 80% on the accuracy of the fitting of the internal state (T_i) values between the simulated model and the real one. This precision has been constant without any significant variation for both building sizes. The interior temperature (T_i) is the fundamental parameter of the study. So, the good results that this models brings has been the main reason to select this option. Furthermore, the chosen heating model has brought good fitting results between the theoretical and the simulated values in the case of the resistances. Moreover, the results for the C_i and C_f capacitances have also been accurate. A wick point has been the bad precision on the C_o capacitance, but, this accuracy has been very bad in all the heating situations.

5. STUDY OF THE IMPACT OF CHANGES ON THE BUILDINGS GEOMETRY AND STRUCTURE ON THE IDENTIFIED PARAMETERS OF THE 4R3C MODEL

In the present chapter, it will be analysed the impact that changes on the building's geometry and structure have on the fitting proportion between the 4R3C parameters obtained by Matlab and the ones calculated theoretically. This analyse will be done in terms of the DTP (Determined/Theoretical Proportion) coefficient, that as it has been explained on the section 2.4, it is a coefficient that compares the fitting proportion of the 4R3C models parameters by dividing the value determined on Matlab with the theoretically calculated one.

As principal goal of this master thesis, on this section the achieved results for the light structured buildings and the ones achieved for a heavy structured ones will be compared. As the study of chapter 4 has revealed, both types of buildings (light and heavy) will be simulated by using the fourth heating situation, where the heating system will get on every day from 06:00 to 18:00 giving a constant power of 2777.78[W] (10000[kJ/h] in TRNSYS units). The details of those buildings have been explained in chapter 3.

In order to do the study, four changes on the building's characteristics will be analysed: the building's floor surface (FS), its width-to-depth ratio (WD), its windows-to-floor surface ratio (WF) and its orientation angle (OA).

The study will begin by analysing the impact that each building's change has on the 4R3C parameters individually. For this first part, the study will be principally focused on the effects on a standard building of 100m², with a WD ratio of two, a WF ratio of 15% and an AO of 0° (100_2_15_0). Then, in order to have a more precise and consistent data and also, to be able to extract more generic conclusions, the 4R3C models parameters will be tested with combined building changes for a wider range of building configurations.

5.1. CHANGING THE FLOOR SURFACE (FS)

In this section the impact that a change on the floor surface (FS) has over the 4R3C model's parameters (resistances and capacitances) DTP will be studied. In order to have realistic results, the floor surface will vary between 50m² and 200m², where the chosen size steps will be of 50m², 75m², 100m², 150m² and 200m².

As it has been explained, this study will analyse and compare the achieved results in both types of buildings (light structured and heavy structured). In addition, in order to make this analyse simpler, a standard building with a WD ratio of two, a WF ratio of 15% and an OA of 0°, where the front wall south oriented, will be employed for this study.

The obtained accuracy values on the fitting proportion on the internal temperature (Ti) between the 4R3C model approximation (Matlab) and the real data (the one provided by TRNSYS) are displayed on Table 7. As it can be appreciated, for both types of buildings the fitting proportion has been above the 80% with very similar values in both buildings and very small fluctuations.

FS [m ²]	50	75	100	150	200
Light Ti fit. [%]	81.68	82.28	82.62	82.97	83.09
Heavy Ti fit. [%]	82.15	82.41	82.52	82.71	81.43

Table 7: Percentage of fitting on the internal state Ti between the 4R3C model approximation (Matlab) and the real data (TRNSYS) for different FS values in X_2_15_0 light and heavy structured buildings.

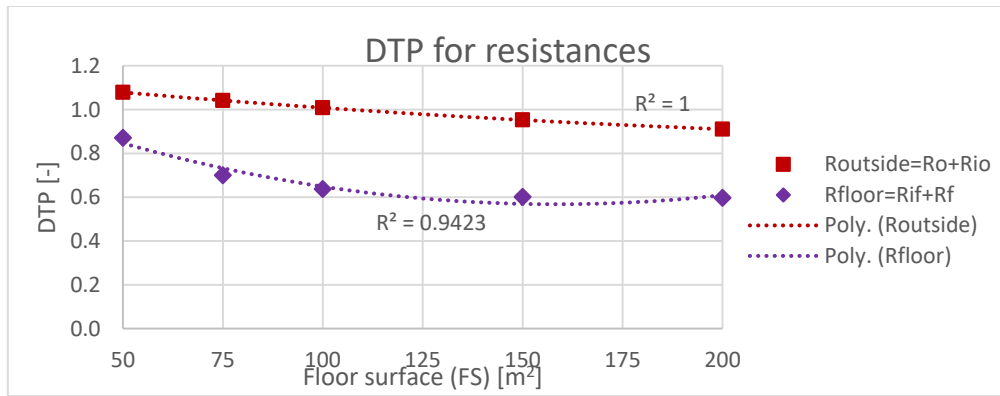


Figure 19: DTP of resistances for different FS in X_2_15_0 light structured buildings.

The first analysed element of the 4R3C model will be the resistances. In the Figure 19 there can be observed the obtained DTP results for the resistances of the light structured building. As this graphic shows, both resistances have been impacted by the FS parameter. In this case the most accurate results have been the ones obtained for the Routside resistance, which has achieved DTP values that were close to 1 in all the studied floor surface sizes. Moreover, its tendency can be represented by polynomial function of second degree which has a coefficient of determination of 1, but, it can also be represented by a linear function with good precision. The highest precision has been acquired for a FS of 100m². For smaller FS the DTP has been above 1 and for the smaller ones the DTP has been under 1. The Rfloor resistances of the light building have been less accurate. All their DTP values have been under 1 in all the studied FS. For this resistance, the best results have been the ones acquired for the smaller FS, where the 50m² building has been the most accurate. In addition, as it has happened in the Routside resistance, the Rfloor resistance evolution has also been represented very precisely by a second degree polynomial function.

When the focus is changed to Figure 20, the obtained DTP results for the resistances of the heavy structured building can be viewed. As it has happened in the light building, the most precise representation for both resistances have been achieved by a second degree polynomial functions with an R² value close to 1. In the case of the Routside resistance, the achieved results have been less precise than in the light building. They have followed a same tendency, but, in the case of the resistance of the heavy structured building, instead of having values for the DTP that are close to 1, they have been close to 0.8. The Rfloor resistance has had a similar tendency to the one seen for the same resistance in the case of the lighter buildings. However, the precision obtained for the smaller surface buildings, the ones which FS is close to 50m², has been higher than the in the light structured building.

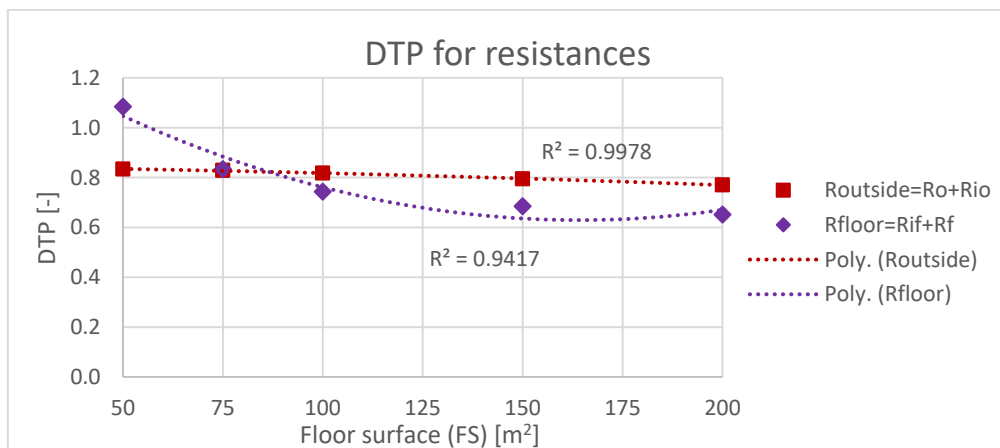


Figure 20: DTP of resistances for different FS in X_2_15_0 heavy structured buildings.

Once having researched the resistances, the next step is to study the capacitances. For that purpose, the obtained capacitances DTP results for the light and heavy structured buildings are represented in Figure 21 and in Figure 22 respectively.

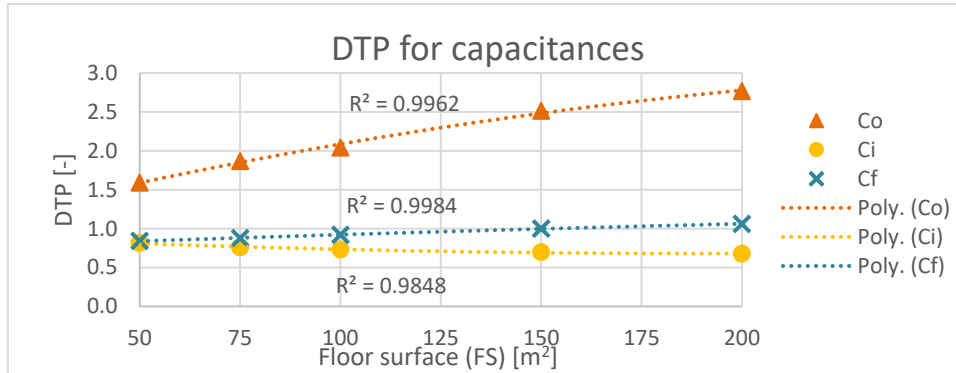


Figure 21: DTP of capacitances for different FS in X_2_15_0 light structured buildings.

As the first results for the light structured building obtained on the study of the chapter 4 have revealed, the accuracy of the Ci and Cf capacitances has been higher than the one obtained for the Co capacitance. Furthermore, the Co capacitance has been the most affected one by the FS changes. In the case of the Co capacitance, the precision has decreased when the FS has become bigger. For all the FS sizes, the DTP values of this capacitance have been above 1.5 and they have increased notoriously their value at the same time that the buildings FS became larger. The Cf capacitance has been the most accurate capacitance. It has acquired DTP values that have been always close to 1. They have improved their precision at the same time that the FS size has become bigger with a very soft curve. The Ci capacitance has also been accurate and has a soft curve, but, unlike the Cf capacitance, the precision has been reduced while the FS has become bigger. For all those capacitances, the closer behaviour representation curve has been achieved with a second degree polynomial function, where the R² has been close to 1.

In the case of the heavy structured building (represented in Figure 22), the behaviour of the DTP has been different. In this case all the capacitances have had a really soft tendencies and they have been less impacted by the FS changes in contrast with the light structured building. As it has happened in the light building, the Cf capacitance has been the most accurate one. Their values have been close to a DTP of 1.2 and they have maintained it in all the analysed building's FS sizes. The Co capacitance has also been the less precise, as it has occurred in the light structured building. In the case of a heavy building, the DTP for the Co capacitance has been close to 0.2 in all the FS sizes with a very small increase with the bigger FS sizes. Finally, the Ci capacitance has had DTP values that have been around 0.6, with a small decrease for the bigger buildings.

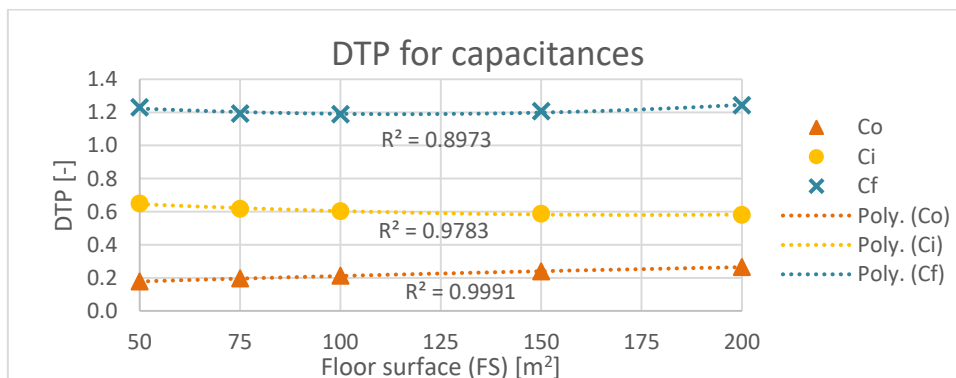


Figure 22: DTP of capacitances for different FS in X_2_15_0 heavy structured buildings.

5.2. CHANGING THE WIDTH-TO-DEPTH RATIO (WD)

In the present section the influence that a change in the width-to-depth (WD) ratio has over the 4R3C model's components DTP will be studied. For this analyse, the WD ratio will vary from 0.25 to 4, where the used steps will be 0.25, 0.5, 1, 2 and 4.

This study will gather the obtained DTP results for light and heavy structured buildings, in order to make their comparison possible. Furthermore, for making an easier analysis, a standard building of 100m² with a WF ratio of 15% and with its front wall south oriented (when the OA is 0°) will be utilized for this part.

The major differences between the buildings with a WD ratio of 0.25 and 4 and for the ones with a WD ratio of 0.5 and 2 is on the surface of each walls window. As it has been described in chapter 3, the building has three windows located in the front south wall and on the east and west side walls (for a building with an OA of 0°). Those windows have been designed to keep the same surface proportion in each wall in all the studied situation. This window proportion is equal to the proportion of area that each wall occupies on the total surface that the walls with windows compose. In order to make it clearer, the following equations describe the calculation of the window surface of each wall:

$$S_{front\ window} = \frac{S_{front\ wall}}{S_{front\ wall} + S_{right\ wall} + S_{left\ wall}} \times S_{Total\ windows} \quad (11)$$

$$S_{right\ window} = \frac{S_{right\ wall}}{S_{front\ wall} + S_{right\ wall} + S_{left\ wall}} \times S_{Total\ windows} \quad (12)$$

$$S_{left\ window} = \frac{S_{left\ wall}}{S_{front\ wall} + S_{right\ wall} + S_{left\ wall}} \times S_{Total\ windows} \quad (13)$$

As it has been commented, the WD ratio affects the windows distribution, so, each wall will have a different windows surface. Nevertheless, its total windows surface remains constant. The following table (Table 8) shows the windows surfaces for the buildings that this study concerns:

WD [-]	0.25	0.5	1	2	4
Front wall window surface [m ²]	1.67	3.00	5.00	7.50	10.00
Right wall window surface [m ²]	6.67	6.00	5.00	3.75	2.50
Left wall window surface [m ²]	6.67	6.00	5.00	3.75	2.50
Back wall window surface [m ²]	0	0	0	0	0
TOTAL windows surface [m ²]	15	15	15	15	15

Table 8: Windows surfaces on each wall for different WD ratios in 100_X_15_0 light and heavy structured buildings.

The Table 9 reflects the obtained accuracy values on the fitting proportion on the internal temperature (Ti) between the 4R3C model approximation (Matlab) and the real data (the one provided by TRNSYS). As it can be noticed, both types of buildings have had a similar fitting proportion that for all the WD ratio variation has been above the 80%, with small fluctuations.

WD [-]	0.25	0.5	1	2	4
Light Ti fit. [%]	82.26	82.37	82.51	82.62	82.70
Heavy Ti fit. [%]	81.76	82.13	82.38	82.52	82.47

Table 9: Percentage of fitting on the internal state Ti between the 4R3C model approximation (Matlab) and the real data (TRNSYS) for different WD values in 100_X_15_0 light and heavy structured buildings.

The first analysed 4R3C model's component will be the resistances. For that purpose, there are Figure 23 and Figure 24 that represent the acquired DTP results for the light and heavy structured buildings respectively. (It must be noticed that a logarithmic scale base 2 for the horizontal axis has been used in both figures).

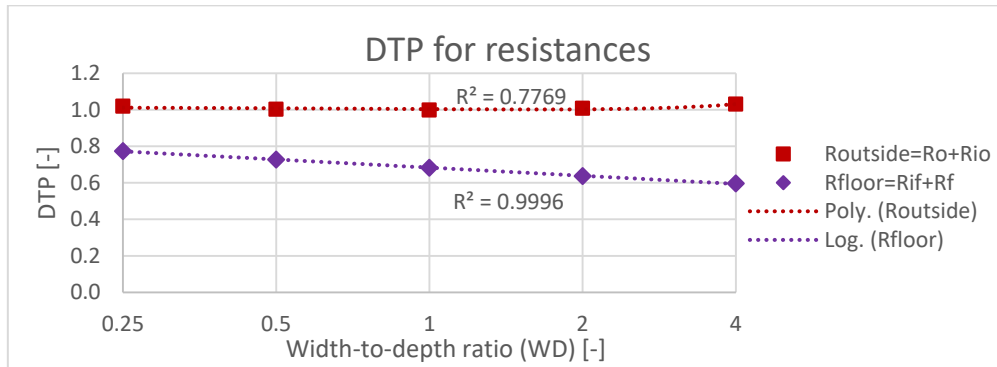


Figure 23: DTP of resistances for different WD in 100_X_15_0 light structured buildings.

As the Figure 23 shows, between the two resistances of the light structured building, the Routside resistance has been the most precise one and the less impacted one by the changes in WD ratio. Its DTP value did not vary significantly with the WD ratio changes. It has obtained DTP values that have been almost equal to 1 in every tested WD ratio. Due to a small increase on the DTP value for a WD ratio of 4, the closest curve to represent its tendency has been a polynomial function of second degree which has a R^2 coefficient of 0.78. The Rfloor resistance has been less accurate than the Routside resistance and it has also been more affected by the WD ratio changes. It has started with a DTP value close to 0.8 for a WD ratio of 0.25 and then, it has been reduced in every WD ratio incremental step. In this case, the most precise curve was a logarithmic one with an R^2 value close to 1.

When the results of the heavy structured building (Figure 24) are studied, it can be observed that the tendencies of both resistances have been the same that the ones discerned in the light structured building. On one hand, there is the Routside resistance. It has had the same evolution that the one show for the light building. Almost for every WD ratio case, it has achieved constant DTP values that have been close to 0.8. Moreover, it can be appreciated that for the bigger WD ratio values the DTP increases its value slightly. Due to this fact, a logarithmic curve is the one that represents better its tendency. On the other hand, there is the Rfloor resistance. As it has occurred with the previous resistance, the tendency of the Rfloor resistance has been the same that the one observed in the light structured building. In this occasion, for the smaller values of WD ratio the Rfloor resistance has been more accurate than Routside with DTP values that have been close to 1 in the proximities of 0.25 WD ratio. Then, as it has happened in the case of the light building, the DTP values have been decreasing with the WD ratio increases.

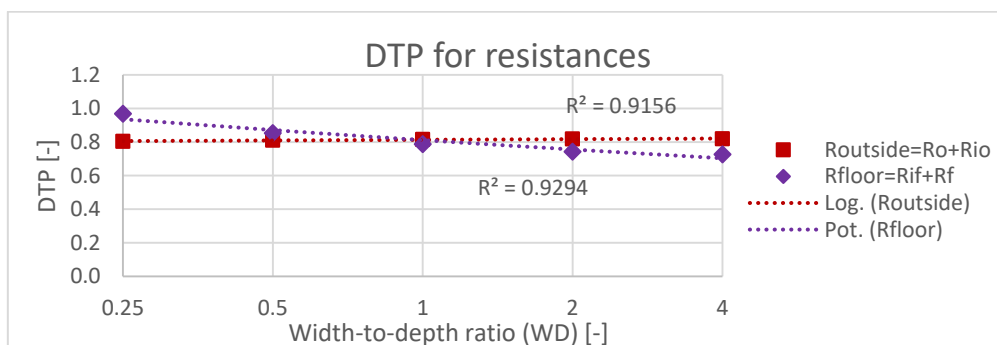


Figure 24: DTP of resistances for different WD in 100_X_15_0 heavy structured buildings.

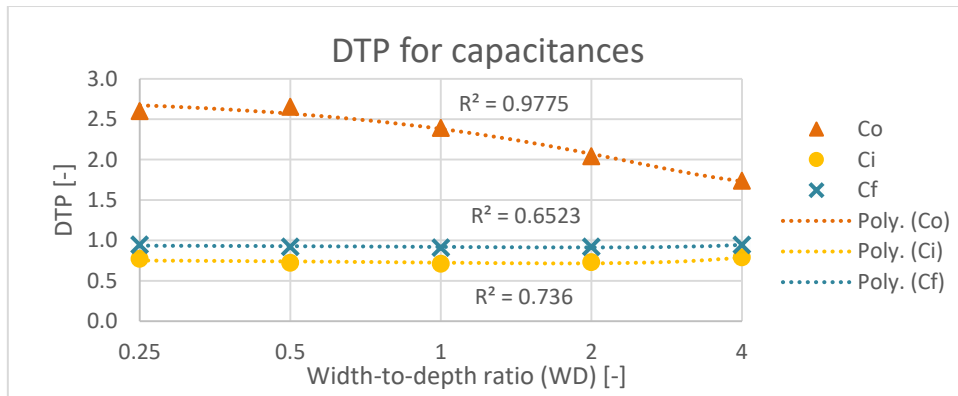


Figure 25: DTP of capacitances for different WD in 100_X_15_0 light structured buildings.

From the obtained results for the light structured building (Figure 25) it can be easily verified that, as it has occurred in the rest of the studied parameters of this master thesis, the Ci and Cf capacitances are more precise than the Co capacitance. Likewise, these two capacitances have not noticed significant impact on the achieved results by the changes on the WD ratio while the Co capacitance has been notoriously affected. The Cf capacitance has been the most accurate one. It has obtained DTP values that have been under 1 but very close to it. Those values did not vary significantly for the different WD ratios employed, maintaining them quite constant in every WD ratio. The Ci capacitance has also acquired precise results but less accurate than the ones for the Cf capacitance. The obtained DTP values for Ci have been around 0.71 and they have experimented a small increase while the WD ratio get bigger. The Co capacitance has reached the less accurate results and has been the most affected one by the WD ratio changes. For a WD ratio of 0.25 the DTP has been 2.6 and while the WD ratio has become bigger, the DTP values have been improved until reaching 1.74 for a WD ratio of 4.

The acquired DTP results for the heavy structured building (Figure 26) have been different from the ones reached in the light structured building. In this case, the noticed impact for the three capacitances with the WD ratio changes has been smaller than in the light building. As it has occurred in the light building the Cf results have been the most precise ones. In this case the DTP values have been above 1 and they have experimented a small precision increase until the middle WD ratio (WD ratio equal to 1, when the building has a square base geometry). For this WD ratio, the Cf capacitance has reached its major precision point with a DTP value of 1.17. Then, the DTP has started to grow with the increases of the WD ratio. The Ci capacitance has obtained very constant DTP values. Those have been around 0.6 in every WD ratio. Finally, as it has occurred in the light structured building, the Co capacitance has been the less accurate. It has begun with a DTP of 0.27 for a WD ratio of 0.25. Then, their DTP values have decreased with the WD ratio increase until reaching a DTP of 0.19 for a WD ratio of 4.

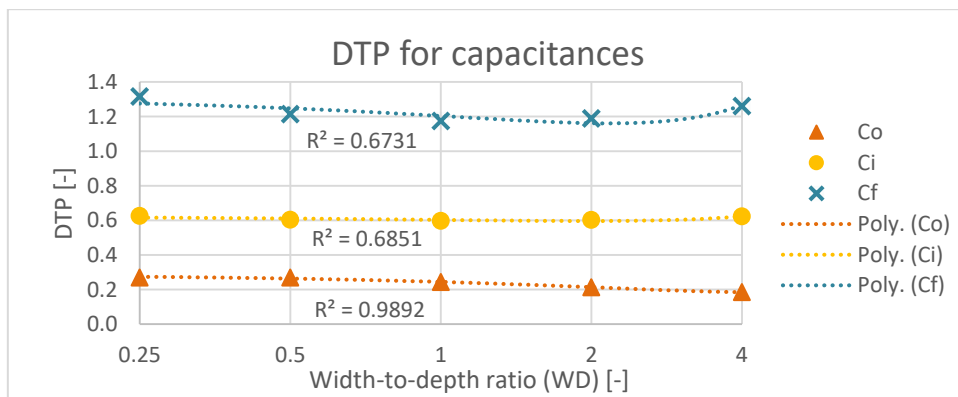


Figure 26: DTP of capacitances for different WD in 100_X_15_0 heavy structured buildings.

5.3. CHANGING THE WINDOWS-TO-FLOOR SURFACE RATIO (WF)

In this section, it will be studied the impact that changes in the windows-to-floor surface (WF) ratio (proportion between the total windows surface and the floor surface) have over the 4R3C model's components (resistances and capacitances). In order to have a realistic analysis, the WF ratio will vary from 5% to 30%, where the chosen steps will be 5%, 10%, 15%, 20% and 30%.

In the present study, the acquired results in both types of buildings (light structured and heavy structured) will be analysed and compared. Furthermore, in order to have a simpler analysis, a standard building of 100m² with a WD ratio of two and an OA of 0° will be employed for studying the impact of the WF ratio.

As it has been explained previously, the windows surface of each wall will keep the same proportion in all the studied cases. In order to make it clearer, the following table (Table 10) presents the obtained windows surfaces on each wall in the studied building (100_2_X_0).

WF [%]	5	10	15	20	30
Front wall window surface [m ²]	2.50	5.00	7.50	10.00	15.00
Right wall window surface [m ²]	1.25	2.50	3.75	5.00	7.50
Left wall window surface [m ²]	1.25	2.50	3.75	5.00	7.50
Back wall window surface [m ²]	0	0	0	0	0
TOTAL windows surface [m ²]	5	10	15	20	30

Table 10: Windows surfaces on each wall for different WF ratios in 100_2_X_0 light and heavy structured buildings.

An important aspect that must be taken into consideration is the influence of the WF ratio on opaque envelope. This ratio affects the total opaque envelope surface. When the WF ratio gets bigger, the total surface of the opaque walls decreases, decreasing the total surface of the opaque envelope. Therefore, the proportion of the opaque walls over the floor surface will be also reduced.

The reached precision values on the fitting proportion on the internal temperature (Ti) between the 4R3C model approximation (Matlab) and the real data (the one provided by TRNSYS) are represented on Table 11. As it can be noticed, the fitting proportion has been over the 80% in every studied situation in both types of buildings, which is a good value.

WF [%]	5	10	15	20	30
Light Ti fit. [%]	82.47	82.73	82.62	82.29	80.97
Heavy Ti fit. [%]	81.84	82.34	82.52	82.40	80.65

Table 11: Percentage of fitting on the internal state Ti between the 4R3C model approximation (Matlab) and the real data (TRNSYS) for different WF values in 100_2_X_0 light and heavy structured buildings.

After having analysed the fitting proportion of the internal temperature (Ti), the first components of the 4R3C model to be studied will be the thermal resistances. In the Figure 27 there are displayed the obtained DTP results for resistances of the light structured buildings and in the Figure 28 there can be noticed the acquired results for the heavy structured building.

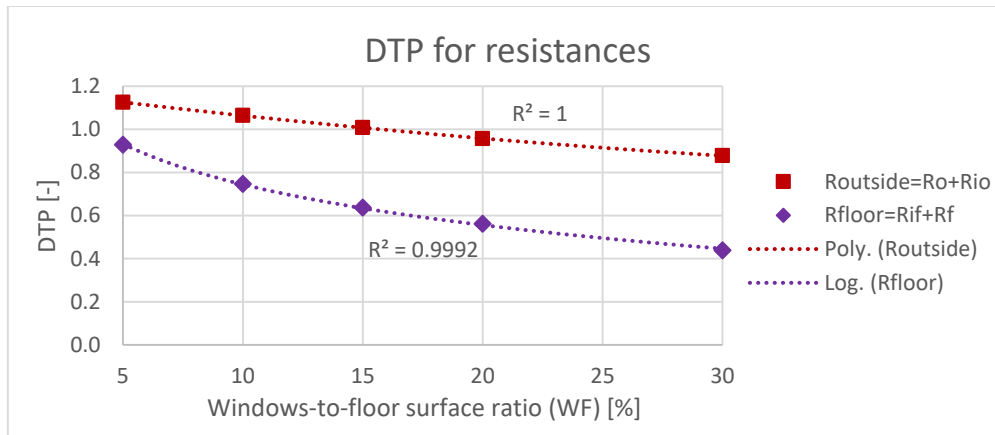


Figure 27: DTP of resistances for different WF in 100_2_X_0 light structured buildings.

As the Figure 27 reflects, the resistances have experimented some impact with the WF ratio parameter, especially the Rfloor resistance. The Routside resistances have been the most precise ones in the light structured building. It has begun with a DTP value of 1.13 for a WF ratio of 5% and these DTP values have fallen down while the WF ratio increases until reaching a DTP of 0.88 for a WF ratio of 30%. The most accurate result has been the one acquired for a WF ratio of 15%, where the DTP has had a value of 1.01. For this resistance, a polynomial function of second degree has been the one that better describes the DTP behaviour, where its R² coefficient has a value of 1. The Rfloor resistance, as it has occurred in all the simulated light structured buildings, has been less precise than the previous resistance. Its DTP value has decreased with the WF ratio increase and a logarithmic function has been the curve that better represents its behaviour. As it has been explained, the most accurate result has been the one obtained for the smaller WF ratio (when WF ratio is equal to 5%) with a DTP value of 0.93, which is quite accurate.

As it can be perceived from the Figure 28, the resistances DTP tendencies for the different WF ratios in the heavy structured buildings have been the same that the ones analysed for the light structured building. The tendency curves have a similar shape, but, their positions inside the graph and consequently the achieved values have been different. The Routside resistance has been around a DTP value of 0.8. It has begun for a WF of 5% with a DTP value of 0.87 and then, it has decreased its DTP values with the WF ratio increments until acquiring a DTP of 0.74 for a WF ratio of 30%. The Rfloor resistance has been also precisely represented by a logarithmic curve where the accuracy has been reduced for the bigger WF ratios. As its tendency curve shows, the most precise values have been the ones obtained for a WF ratio between 5% and 10%. Therefore, it has been proved that resistances of the heavy structured buildings are affected on their precision by the WF ratio.

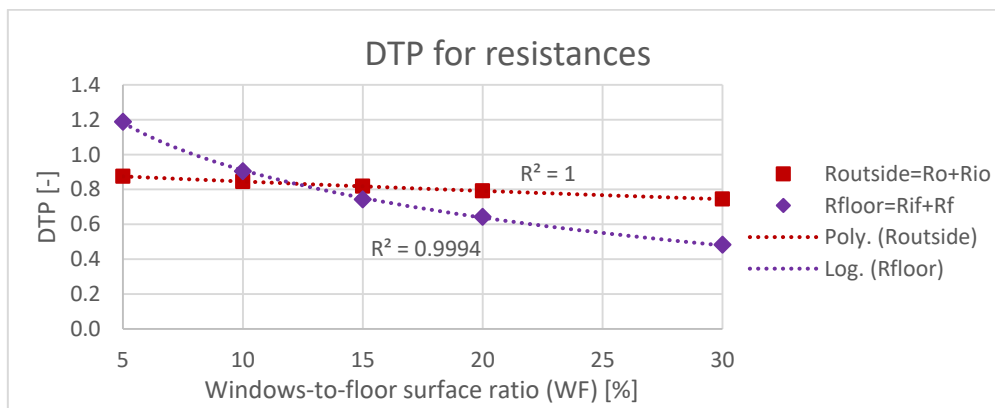


Figure 28: DTP of resistances for different WF in 100_2_X_0 heavy structured buildings.

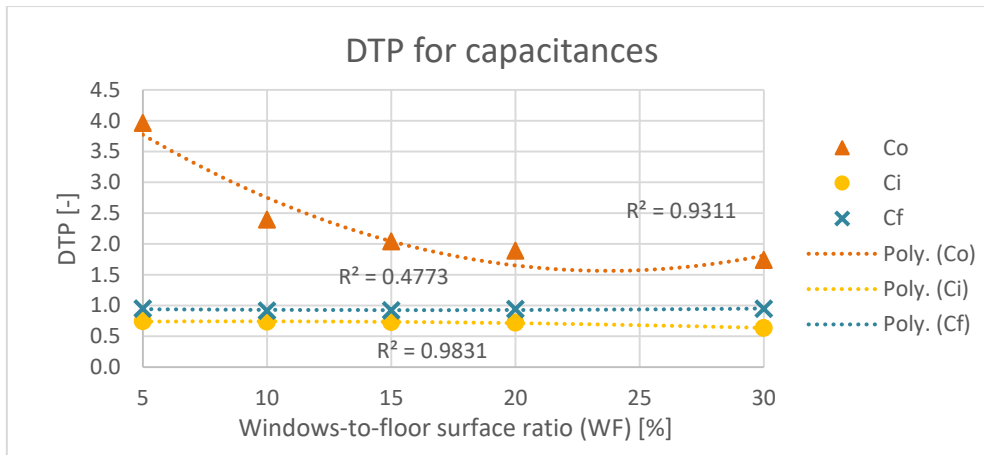


Figure 29: DTP of capacitances for different WF in 100_2_X_0 light structured buildings.

As the Figure 29 reflects and as it has been observed over the rest of the analysis, the Cf and Ci capacitances have been the most precise ones in the light structured building. It can be also noticed that both capacitances (Cf and Ci) have not been influenced by the different WF ratios. They have obtained very constant results in all the tested WF ratios. For the case of the Cf capacitance, the DTP has been next to 0.95 and in the case of the Ci capacitance it has been around 0.73. The Co capacitance has been the most imprecise one. It has been affected notoriously by the WF ratio changes. For the smallest tested WF ratio value (5%) the DTP has almost reached a value of 4. Then, in each WF ratio increment the DTP value has got closer to 1. In the last WF ratio (30%), this capacitance has reached its most accurate result by acquiring a DTP value of 1.74. For all the capacitances, the best fitting curves have been the ones that are formed by a second-degree polynomial function.

The results for the heavy structured buildings have been different from the ones achieved in the light structured building. In this case the three capacitances have been quite constant in all the simulated WF ratios. Therefore, the WF ratio did not have any relevant impact on the precision of the capacitances. In this case, as it has occurred in the light building, the most precise results have been the ones acquired for the Cf capacitance, followed by the Ci capacitance and with the Co capacitance as the less accurate one. The Cf capacitance has experimented a small precision increase. For a WF ratio of 5% it has reached a DTP of 1.3. Then the DTP has been established close to a DTP of 1.2. The Ci capacitance have been the most constant ones with all their values near a DTP of 0.6. The results for the last capacitance (Co) have suffered from a minimal precision decrease. It has begun with a DTP of 0.3 (for a WF ratio of 5%) and then it has been reduced until establishing a value around 0.2.

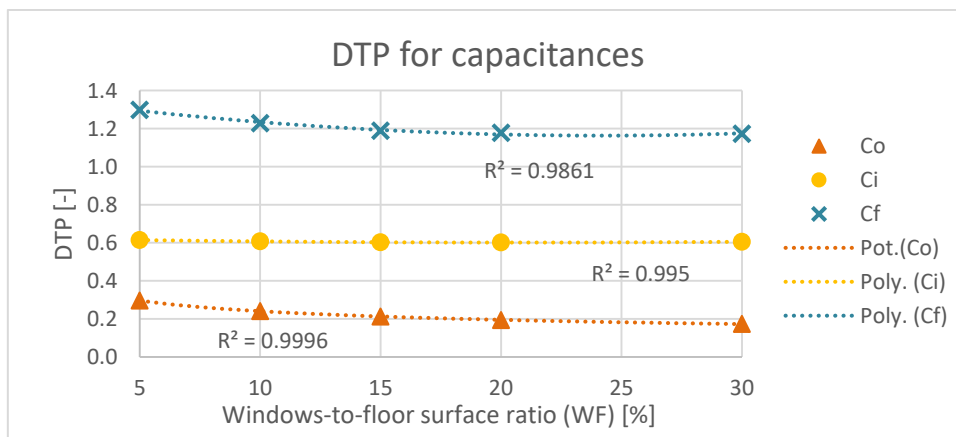


Figure 30: DTP of capacitances for different WF in 100_2_X_0 heavy structured buildings.

5.4. CHANGING THE ORIENTATION ANGLE (OA)

The present section will present the influence that the orientation angle (OA) parameter has over the 4R3C model's components (resistances and capacitances). For this study, the buildings orientation will vary from 0° to 180°. In a building where the OA has a value of 0°, the front wall (the one that has the bigger windows) will be facing the south while the wall without windows will have a north orientation. The chosen steps for the OA have been the followings: 0°, 45°, 90°, 135° and 180°.

In this analysis the light structured and heavy structured buildings with a heated surface of 100m² with WD ratio of two and a WF ratio of 15% will be simulated.

On Table 12 there can be observed the obtained precision values on the fitting proportion on the internal temperature (Ti) between the 4R3C model approximation (Matlab) and the real data (the one provided by TRNSYS). In all the simulated buildings the fitting proportion has been over the 80% which is an accurate result.

OA [°]	0	45	90	135	180
Light Ti fit. [%]	82.62	83.07	82.21	81.96	81.98
Heavy Ti fit. [%]	82.52	82.40	82.19	81.79	81.53

Table 12: Percentage of fitting on the internal state Ti between the 4R3C model approximation (Matlab) and the real data (TRNSYS) for different OA values in 100_2_15_X light and heavy structured buildings.

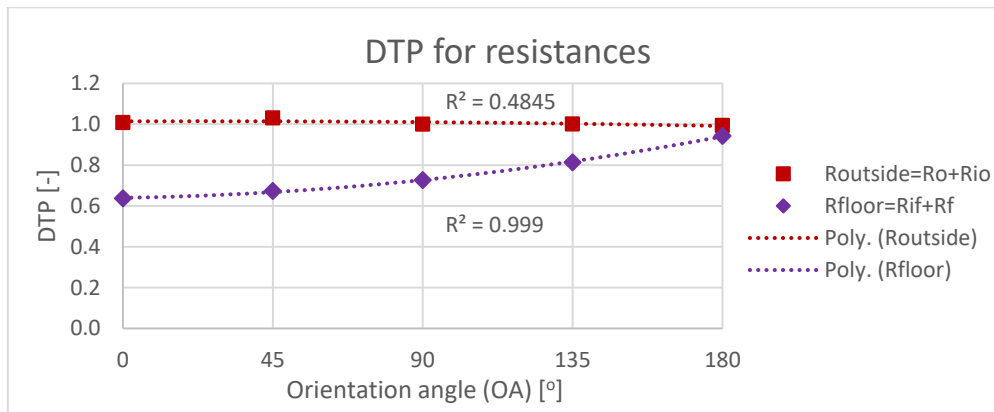


Figure 31: DTP of resistances for different OA in 100_2_15_X light structured buildings.

The Figure 31 shows the DTP results with the OA variations for the resistances of the light structured building. As the figure reveals, the Routside resistance has been really precise and it has not been notoriously impacted by the OA changes. All its values have been around a DTP of 1 and they did not suffer any remarkable variation. The Rfloor resistance has had a different behaviour from the one shown in the Routside resistance. In this occasion, the Rfloor resistance has suffered a visible impact with the OA variations. It has begun (for an OA of 0°) with a DTP value of 0.64. The precision has been improving in every OA increment until acquiring a DTP of 0.94 for an OA of 180°. For both resistances, a second-degree polynomial function has been the one that better describes the observed tendency.

When the obtained results for the resistances of heavy structured buildings (Figure 32) are observed, it can be observed that they got some similarities with the results of the light structured buildings. As it has happened in the Routside resistance in the light structured building, the Routside resistance of the heavy structured building has almost not been impacted by the OA variations. It has achieved DTP results that have been close to 0.8 in every tested OA. The tendency of the Rfloor resistance of the heavy structured building has been similar to the one observed in the light structured building. It has

begun (for an OA of 0°) with a DTP of 0.74. Then with each OA increase the DTP value has increased until obtaining a DTP of 1.27 for an OA of 180°. As the used polynomial curve shows, the most accurate result for the Rfloor resistance will be the one obtained for an OA between 90° and 135°.

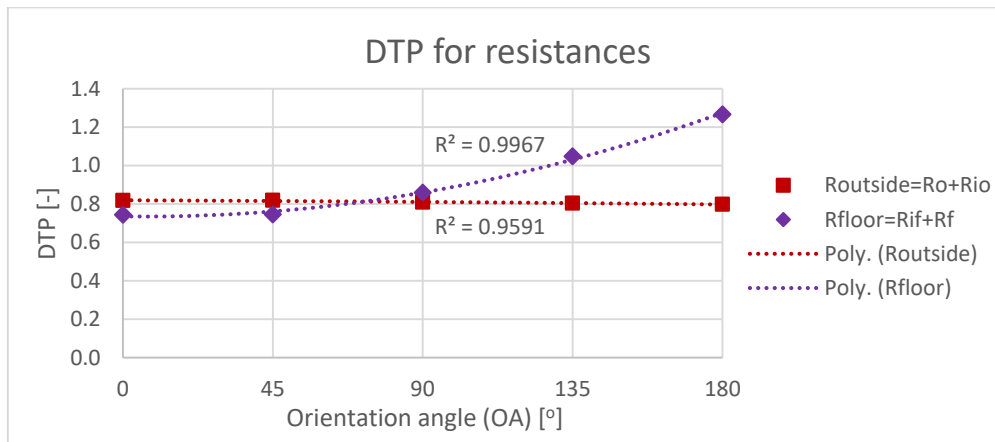


Figure 32: DTP of resistances for different OA in 100_2_15_X heavy structured buildings.

Once having analysed the results of the resistances, the following step is to analyse the behaviour of the capacitances. For that objective, the obtained results are displayed in Figure 33 (for light structured buildings) and in Figure 34 (for heavy structured buildings).

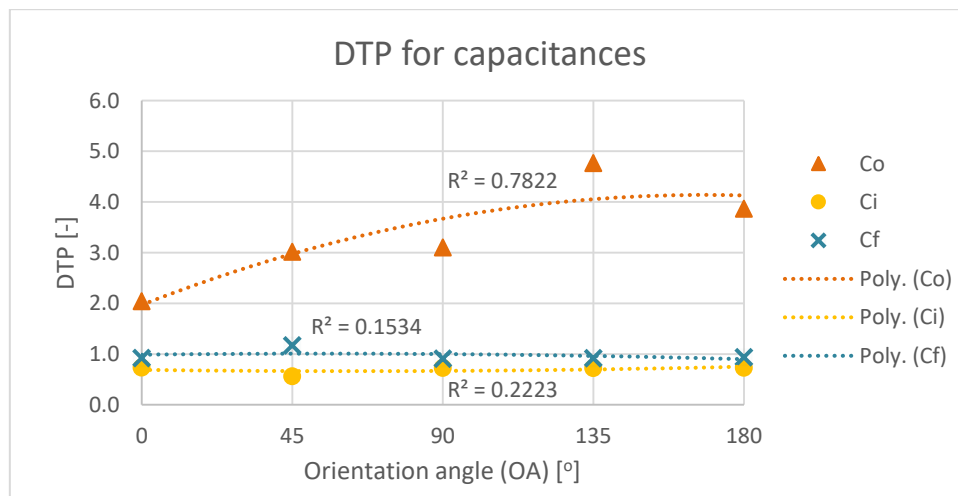


Figure 33: DTP of capacitances for different OA in 100_2_15_X light structured buildings.

As Figure 33 reflects, the Ci and Cf capacitances have been barely impacted by the OA changes while the Co capacitances have been notably affected. Moreover, as it has been occurring in all this master thesis, the Cf capacitance has been the most accurate one of the light structured building followed by the Ci capacitance and with the Co capacitance in the last place. The Cf capacitance has acquired DTP values that have been around 0.92 in all the tested situations. There is an exception on the DTP results for an OA of 45°, where the DTP has been 1.17. The same thing has happened to the Ci capacitance. All its DTP have been close to 0.73 except from the one acquired for an OA of 45° where the DTP has decreased to 0.56. As it has occurred in all the studies, the results for the Co capacitance have been very unprecise. In all the situations the DTP has been over 2 and it has got bigger with the OA increments.

The situation of the capacitances of the heavy structured buildings (Figure 34) has been different from the one observed in the light structured building. In general, these

capacitances have been less impacted by the OA changes. The Cf capacitance has been again the most precise one. It has had DTP values that have been close to 1.2. With the increment of the OA the DTP values have got bigger (1.19 for an OA of 0° and 1.26 for an OA of 180°). The Ci capacitance has been the less affected one by the OA changes. It has obtained DTP values that have been near 0.6 in all the tested OA. Finally, as it has occurred in the light structured building, the Co capacitance has been the less accurate one and the most affected one by the OA variations. It has begun with a DTP value of 0.21 (for an OA of 0°) and it has improved its precision in all the OA increments until reaching a DTP of 0.42 for an OA of 180°.

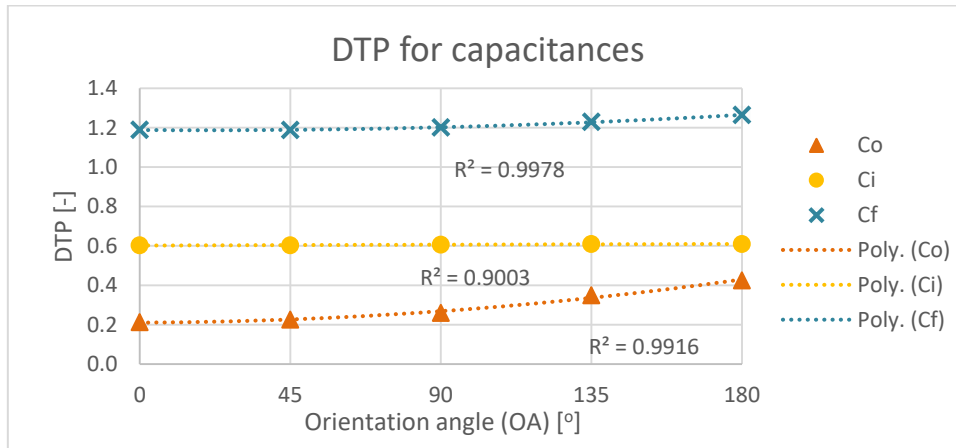


Figure 34: DTP of capacitances for different OA in 100_2_15_X heavy structured buildings.

5.5. COMBINING THE CHANGES

The first four sections of chapter 5 have studied individually the influence that changes in four different building’s parameters (FS, WD, WF and OA) have over the DTP of the components of the 4R3C model for light and heavy structured buildings. This study has been done using a building model with a 100m² FS, a WD ratio of two, a WF ratio of 15% and an OA of 0° (100_2_15_0). However, in order to have wider perspective and a more consistent data, the study must consider a wider range of buildings with different configurations.

In the present section, the impact of the previously mentioned four parameters (FS, WD, WF and OA) will be studied over the 4R3C models components for a wider range of building configurations. As a goal of the thesis, the study will analyse and compare the achieved results in light and heavy structured buildings in order to find the proper correlation for each model’s component accordingly to the four parameters. The Table 13 shows the buildings configurations (for light and heavy structured buildings) that have been simulated to obtain the data to carry out the study. It must be noticed that in Table 13 the OA has not been represented. Nevertheless, every building configuration has been simulated for all the OA (0°, 45°, 90°, 135° and 180°).

WD ratio [-]		0.25	0.5				1				2				4							
WF ratio [%]		5	10	15	20	30	5	10	15	20	30	5	10	15	20	30	5	10	15	20	30	
FS [m ²]	50		X	X	X	X	X	X	X	X	X	X	X	X	X	X						X
	75		X									X	X	X	X	X						X
	100		X				X	X	X	X	X	X	X	X	X	X						X
	150		X				X	X	X	X	X	X	X	X	X	X						X
	200		X				X	X	X	X	X	X	X	X	X	X						X

Table 13: Representation of the buildings configurations (for light and heavy structured buildings) that have been studied. It has to take into account that the OA has not been represented in the table. However, all the displayed building configurations have been tested for all the OA (0°, 45°, 90°, 135° and 180°).

In order to have a global view of the impact, the changes in the four parameters have to be combined between each other. The fact of having four different parameters to observe their influence on the components DTP evolution, make impossible to represent all them in a two-dimensional plan. Therefore, the adopted solution will be to represent all the combined situations in several graphs.

In order to generate the graphs, the first step will be to choose the parameters that will be represented on it. The WF ratio seems to be the parameter that has the bigger impact on the components (resistances and capacitances) DTP. Due to this fact, it has been decided to display the DTP for different WF ratios on the same graph. Then, from the remaining parameters, the OA has been the one chosen to represent the components DTP evolution. The remaining parameters (FS and WD ratio) will vary from one graph to another.

Considering that five different FS and five distinct WD ratios have been studied, this generates 25 graphs per each 4R3C model's components (resistances and capacitances). As it has been explained, each graph will represent the DTP variation with OA for the different WF ratio. Those graphs are represented in the appendixes. The light structured buildings components are displayed from Appendix D to Appendix H. The ones for the heavy structured buildings are represented from Appendix I to Appendix M.

The following subsections will analyse individually, for light and heavy structured building, the next resistances and capacitors: Routside, Rfloor, Co, Ci and Cf. In each subsection the evolution of the DTP will be studied by analysing the variation of the four building's parameters: the floor surface (FS), the width-to-depth ratio (WD), the windows-to-floor surface ratio (WF) and the orientation angle (OA).

The present section will try to find the relationships that exist between the 4R3C model's components and the changes on the parameters (FS, WD, WF and OA). Nevertheless, this study serves as a guide. It attempts to explain which changes affect the components DTP and with which consequence. This could be used as a base for further studies on this subject.

5.5.1. RESISTANCE OF THE OUTSIDE ENVELOPE ($R_{OUTSIDE}=R_O+R_{IO}$)

The Appendix D and I compile the graphs with the DTP results for the Routside resistance for light and heavy structured buildings respectively. Those results will be employed to analyse the impact of the studied parameters (FS, WD, WF and OA) on the Routside resistance.

IMPACT OF THE OA

As it can be perceived from the graphs of the light structured building (Appendix D), the Routside's DTP has apparently had a linear evolution with the studied OA. In all the cases, the DTP has acquired results that have not varied significantly with the OA increments. However, as the Figure 35 and Figure 36 show, the linear tendency has not been that clear. As both figures reflect, the obtained R^2 values for a linear regression have not been as precise as it was expected. As it can be extracted from those representations, it seems that in the situations where WD ratio has a value of 1 (a squared building base) and the WF ratios of 10% and 20% brings the best results for a linear regression. Nevertheless, the acquired DTP values have been almost the same in each OA. Due to this fact, the small slope of the DTP values could be the reason that explains the obtained results with the linear regressions.

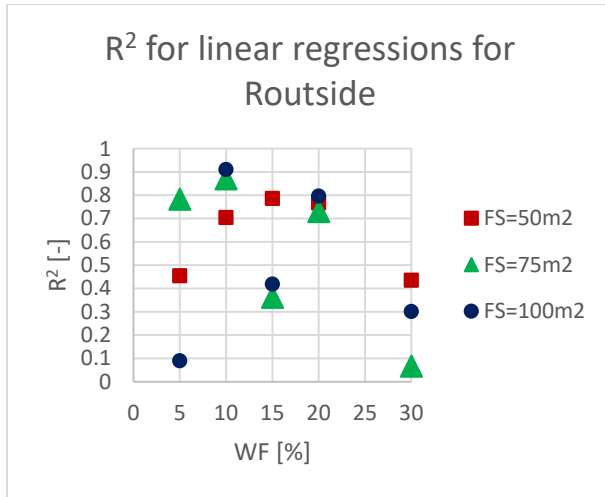


Figure 35: R² for linear regressions for Routside's DTP for light structured buildings with FS between 50m² and 100m² with a WD ratio of two for several WF ratios while the OA varies.

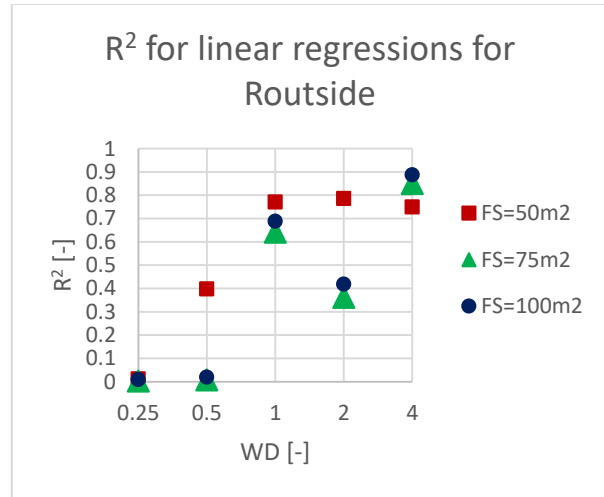


Figure 36: R² for linear regressions for Routside's DTP for light structured buildings with FS between 50m² and 100m² with a WF ratio of 15% for several WD ratios while the OA varies.

If the obtained results for the light structured building are compared with the ones achieved for the heavy structured building (Appendix I), there can be noticed some similarities. As it has occurred in the previous type of building, the DTP values have been very constant, experimenting few variations on each OA increment. This seems to coincide with a linear tendency. In order to prove it, the representations that have been done for the light building, have also been made for the heavy one. Those results are displayed on Figure 37 and Figure 38. As it can be perceived from those figures, the acquired results have been better than the previous ones achieved for the light structured buildings. In this occasion, the linear tendency has not have the same precision in all the situations. In the situations with a big FS (75m² and 100m²) the linear regression has obtained R² values that have been more precise than the ones achieved for the small FS. As the results show, the best coincidence with a linear regression has been reached for the buildings with a WD ratios between 2 and 4 and with big values for the WF ratio.

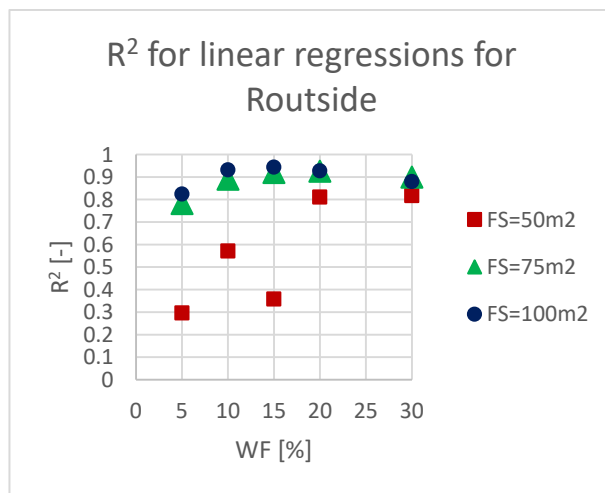


Figure 37: R² for linear regressions for Routside's DTP for heavy structured buildings with FS between 50m² and 100m² with a WD ratio of two for several WF ratios while the OA varies.

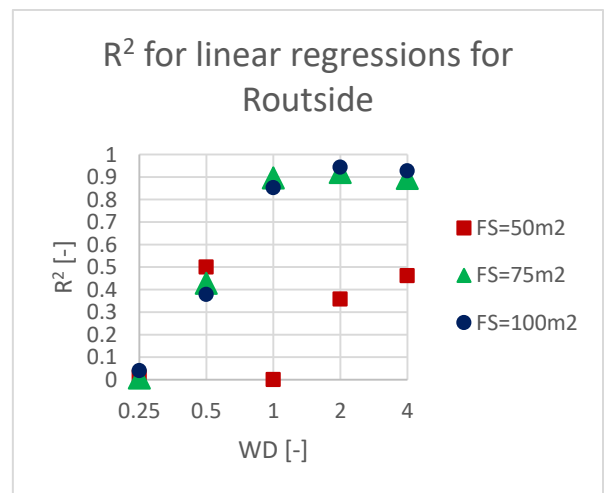


Figure 38: R² for linear regressions for Routside's DTP for heavy structured buildings with FS between 50m² and 100m² with a WF ratio of 15% for several WD ratios while the OA varies.

IMPACT OF THE WF

In the present subsection the influence of the WF ratio on the Routside's DTP evolution will be analysed. The light structured building will be the first one to analyse. The DTP results for this type of building have revealed an existing relationship with the WF ratio. The highest values for the DTP have been the ones acquired for the smallest WF ratios. Then, the DTP has decreased its value in each WF ratio increment. This tendency can be observed in the Figure 39.

Then when the DTP results for the heavy structured buildings are studied, there can be observed that they have the same tendency that the light structured buildings. The highest and most accurate DTP values have been obtained with the smallest WF ratio. In addition, the DTP has decreased its value and precision in each WF ratio augmentation (see Figure 40). The differences between those types of buildings reside on the DTP values. In the case of the heavy building, all the DTP values have been under 0.92 and in the case of the light structured buildings, in some configurations the DTP has reached values that have been above 1.

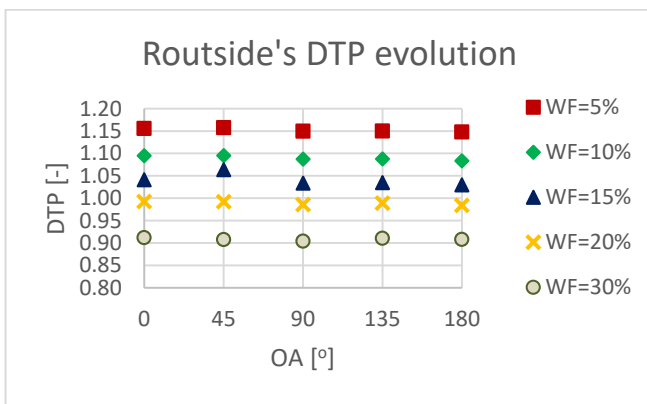


Figure 39: Routside's DTP evolution for 75_2_X_Y light structured building.

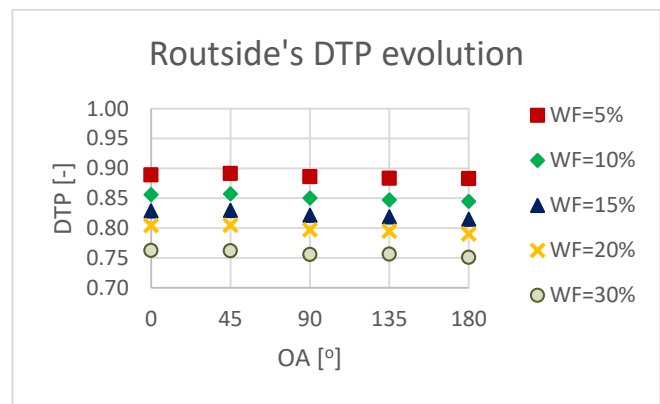


Figure 40: Routside's DTP evolution for 75_2_X_Y heavy structured building.

IMPACT OF THE WD

When the influence of the WD ratio is analysed for the light structured building, there can be observed a particular aspect. It has been shown that the biggest DTP values are the ones achieved for the WD ratios of 0.25 and 4. Then the DTP decreases symmetrically until achieving the smallest value for a WD ratio of 1 (WD ratios of 0.5 and 2 have similar DTP values). This relation can be appreciated on Figure 41.

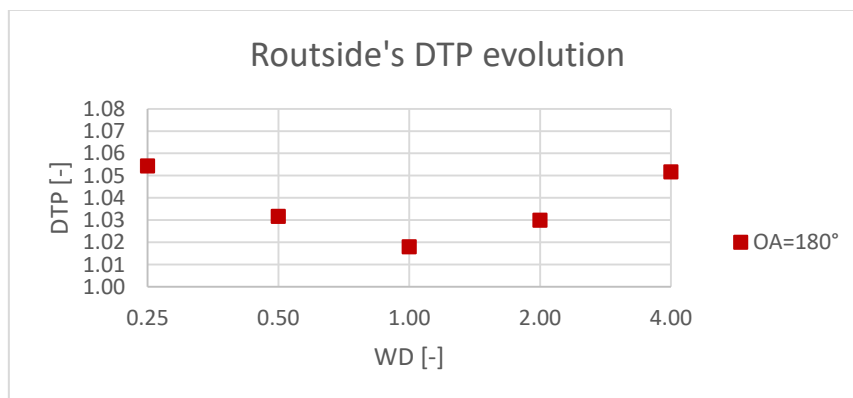


Figure 41: Routside's DTP evolution for 75_X_15_180 light structured building.

The case of the heavy structured buildings is different from the one observed in the light building. In this case the WD ratio did not impact the Routside's DTP. The acquired DTP values have not varied with the WD ratio changes.

IMPACT OF THE FS

When the DTP results for Routside resistance of the light structured building are observed, it can be appreciated a clear impact from the FS. The highest DTP values are obtained for the smallest FS (when FS has a value of 50m²). Then, with each FS increase the DTP decreased its values. The smallest DTP values are acquired for the biggest FS (200m²). This behaviour can be noticed in Figure 42.

The tendency on the heavy structured building is essentially the same as the one shown in the light structured building (Figure 43). The DTP reduces its value in each FS increment. The difference between both types of buildings resides in the total DTP decrease suffered from the smallest FS to the biggest one. The total DTP reduction has been bigger on the light structured building.

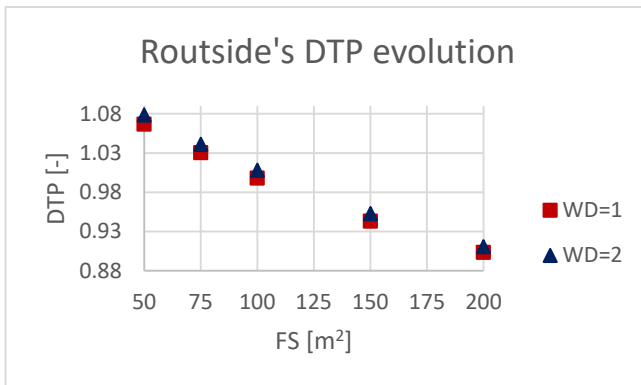


Figure 42: Routside's DTP evolution for X_Y_15_0 light structured building.

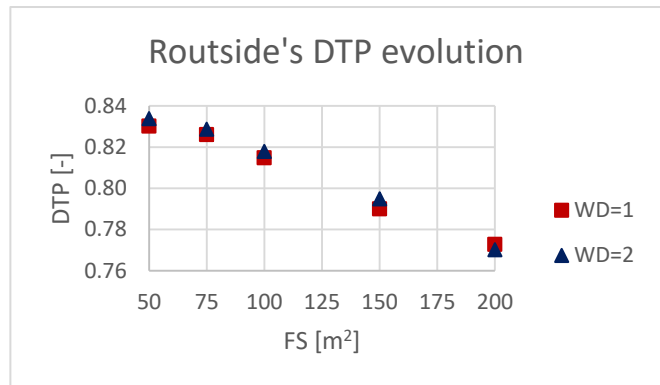


Figure 43: Routside's DTP evolution for X_Y_15_0 heavy structured building.

5.5.2. RESISTANCE OF THE FLOOR ($R_{FLOOR}=R_{IF}+R_F$)

Appendix E and J gather the achieved DTP results for the Rfloor resistance, where the first appendix contains the results for the light structured buildings and the second one the ones for the heavy structured buildings.

IMPACT OF THE OA

Firstly the acquired DTP results for the light structured building will be analysed. As those results reflect, the DTP values of the Rfloor resistance tend to get bigger with the OA increments. In comparison with the results of the Routside resistance, the obtained values have suffered a bigger impact. The difference between the DTP value for an OA of 0° and the DTP value for an OA of 180° (maintaining the same FS, WD ratio and WF ratio) has reached a maximum value of 0.51. In the case of the Routside resistance, this difference has been between 0 and 0.01 in the majority of the cases (where the maximum difference has reached a value of 0.17).

The DTP values of the Rfloor resistance in the case of the heavy structured building have had a similar behaviour as the one shown in the light building. As it has happened in the previous type of building, the DTP has incremented its value in each OA increase. Moreover, the difference between the DTP value for the smallest OA and the biggest OA (0° and 180° respectively) have been bigger than the one obtained for the Routside resistance.

IMPACT OF THE WF

When the impact of the WF ratio on the Rfloor resistance is studied, it can be noticed through the simulated data that the behaviour of the DTP has been very similar to the one shown in the Routside resistance. In both types of buildings (light and heavy structured buildings) the DTP's tendency has been similar. The highest values of DTP have been acquired for the smallest WF ratio (5%). Then, in every WF ratio increase the

DTP has become smaller. This can be observed in Figure 44 (light structured building) and in Figure 45 (heavy structured building).

In this occasion, both types of buildings have obtained DTP values that have been above 1 (in previous case for the Routside resistance in a heavy structured building, those values have been under 0.92).

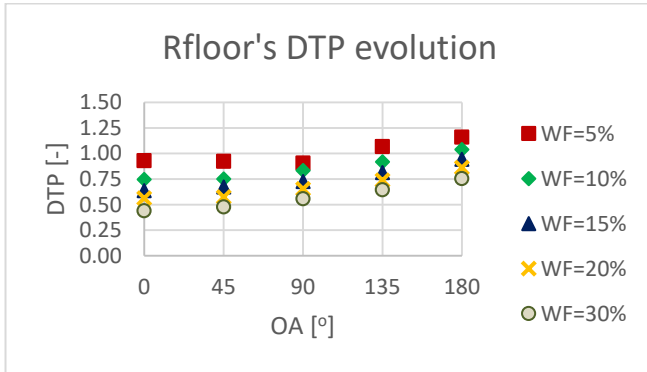


Figure 44: Rfloor's DTP evolution for 100_2_X_Y light structured building.

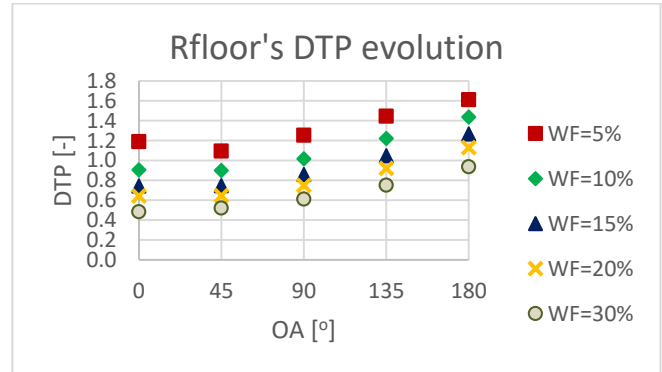


Figure 45: Rfloor's DTP evolution for 100_2_X_Y heavy structured building.

One remarkable aspect from the obtained DTP results for the Rfloor resistance of the heavy structured buildings is the achieved result for the 50_05_15_180 building. This building has acquired an anomalous DTP value of 8.46 which has not had any explainable correlation.

IMPACT OF THE WD

When the impact of the WD ratio over the Rfloor's DTP is analysed, it can be shown that the DTP's behaviour has been different from the one observed in the Routside resistance.

If the results for the light structured building are studied, there can be appreciated the tendency that is represented on Figure 46. As it can be observed, the influence on the Rfloor resistance's DTP by the WD ratio is also linked with the OA. For each OA, the WD ratio produces a different behaviour on the Rfloor's DTP. For the smaller OA (0° and 180°) the DTP tends to decrease in every WD ratio increment. In the case of the middle OA (90°), the Rfloor resistance maintains its DTP values approximately constant in each WD ratio increase. Finally, for the bigger OA (135° and 180°) the DTP increases its value with the WD ratio increments.

The case for the heavy structured buildings is also similar to the one observed in the light structured building. The DTP is affected by the WD ratio changes and the way in which they affect the DTP is determined by the OA (Figure 47).

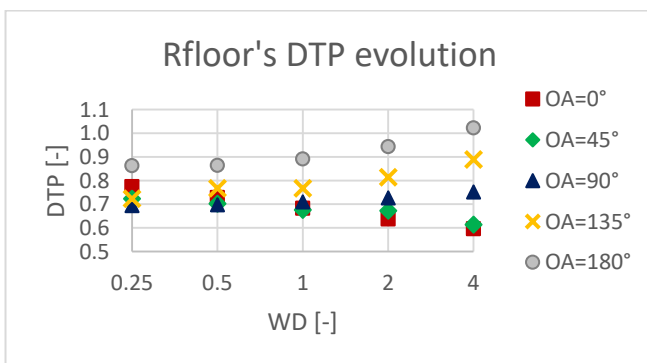


Figure 46: Rfloor's DTP evolution for 100_X_15_Y light structured building.

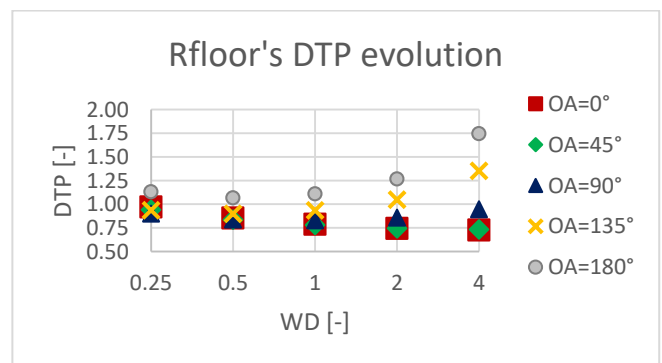


Figure 47: Rfloor's DTP evolution for 100_X_15_Y heavy structured building.

IMPACT OF THE FS

In the present subsection the impact of the FS on the Rfloor resistance's DTP will be studied. In this occasion, the light and the heavy structured buildings Rfloor's DTP behave in a similar way. As Figure 48 (for light structured buildings) and Figure 49 (for heavy structured buildings) show, the DTP reaches its highest values for the smallest FS (50m²). Then, in each FS increase the Rfloor's DTP reduces its value until obtaining the smallest one for the biggest FS (200m²).

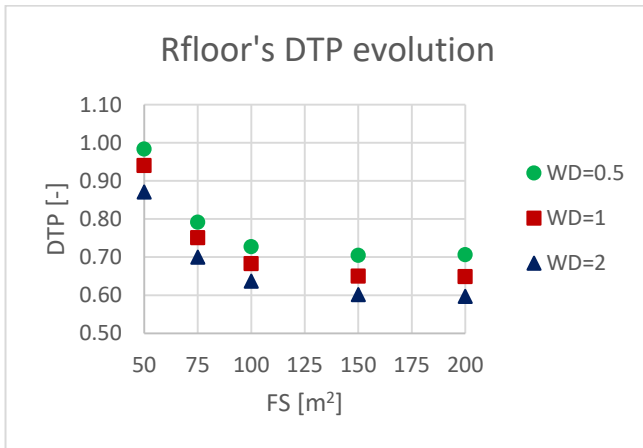


Figure 48: Rfloor's DTP evolution for X_Y_15_0 light structured building.

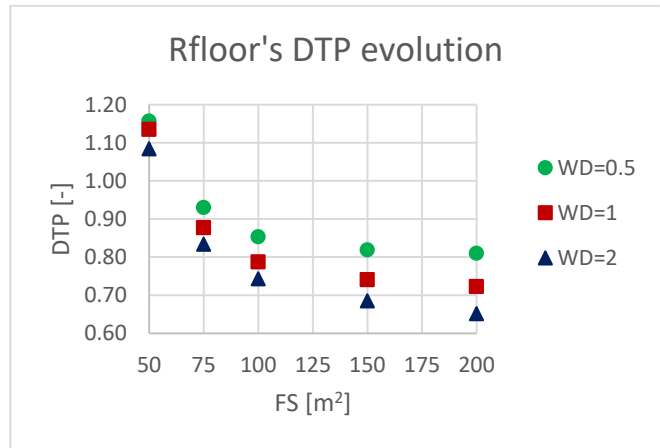


Figure 49: Rfloor's DTP evolution for X_Y_15_0 heavy structured building.

5.5.3. CAPACITANCE OF THE OUTSIDE ENVELOPE (Co)

The results for the Co capacitance of the light structured building are displayed on Appendix F while the ones acquired for the heavy structured one can be observed in Appendix K.

IMPACT OF THE OA

In the present subsection the influence of the OA on the Co capacitance's DTP evolution will be analysed. The first studied building will be the light structured one, whose results are located in Appendix F. As they reflect, their DTP tends to get higher values with the OA increments. In each type of building (with a specific FS, WD ratio and WF ratio) the smallest DTP value has been obtained for the smallest OA (0°) and its biggest DTP value has been obtained for biggest OA. If the DTP values are observed, it can be shown that those have been over 1.31 in all the simulated cases with a maximum value of 9.32. Those values have been much more imprecise than the ones achieved for the previous resistances (Routside and Rfloor).

Taking a look to the Co capacitance's DTP results for the heavy structured buildings (Appendix K), it can be noticed that the DTP behaves in a similar way to the previous one (light structured building). The DTP increases its values with the OA increments. The major difference between the DTP's of the heavy and light structured buildings resides in the rank of values. In the case of the heavy building, all the DTP's have been under 0.8 where the minimum has been 0.15.

IMPACT OF THE WF

When the influence of the WF ratio over the Co capacitance is studied for the light structured building, it has been noticed that the DTP behaviour with the WF ratio changes has been very similar to the one observed for the resistances. As Figure 50 reflects, the highest DTP values are obtained for the smallest WF ratios. Then, the DTP decreases its value with the increments of the WF ratio. There is an exception for an OA of 180°. For this particular OA the observed tendency is not that clear in all the simulated buildings.

By observing the data for the heavy structured building, it has been seen that the Co capacitance's DTP behaves like the Co's DTP for the light structured building. As Figure 51 reflects, the biggest DTP values are acquired for the smallest WF ratio and they are reduced with the WF ratio increases. Furthermore, the anomaly for the OA of 180° is still present in the heavy structured buildings.

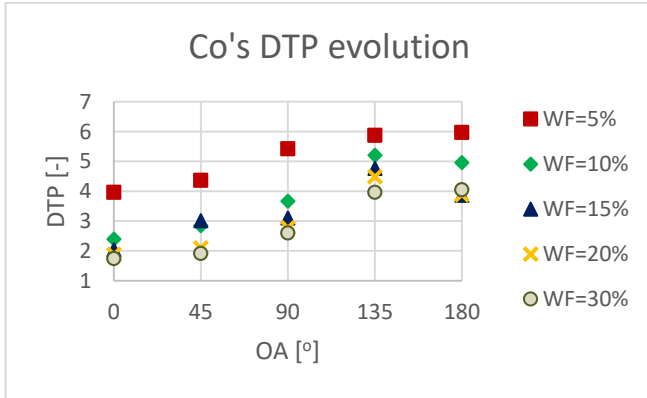


Figure 50: Co's DTP evolution for 100_2_X_Y light structured building.

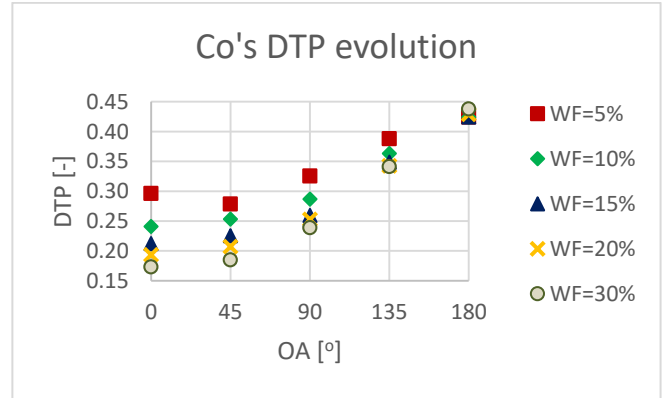


Figure 51: Co's DTP evolution for 100_2_X_Y heavy structured building.

IMPACT OF THE WD

As it can be perceived from the graphs of the light structured building (Appendix F), the Co's DTP is impacted by the WD ratio. Furthermore, the influence of the WD ratio acts differently depending on the OA. This influence is reflected in Figure 52. As it shows, for an OA of 0° the Co's DTP decrease with the WD ratio increases. In the case of an OA of 45°, the DTP approximately maintains its values constant with a small increase with the WD ratio increments. Finally, in the resting OA the DTP increases with the WD ratio increase.

The situation of the heavy structured building is similar to the one observed in the light structured building. In this case, as the Figure 53 shows, the DTP descending behaviour is hold for the OA of 0° and 45°. Then, the situation where the DTP maintains constant values is hold for an OA of 90°. For the rest of the OA, the DTP increases its value with the WD ratio increase.

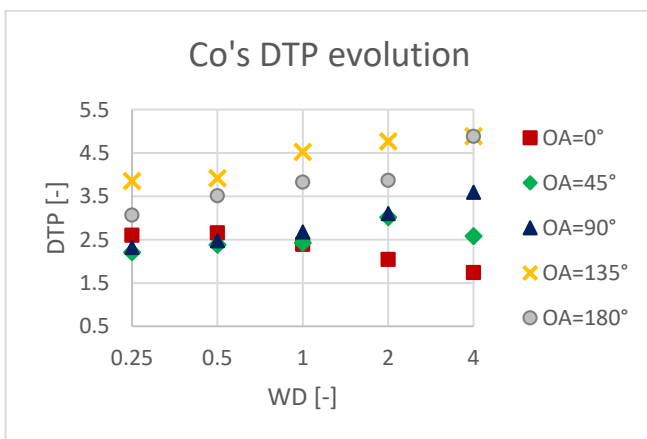


Figure 52: Co's DTP evolution for 100_X_15_Y light structured building.

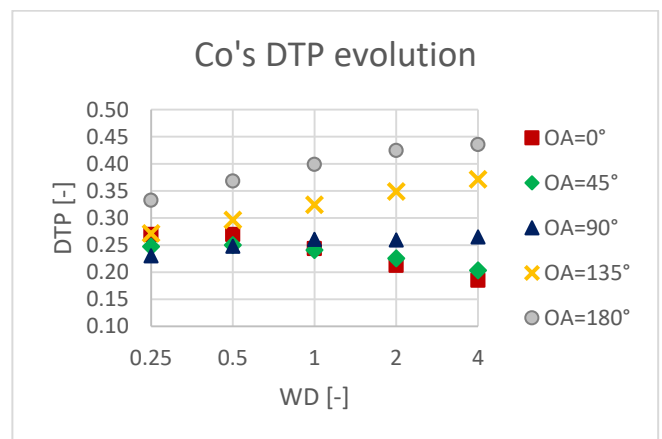


Figure 53: Co's DTP evolution for 100_X_15_Y heavy structured building.

IMPACT OF THE FS

When the influence of the FS over the Co capacitance is studied, it can be observed that for light structured and for heavy structured buildings the impact of the FS parameter is the same. As Figure 54 (for light structured buildings) and Figure 55 (for

heavy structured buildings) show, the tendency is clear: the Co's DTP increase its value with the FS parameter increments. As it can be noticed, the smallest DTP values are acquired for the smallest FS (50m²) and the highest DTP values are reached for the biggest FS (200m²).

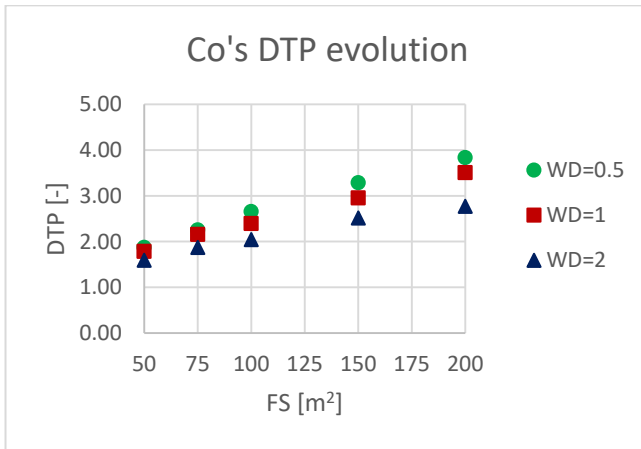


Figure 54: Co's DTP evolution for X_Y_15_0 light structured building.

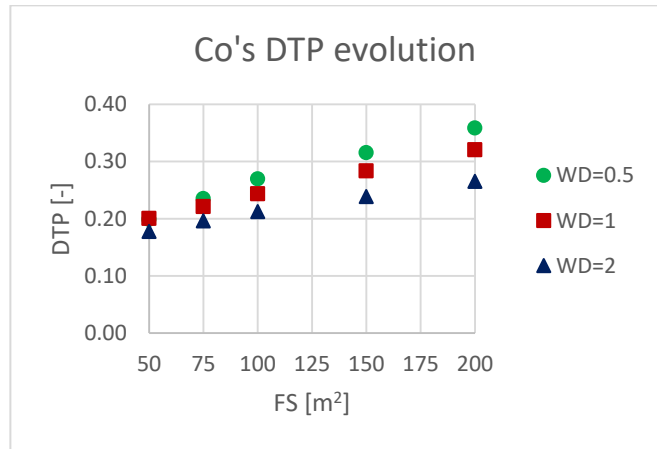


Figure 55: Co's DTP evolution for X_Y_15_0 heavy structured building.

5.5.4. INTERNAL CAPACITANCE (CI)

Appendix G compiles the obtained DTP results for the Ci capacitance of the light structured building while Appendix L collects the results for the Ci capacitance of the heavy structured building.

IMPACT OF THE OA

In this subsection the influence of the OA over the Ci capacitance's DTP values will be analysed. In the results for the light structured building (Appendix G) there can be noticed that the OA barely affects the Ci's DTP. In practically all the simulated buildings, for a specific FS, WD ratio and WF ratio the value of the Ci capacitance's DTP did not vary significantly. Furthermore, the acquired results have been quite accurate and in all the cases the DTP has been under 1. The highest DTP has reached a value of 0.91 while the smallest has been 0.55.

When the results for the heavy structured building are searched, the situation coincides with the one observed for the light structured building. The changes on the OA parameter practically did not have an impact on the DTP. The DTP has not varied its values with the OA changes. In this type of buildings (heavy structured ones) the reached precision has been smaller than in the light structured building. In the heavy buildings the DTP values have been between 0.51 and 0.68.

IMPACT OF THE WF

When the WF ratio's impact over the Ci capacitance's DTP values is studied, the same behaviour that have been observed in the rest of the 4R3C model's components has been shown in the Ci capacitance. The achieved results for the light and heavy structured buildings reveal that both types of buildings have a similar behaviour. As Figure 56 and Figure 57 reflect, the highest value for the DTP has been acquired for the smallest WF ratio. Then, each increasing step of the WF ratio has supposed a reduction on the DTP values. Due to this fact, the smallest DTP values have been obtained for the biggest WF ratio (30%). The major difference between the obtained results for light and heavy structured buildings is held on the existing differences between the DTP values for different WF ratios. In the case of the heavy building, those differences are smaller than in the light building.

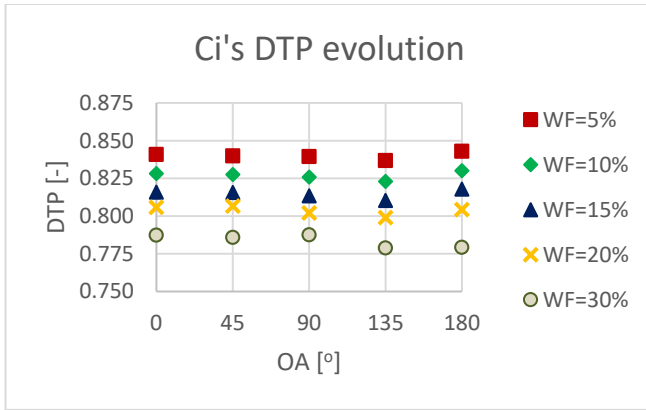


Figure 56: Ci's DTP evolution for 50_2_X_Y light structured building.

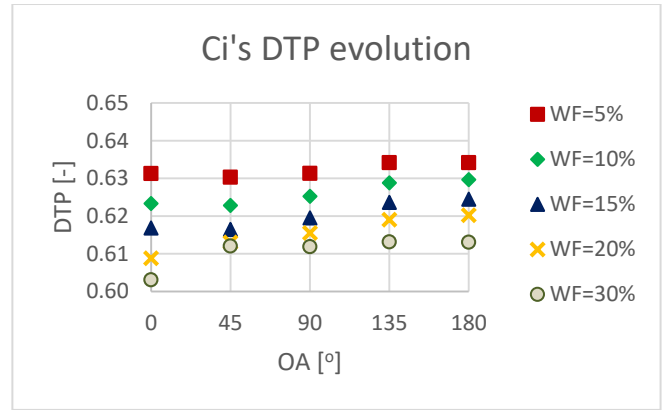


Figure 57: Ci's DTP evolution for 75_2_X_Y heavy structured building.

IMPACT OF THE WD

By analysing the data of the Ci capacitance for light and heavy structured buildings, it has been shown that both types of buildings have a similar impact with the WD ratio changes. The observed behaviour of the DTP has been practically the same. In addition, the regarded tendency has been the same as the one shown for the Routside resistance. As Figure 58 (for light buildings) and Figure 59 (for heavy buildings) reflect, the DTP variates with the WD changes in a symmetrical way. The highest DTP values have been acquired for the WD ratios of 0.25 and 4 with similar DTP values in both WD ratios. Then, for the WD ratios of 0.5 and 2 the DTP has decreased its values in an analogous proportion for both WD ratios. Finally, the smallest DTP values have been reached for a WD ratio of 1.

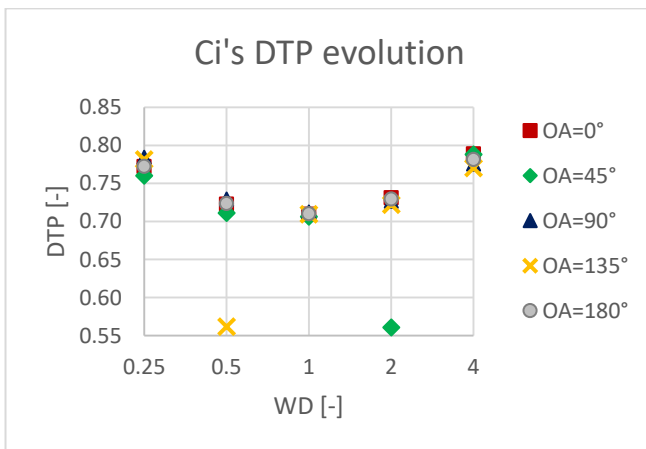


Figure 58: Ci's DTP evolution for 100_X_15_Y light structured building.

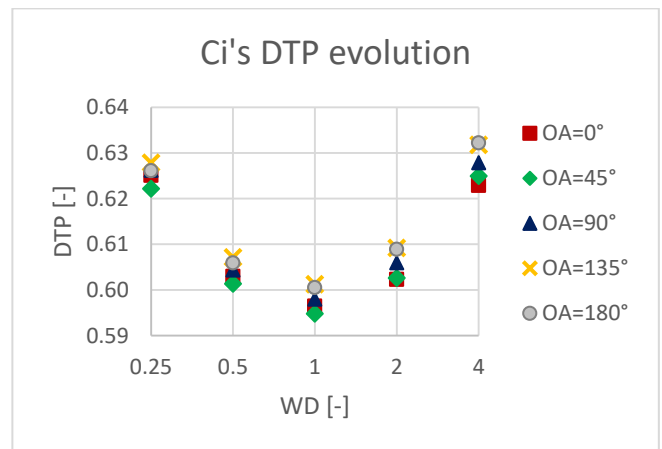


Figure 59: Ci's DTP evolution for 100_X_15_Y heavy structured building.

If the focus is pointed on Figure 58, there can be observed two anomalous values: the first one for a WD ratio of 0.5 and an OA of 135° and the second one for a WD ratio of 2 and an OA of 45°. Those values have been an exception. In the rest of the cases the behaviour of the DTP with the changes on the WD ratio has been the one described in the previous paragraph.

IMPACT OF THE FS

When the impact of the FS on the Ci capacitance's DTP values is studied, it can be observed that for both types of building (light and heavy structured buildings) the influence and the tendency have been the same. Furthermore, this tendency is the same as the one analysed on Routside and Rfloor resistances. The highest DTP values have

been achieved with the smallest FS (50m²). Then, in each FS increase the DTP has decreased its value until reaching the smallest one for a FS of 200m².

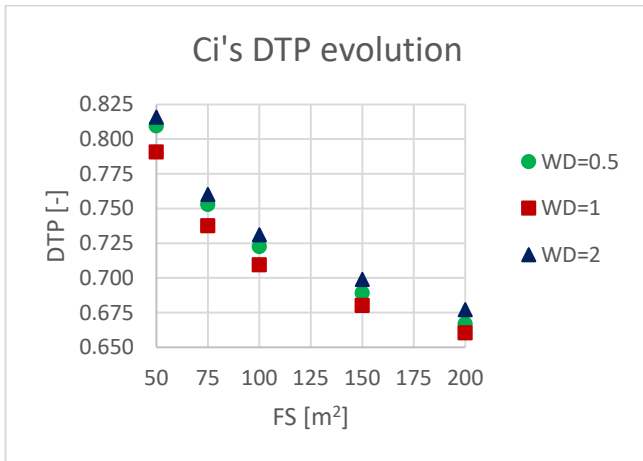


Figure 60: Ci's DTP evolution for X_Y_15_0 light structured building.

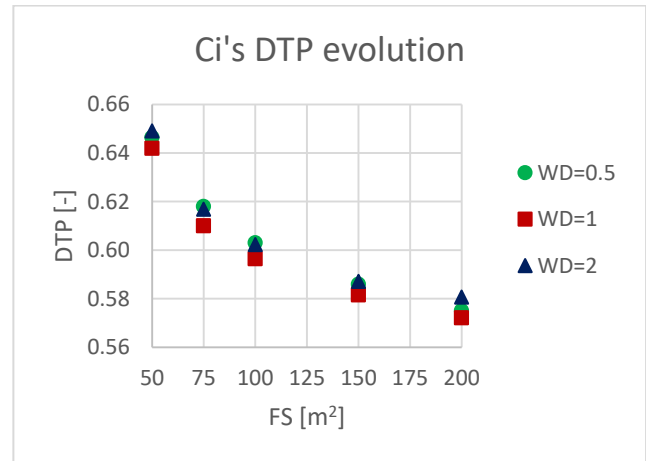


Figure 61: Ci's DTP evolution for X_Y_15_0 heavy structured building.

5.5.5. CAPACITANCE OF THE FLOOR (Cf)

The DTP results for the Cf capacitance are gathered in Appendix H and M. The first one has the results for the light structured building while the second one compiles the ones for the heavy structured building.

IMPACT OF THE OA

In this subsection the impact of the OA over the Cf capacitance's DTP values will be analysed. In the results for the light structured building (Appendix H) there can be noticed that the Ci's DTP has been affected by OA in a small proportion. The curve that the DTP forms with the increments of the OA seems to be horizontal. In some of the buildings the DTP has suffered a small increase with biggest OA.

In the case of the results of the heavy structured building (Appendix M), the impact has been similar to the one observed in the light structured buildings. In this occasion, it seems to be a small rise on the DTP value with the increment of the OA.

The DTP values in both buildings have been quite precise. In the case of the light structured building, the DTP has been between 0.78 and 1.35. In the other hand, the DTP of the heavy structured building have been always over 1, with all its values between 1.07 and 1.37.

IMPACT OF THE WF

When the influence of WF ratio on the Cf capacitance's DTP values is studied, it can be observed for both types of buildings (light and heavy structured buildings) that the impact has been the same as the ones observed in the rest of components of the 4R3C model. As it can be observed in Figure 62 (for light buildings) and on Figure 63 (for heavy buildings), the DTP decreases with the augmentation of the WF ratio. Due to this, the highest DTP values have been obtained for a WF ratio of 5% and the smallest ones have been acquired for a WF of 30%.

In the case of the light structured buildings, this tendency has not been that clear. As the Figure 62 shows, there have been some points where the previous tendency has not been applied.

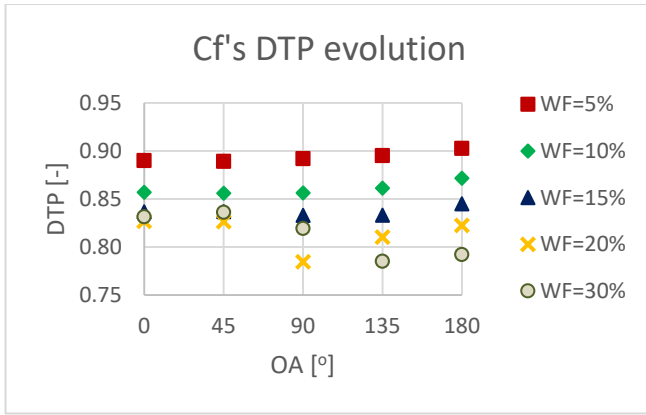


Figure 62: Cf's DTP evolution for 50_1_X_Y light structured building.

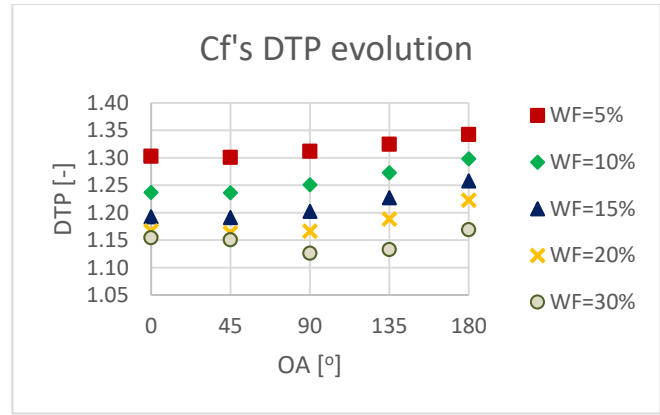


Figure 63: Cf's DTP evolution for 75_2_X_Y heavy structured building.

IMPACT OF THE WD

By studying the data of the Cf capacitance for light and heavy structured buildings, it has been observed that both types of buildings have an analogous influence with the WD ratio variations. The noticed tendency has been the same as the one shown for the Routside and Ci components. As Figure 64 and Figure 65 show, the WD changes causes a symmetrical evolution of the DTP values. The highest DTP values have been obtained for the WD ratios of 0.25 and 4, where the DTP in both WD ratios has had similar values. Then, for the WD ratios of 0.5 and 2 the DTP values have been reduced in a similar proportion for both WD ratios. Finally, the smallest DTP values have been acquired with a WD ratio of 1.

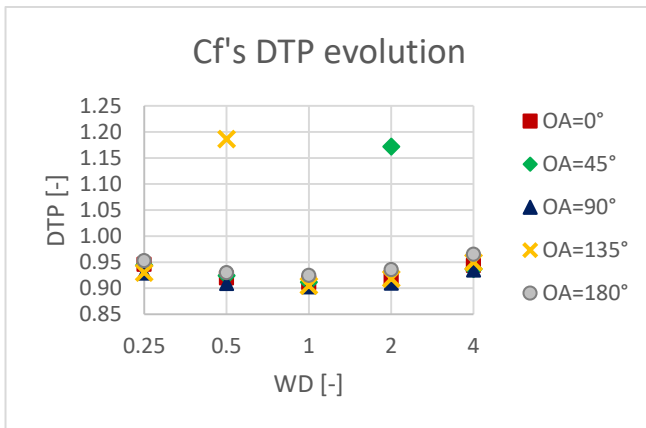


Figure 64: Cf's DTP evolution for 100_X_15_Y light structured building.

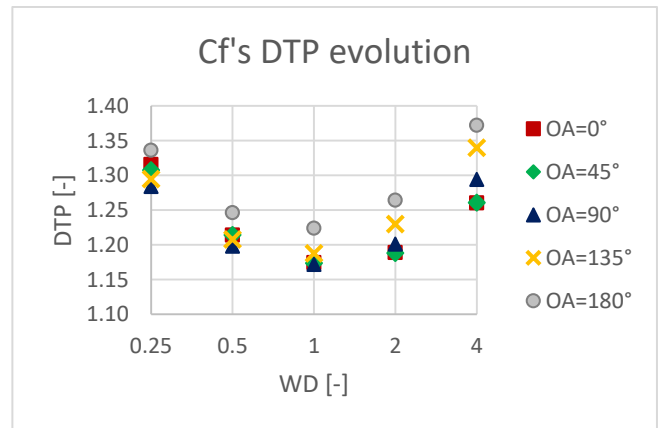


Figure 65: Cf's DTP evolution for 100_X_15_Y heavy structured building.

As it has occurred in the Ci capacitance for the light structured building, the Figure 64 shows two anomalous values that have been an exception.

IMPACT OF THE FS

When the results for the light structured building (Appendix H) are studied, there can be observed that the DTP values increases with the augmentation of the FS parameter. This tendency can be appreciated on Figure 66.

The situation of the heavy structured buildings is different. In this case, as Figure 67 reveals, the Cf's DTP decreases from the FS of 50m² to the FS of 75m². Then, the DTP begins to increase its value for the resting FS value increments. The final values for a FS of 200m² are a bit bigger than the ones obtained for a FS of 50m².

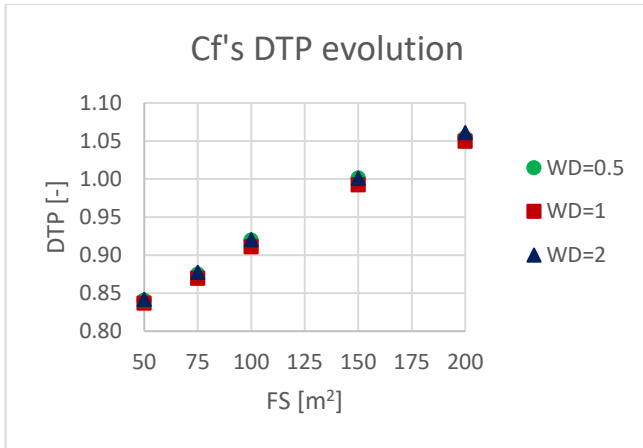


Figure 66: Cf's DTP evolution for X_Y_15_0 light structured building.

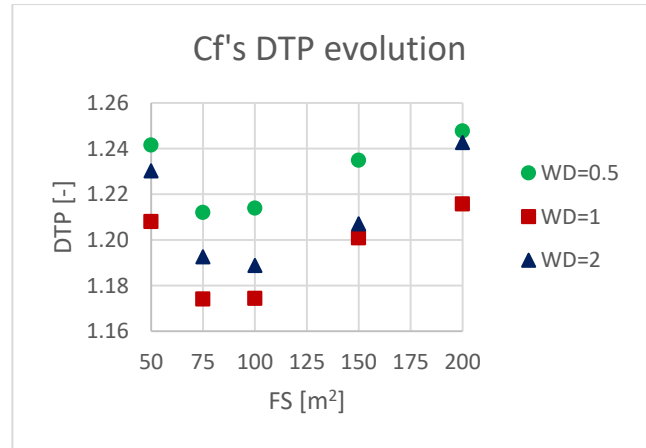


Figure 67: Cf's DTP evolution for X_Y_15_0 heavy structured building.

6. SIMULATION VERIFICATION

The simulations of light and heavy structured buildings of the present master thesis have been done by using a simulation period that corresponds to the first 1000 hours of the year. This chapter will serve to prove that the used simulation period is correct and to verify that the obtained results by using a bigger time period will be also right and accurate in the two types of buildings (light and heavy structured buildings) that have been studied.

In order to do the verification, a time period of a whole year has been selected (8760 hours). Moreover, the utilized building for light structured and heavy structured buildings will have the following characteristics: a floor surface (FS) of 100m², a width-to-depth ratio (WD) of two, a windows-to-floor surface ratio (WF) of 15% and an orientation angle (OA) of 0°.

The Table 14 displays the acquired results for both types of buildings with a simulation period of 8760 hours:

Parameters	Light structured building 100_2_15_0	Light structured building 100_2_15_0
Routside's DTP [-]	1.01	0.80
Rfloor's DTP [-]	0.64	0.87
Co's DTP [-]	3.60	0.25
Ci's DTP [-]	0.79	0.60
Cf's DTP [-]	1.21	1.37
Ti fitting [%]	87.03	89.36

Table 14: Obtained results for 100_2_15_0 light and heavy structured buildings in an 8760 hours simulation.

As the Table 14 shows, the achieved results for a year simulation period have been really precise in both types of buildings. In comparison with the previous simulations where the simulation period has a value of 1000 hours, the Ti fitting proportion has increased its value around a 5% in both buildings. Furthermore, the obtained values of DTP for the components of the 4R3C model have been close to the ones achieved in the previous simulations.

As the results reflect, the used model brings very good results for a year simulation period. Therefore, due to the obtained results, it can be concluded that the used model and its time period are correct.

CONCLUSIONS

The present master thesis has been done within the frame of the RESIZED project at the Department of Thermal Engineering and Combustion at the Faculty of Engineering of the University of Mons. It forms part of a bigger research whose main objective consists in simulating the energy consumption and the thermal behaviour of a whole district composed by different typologies of buildings by utilizing simplified thermal models.

Based on the researches of Mr A. Bagheri and on the studied done by Ms Y. Touly, the present master thesis has been focused on the studying the behaviour of the 4R3C simplified model's components (resistances and capacitors) on the light structured buildings. In addition, those results have been compared with the ones achieved on heavy structured buildings.

In order to study the behaviour of the model, two different parameters have been observed. In one hand, it has been examined the fitting proportion on the building's internal temperature (T_i) between the "real" data (provided by TRNSYS software, which uses measuring data) and the one obtained through an optimization process (by using Matlab software). In the other hand, it has been analysed the relation that the 4R3C model's components have between the theoretically calculated values (by employing the building's physical characteristics) and the ones provided by an optimization process implemented in Matlab. The optimization process determines the most suitable values for the 4R3C model's components in order to reach the highest fitting proportion on the internal temperature (T_i) with the output that TRNSYS gives.

The first study of the present master thesis has been focused on analysing the impact of different heating loads and indoor conditions on the precision of the fitting proportion of the internal temperature (T_i) and on the 4R3C model's components. This study has revealed that the best results in light and heavy structured buildings are the ones achieved in situations where the building has a thermal heating system. Moreover, it has been observed that the simulations of buildings without any heating system brought less accurate results.

The second study has analysed the influence that changes on the buildings geometry and structure have over the 4R3C model's components. In this study it has been observed the impact of changes in four different parameters: the building's floor surface, the building's width-to-depth ratio, the building's windows-to-floor surface ratio and the buildings orientation angle. In order to study their impact, the used parameter has been the DTP (Determined/Theoretical Proportion). This parameter is referred to the acquired proportion between the values of the 4R3C model's components ($R_{outside}$, R_{floor} , C_o , C_i and C_f) determined by the optimisation process in Matlab and the theoretically calculated ones.

The first thing that this study has revealed is that both types of buildings are affected by changes on the buildings geometry and structure. The influence of each change has affected the 4R3C model's components results in different ways. In most of the cases, the components DTP behaviour can be described with good precision by using linear, logarithmic or second degree polynomial functions.

When the fitting proportion of the internal temperature (T_i) has been observed, it has been noticed that both types of buildings (light and heavy structured), with no matter on the analysed building's physical characteristics, have reached fitting proportion values that have been above the 80%, which are quite accurate results.

From a general point of view, both types of buildings have obtained DTP values for the resistances that have been more accurate than the capacitances ones. Between the 4R3C model's two resistances, the $R_{outside}$ has been the most precise one in both types

of buildings. However, if the achieved results for the Routside resistance between the two types of buildings are compared, the ones acquired for the light structured buildings have been the most accurate ones. Nevertheless, in the case on the Rfloor resistance the heavy structured building has obtained more precise results than the light structured building.

The capacitances have obtained less accurate results than the resistances. In both types of buildings the Cf capacitance has been the most precise one, followed by the Ci capacitance and with the Co capacitance as the less precise one. In the case of the Co capacitance, the obtained results for the heavy structured building have been the most accurate ones, while the ones reached on the light structured building have been very imprecise. Nevertheless, the situation with the other two capacitances has been different. In the case of the Ci and the Cf capacitances, the light structured building has been the one that has reached the best results. In addition, the obtained difference between the acquired precision for Co capacitance and the ones reached for Ci and Cf capacitances has been remarkable in both types of buildings.

There has also been done a verification of the utilized model. In order to do it, it has been realized a simulation of a whole year with the light and heavy structured buildings. This analysis has revealed that the used model is correct for the chosen period of time.

Finally, it can be concluded that the observations made from the studies done in this master thesis could serve as an initial guide for further researches on the subject of RC models. In addition, a further case of study could be centred on studying the buildings behaviour in different seasons of the year, in order to see how the model's components are affected by the different seasons.

BIBLIOGRAPHY

- [1] L.G. Swan, V.I. Ugursal, Modeling of end-use energy consumption in the residential sector: a review of modelling techniques, *Renew. Sustain. Energy Rev.* 13 (2009) 1819-1838. doi:10.1016/j.rser.2008.09.033.
- [2] R. Kramer, J. van Schijndek, H. Schellen, Simplified thermal and hygric building models: A literature review, *Front. Archit. Res.* 1 (2012) 318-325. doi:10.1016/j.foar.2012.09.001
- [3] F. Amara, K. Agbossou, A. Cardenas, Y. Dubé, S. Kelouwani, Comparison and simulation of building thermal models for effective energy management, *Smart Grid Renew. Energy.* 6 (2015) 95-112. doi:10.4236/sgre.2015.64009.
- [4] A. Bagheri, V. Feldheim, D. Thomas, C. S. Ioakimidis, Coupling building thermal network and control system, the first step to smart buildings, 2016 IEEE International Smart Cities Conference (ISC2) (2016) 1-6. doi: 10.1109/ISC2.2016.7580820.
- [5] O. T. Ogunsola, L. Song, Application of a simplified thermal network model for a real-time thermal load estimation, *Energy and buildings* 96 (2015) 309-318. doi: 10.1016/j.enbuild.2015.03.044.
- [6] G. Fraisse, C. Viardot, O. Lafabrie, G. Achard, Development of a simplified and accurate building model based on electrical analogy, *Energy Build.* 34 (2002) 1017-1031. doi: 10.1016/S0378-7788(02)00019-1.
- [7] Y. Touly, Study of the impact of changes in a building's geometry and envelope on its 4R3C model's components, Master Thesis, 2017.
- [8] A. Bagheri, Literature review and developing a simplified thermal network of a building, First committee, 2016.
- [9] A. Bagheri, V. Feldheim, D. Thomas, C. S. Ioakimidis, The adjacent walls effects in simplified thermal model of buildings, *Energy Procedia* (Vol. 122) (2017) 619-624. doi: 10.1016/j.egypro.2017.07.359
- [10] A. Bagheri, V. Feldheim, C. S. Ioakimidis, On the evolution and application of the thermal network method for energy assessments in buildings, *Energies.* 11(4) (2018). doi: 10.3390/en11040890
- [11] S. N. Al-Saadi, Z. Zhai, A new validated TRNSYS module for simulating latent heat storage walls. *Energy and Buildings.* 109 (2015) 274-290. doi: 10.1016/j.enbuild.2015.10.013
- [12] S. Schmidt, M. Lindauer, M. Hoppe, Comparing TRNSYS and WUFI ® plus simulation models-illustrated on models validated on measurements at Schack-Gallery Munich. In 5th IBPC, Kyoto. (2012) 1143-1148.
Retrieved from: <https://mediatum.ub.tum.de/doc/1251331/1251331.pdf>

TABLE OF APPENDIXES

Appendix A: Physical characteristics of basic light structured building	- 69 -
Appendix B: Physical characteristics of basic heavy structured building	- 70 -
Appendix C: Modelling hypothesis used in TRNSYS modelling	- 71 -
Appendix D: Evolution of Routside's DTP in light structured buildings for different FS, WD, WF and OA	- 72 -
Appendix E: Evolution of Rfloor's DTP in light structured buildings for different FS, WD, WF and OA	- 73 -
Appendix F: Evolution of Co's DTP in light structured buildings for different FS, WD, WF and OA	- 74 -
Appendix G: Evolution of Ci's DTP in light structured buildings for different FS, WD, WF and OA	- 75 -
Appendix H: Evolution of Cf's DTP in light structured buildings for different FS, WD, WF and OA	- 76 -
Appendix I: Evolution of Routside's DTP in heavy structured buildings for different FS, WD, WF and OA	- 77 -
Appendix J: Evolution of Rfloor's DTP in heavy structured buildings for different FS, WD, WF and OA	- 78 -
Appendix K: Evolution of Co's DTP in heavy structured buildings for different FS, WD, WF and OA	- 79 -
Appendix L: Evolution of Ci's DTP in heavy structured buildings for different FS, WD, WF and OA	- 80 -
Appendix M: Evolution of Cf's DTP in heavy structured buildings for different FS, WD, WF and OA	- 81 -

APPENDIX A – PHYSICAL CHARACTERISTICS OF BASIC LIGHT STRUCTURED BUILDING

The Table 15 brings the physical characteristics of the roof, walls, windows and floor of the light structured building used for the study.

Wall type	Layer (inside --> outside)	Physical properties	
ROOF	Mineral Wool	Thickness [m]	0.15
		Conductivity [W/m.K]	0.045
	Wood	Thickness [m]	0.02
		Conductivity [W/m.K]	0.12
Capacity [J/kg.K]		2500	
		Density [kg/m ³]	400
	Solar absorption coefficient [-]		0.75
LIGHT WALL	Plasterboard	Thickness [m]	0.01
		Conductivity [W/m.K]	0.331
		Capacity [J/kg.K]	801
		Density [kg/m ³]	790
	Composite	Thickness [m]	0.14
		Conductivity [W/m.K]	0.671
		Capacity [J/kg.K]	876
		Density [kg/m ³]	60.8
Glass wool	Thickness [m]	0.09	
	Conductivity [W/m.K]	0.041	
	Capacity [J/kg.K]	840	
	Density [kg/m ³]	12	
	Solar absorption coefficient [-]		0.6
WINDOWS	Glazing	U-value [W/m ² .K]	1.1
		Solar transmission coefficient [-]	0.609
	Frame	U-value [W/m ² .K]	1.8
FLOOR	Tiles	Thickness [m]	0.01
		Conductivity [W/m.K]	1.705
		Capacity [J/kg.K]	700
		Density [kg/m ³]	2300
	Cement mortar	Thickness [m]	0.08
		Conductivity [W/m.K]	1.4
		Capacity [J/kg.K]	1000
		Density [kg/m ³]	2000
Concrete	Thickness [m]	0.2	
	Conductivity [W/m.K]	2.1	
	Capacity [J/kg.K]	1000	
	Density [kg/m ³]	2400	
Polyurethane	Thickness [m]	0.16	
	Conductivity [W/m.K]	0.03	
	Capacity [J/kg.K]	837	
	Density [kg/m ³]	35	
INTERIOR WALL	CAR_PL_70	Thickness [m]	0.07
		Conductivity [W/m.K]	0.351
		Capacity [J/kg.K]	801
		Density [kg/m ³]	790
AIR + FURNITURE		Capacity factor [J/K.m ³]	2400

Table 15: Physical properties of the light structured building.

In Table 16 there can be observed the values of the thermal surface resistances used in TRNSYS and employed for the calculation of the building's thermal resistances.

	Heat Flux Direction		
	Ascending (roof)	Horizontal (walls)	Descending (floor in contact with the ground)
Rsi [m ² .K/W]	0.33	0.33	0.33
Rse [m ² .K/W]	0.06	0.33	0

Table 16: Values of the thermal surface resistances used for the calculation of the building's thermal resistances.

APPENDIX B – PHYSICAL CHARACTERISTICS OF BASIC HEAVY STRUCTURED BUILDING

The Table 17 brings the physical characteristics of the roof, walls, windows and floor of the heavy structured building used for the study. In Table 16 (displayed on Appendix A) there can be observed the values of the thermal surface resistances used in TRNSYS and employed for the calculation of the building's thermal resistances.

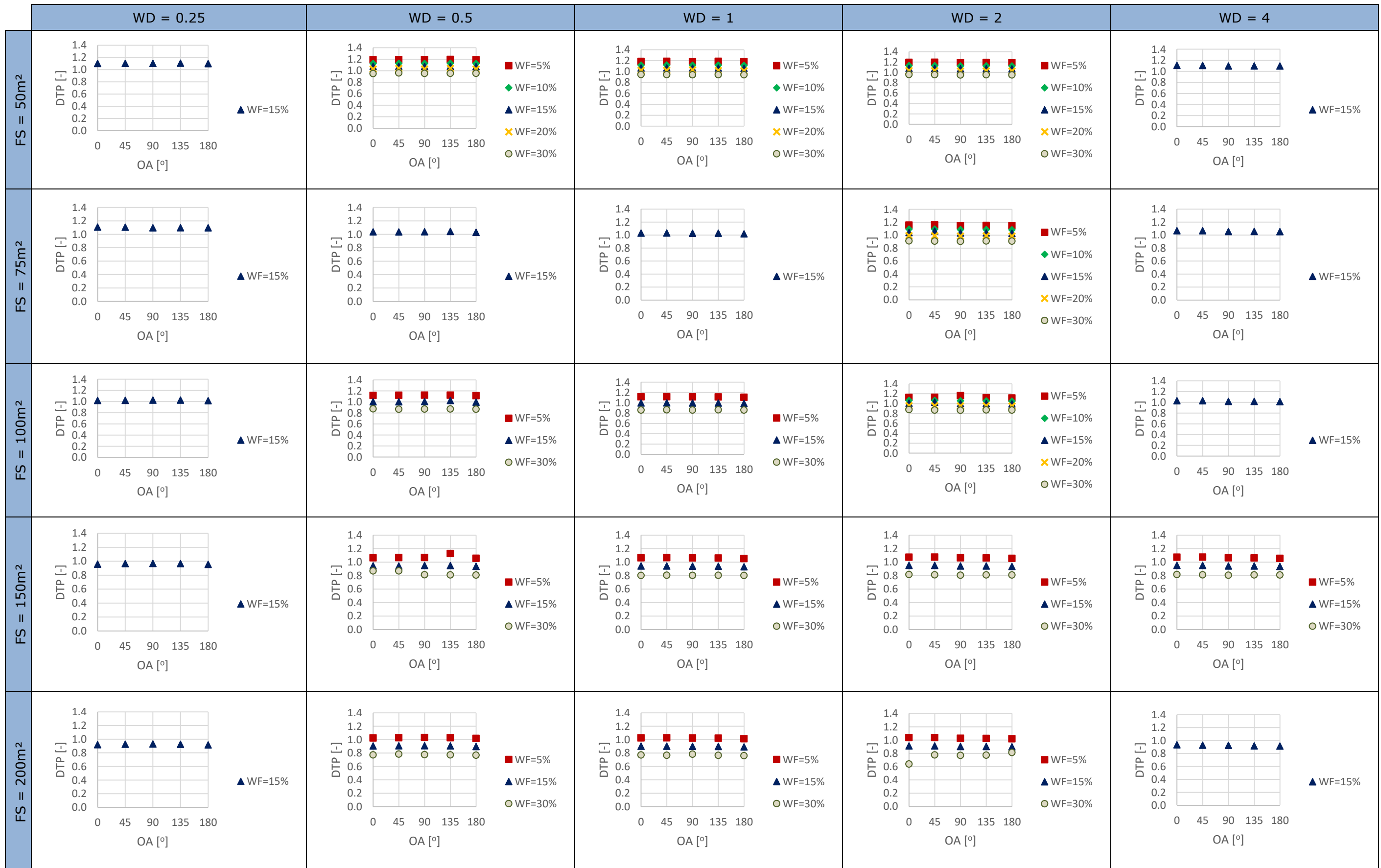
Wall type	Layer (inside --> outside)	Physical properties	
ROOF	Mineral Wool	Thickness [m]	0.15
		Conductivity [W/m.K]	0.045
	Wood	Thickness [m]	0.02
		Conductivity [W/m.K]	0.12
Capacity [J/kg.K]		2500	
		Density [kg/m ³]	400
	Solar absorption coefficient [-]		0.75
HEAVY WALL	Plaster	Thickness [m]	0.01
		Conductivity [W/m.K]	0.351
		Capacity [J/kg.K]	1000
		Density [kg/m ³]	1500
	Concrete blocs	Thickness [m]	0.2
		Conductivity [W/m.K]	1.053
		Capacity [J/kg.K]	650
			Density [kg/m ³]
Polystyrene expanded	Thickness [m]	0.16	
	Conductivity [W/m.K]	0.039	
	Capacity [J/kg.K]	1380	
		Density [kg/m ³]	25
Exterior coat	Thickness [m]	0.01	
	Conductivity [W/m.K]	1.153	
	Capacity [J/kg.K]	1000	
	Density [kg/m ³]	1700	
	Solar absorption coefficient [-]		0.6
WINDOWS	Glazing	U-value [W/m ² .K]	1.1
		Solar transmission coefficient [-]	0.609
	Frame	U-value [W/m ² .K]	1.8
FLOOR	Tiles	Thickness [m]	0.01
		Conductivity [W/m.K]	1.705
		Capacity [J/kg.K]	700
		Density [kg/m ³]	2300
	Cement mortar	Thickness [m]	0.08
		Conductivity [W/m.K]	1.4
		Capacity [J/kg.K]	1000
			Density [kg/m ³]
Concrete	Thickness [m]	0.2	
	Conductivity [W/m.K]	2.1	
	Capacity [J/kg.K]	1000	
		Density [kg/m ³]	2400
Polyurethane	Thickness [m]	0.16	
	Conductivity [W/m.K]	0.03	
	Capacity [J/kg.K]	837	
	Density [kg/m ³]	35	
INTERIOR WALL	CAR_PL_70	Thickness [m]	0.07
		Conductivity [W/m.K]	0.351
		Capacity [J/kg.K]	801
		Density [kg/m ³]	790
AIR + FURNITURE		Capacity factor [J/K.m ³]	2400

Table 17: Physical properties of the heavy structured building.

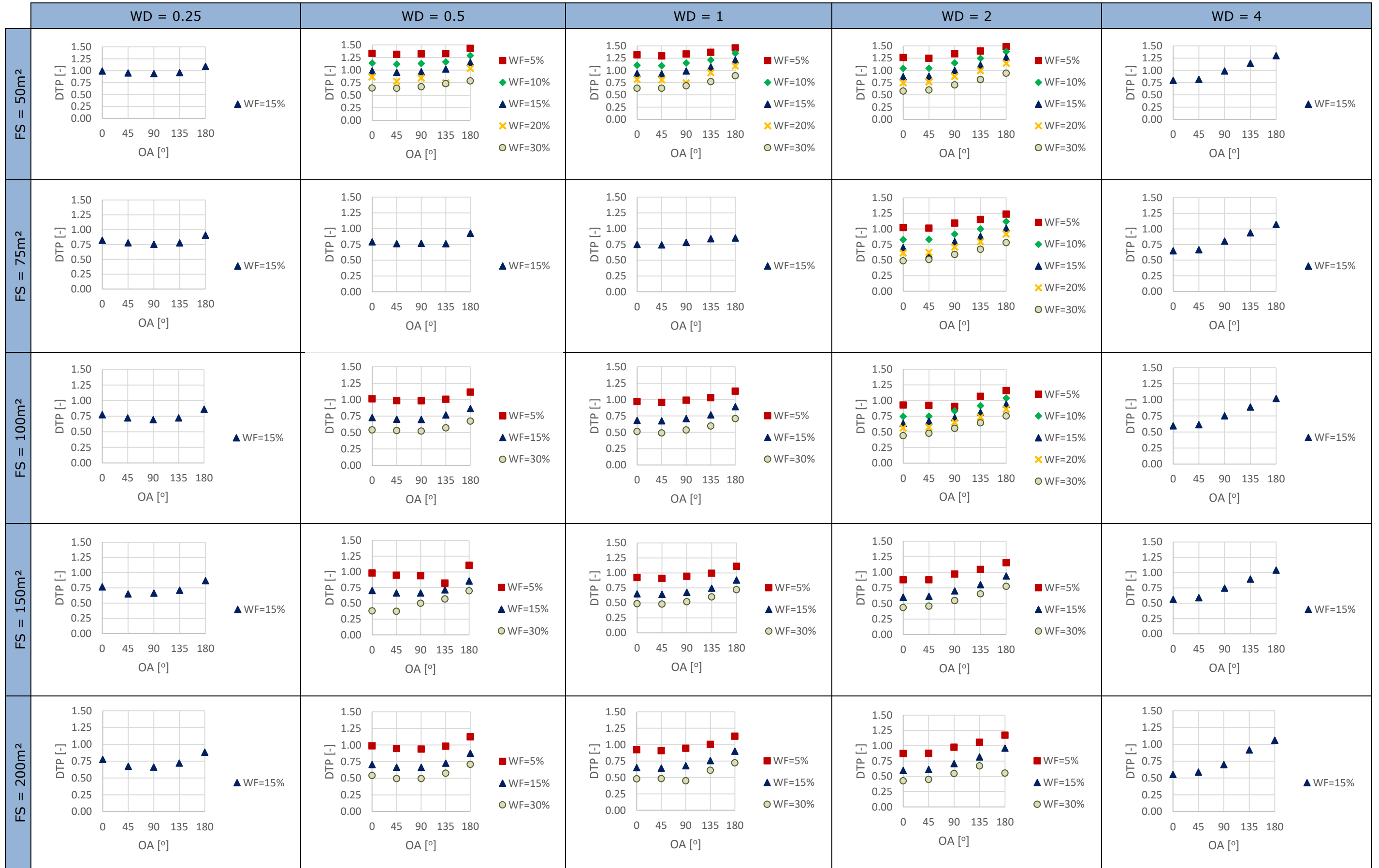
APPENDIX C – MODELLING HYPOTHESIS USED IN TRNSYS MODELLING

Weather data	Location:	Uccle (Belgium)		
Infiltration Type Manager				
	Infiltration Type :	LEAKY		
	Airchange of Infiltration :	0.24 /h		
Ventilation Type manager				
	Ventilation Type :	VENTMECH		
	AirFlow :	air change rate	S : 2*ROOM1+1	/h
	Temperature of Air Flow :	other :	20.00 °C	
	Humidity of Air Flow :	relative humidity		
		other :	50.00 %	
Heating Type Manager				
	Heating Type :	HEAT1		
	Room Temperature Control :	set temperature :	99999	°C
	Heating Power :	limited	S:10000*DAY1	kJ/h
	Humidification :	off		
Cooling Type Manager				
	Cooling Type :	COOL1		
	Room Temperature Control :	set temperature :	S : -	°C
	Cooling Power :	limited	5*ROOM1+33	0.00 kJ/h
	Dehumidification :	off		
Gain Type Manager				
	Gain Type :	GAIN_SP		
	Radiative Power :	0.00 kJ/h		
	Convective Power :	0.00 kJ/h		
	Abs. Humidity :	0.00 kg/h		
Comfort Type Manager				
	Comfort Type :	COMF001		
	Clothing Factor :	S : 1*ROOM1+1	clo	
	Metabolic Rate :	S : 1*ROOM1+1	met	
	External Work :	S : 1*ROOM1+1	met	
	Relative Air Velocity	S : 1*ROOM1+0.3	m/s	
Schedule Type Manager				
	Schedule Type	ROOM1		
		weekly	Monday	DAY1
			Tuesday	DAY1
			Wednesday	DAY2
			Thursday	DAY2
			Friday	DAY1
			Saturday	DAY1
			Sunday	DAY2
	DAY1			value
	daily	0:00	6:00	0
		6:00	18:00	1
		18:00	0:00	0
	DAY2			value
	daily	0:00	6:00	0
		6:00	18:00	0.75
		18:00	0:00	0

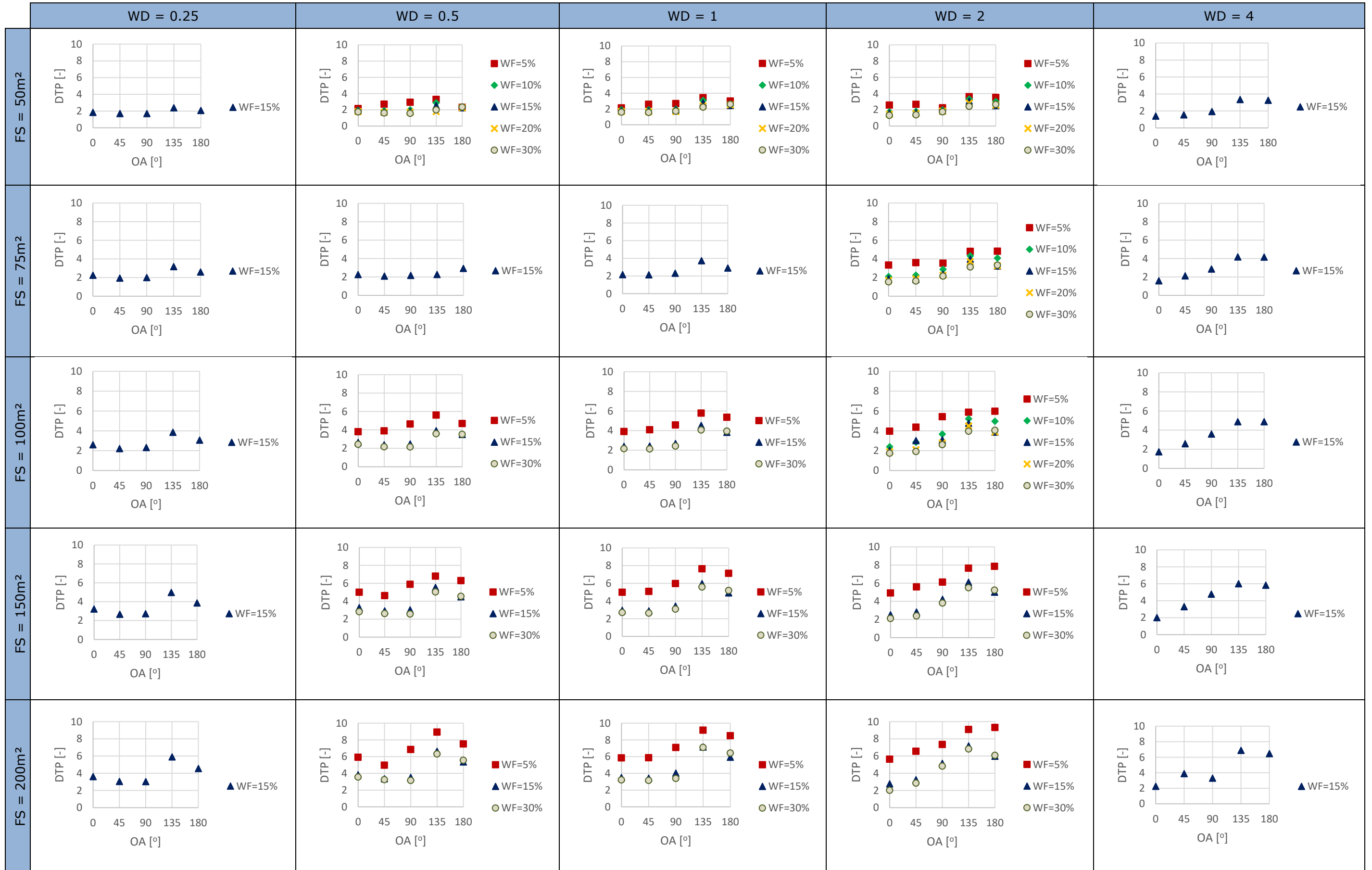
APPENDIX D - EVOLUTION OF ROUTSIDE'S DTP IN LIGHT STRUCTURED BUILDINGS FOR DIFFERENT FS, WD, WF AND OA



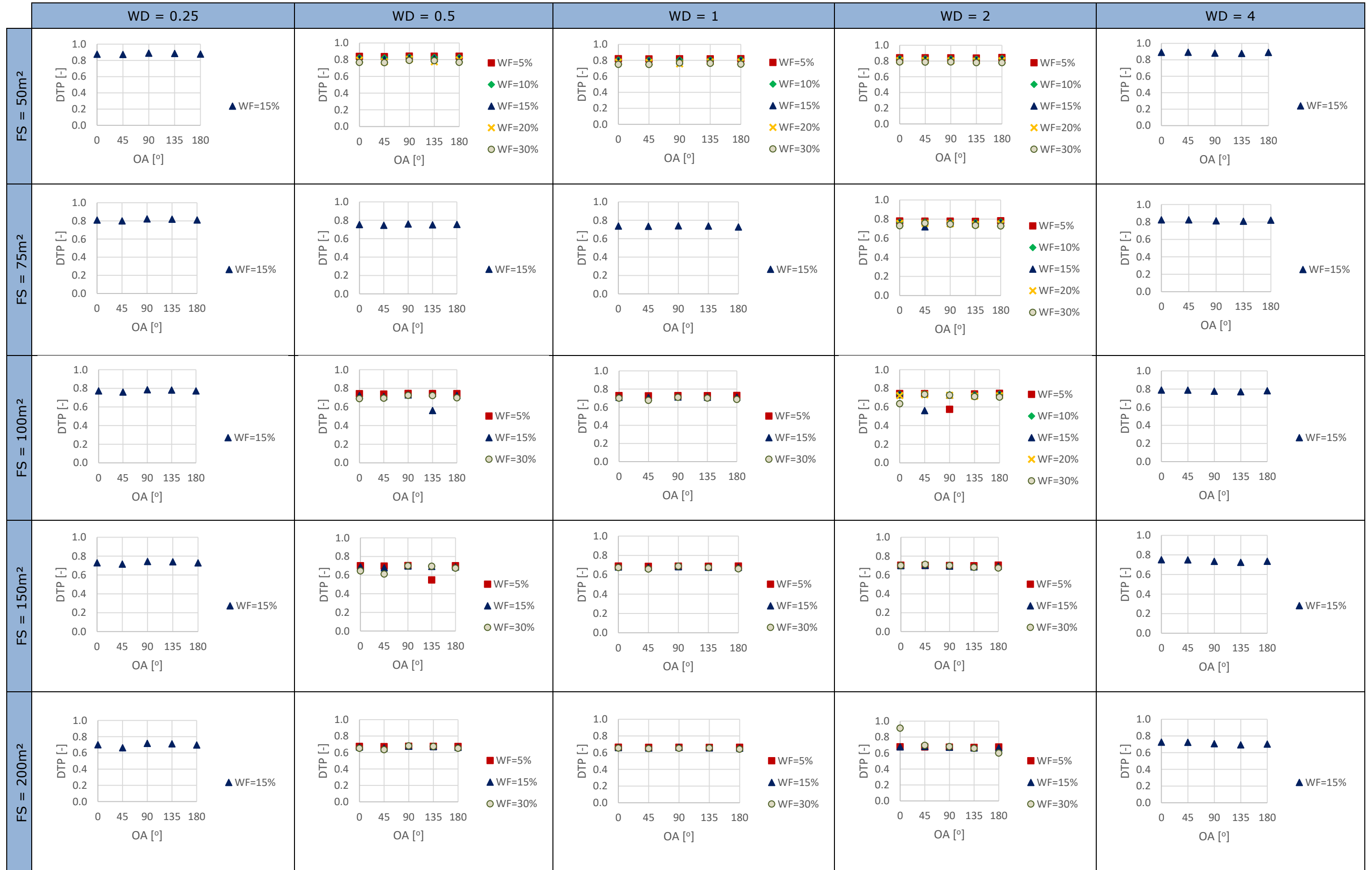
APPENDIX E - EVOLUTION OF RFLOOR'S DTP IN LIGHT STRUCTURED BUILDINGS FOR DIFFERENT FS, WD, WF AND OA



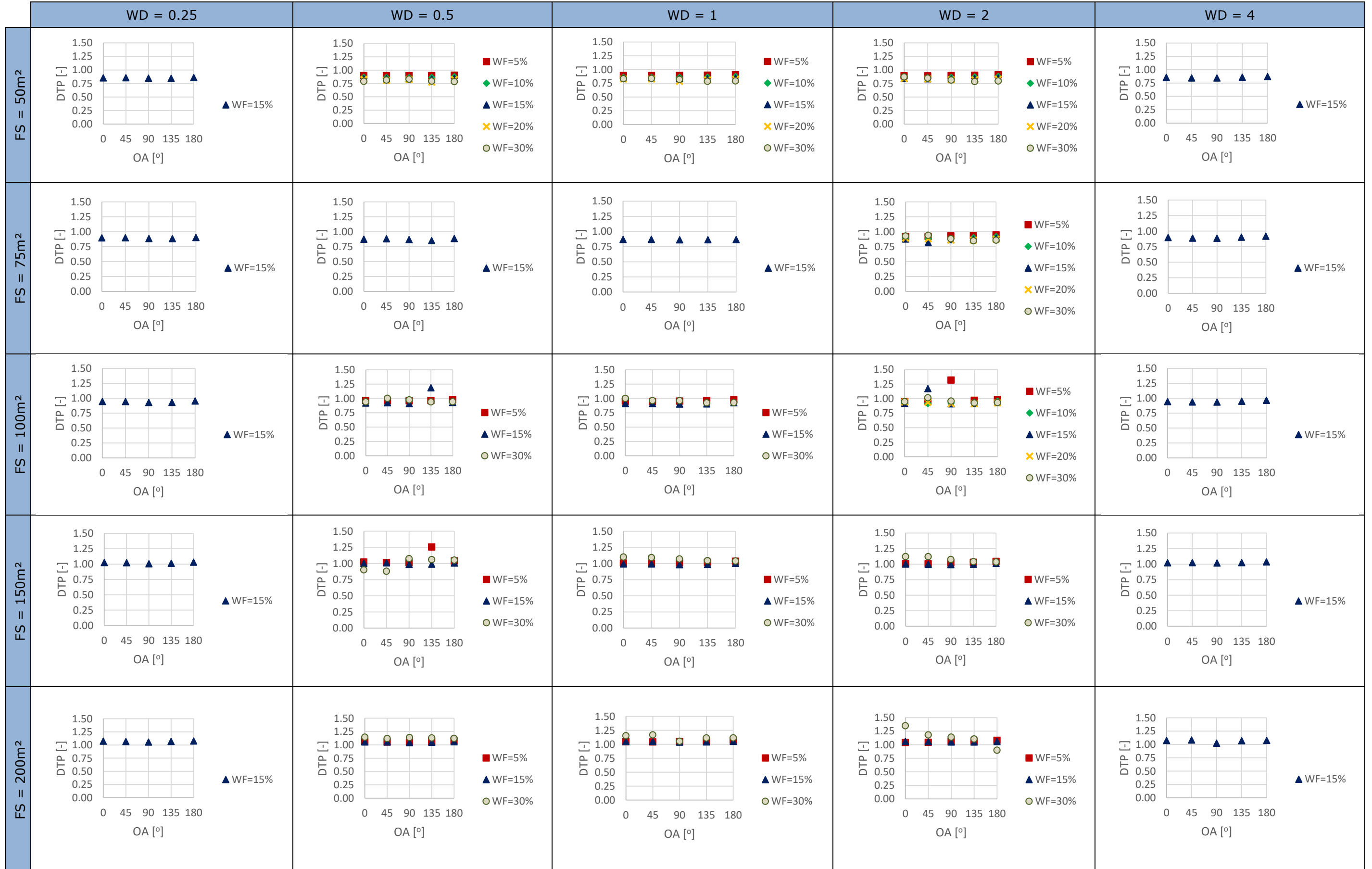
APPENDIX F - EVOLUTION OF Co'S DTP IN LIGHT STRUCTURED BUILDINGS FOR DIFFERENT FS, WD, WF AND OA



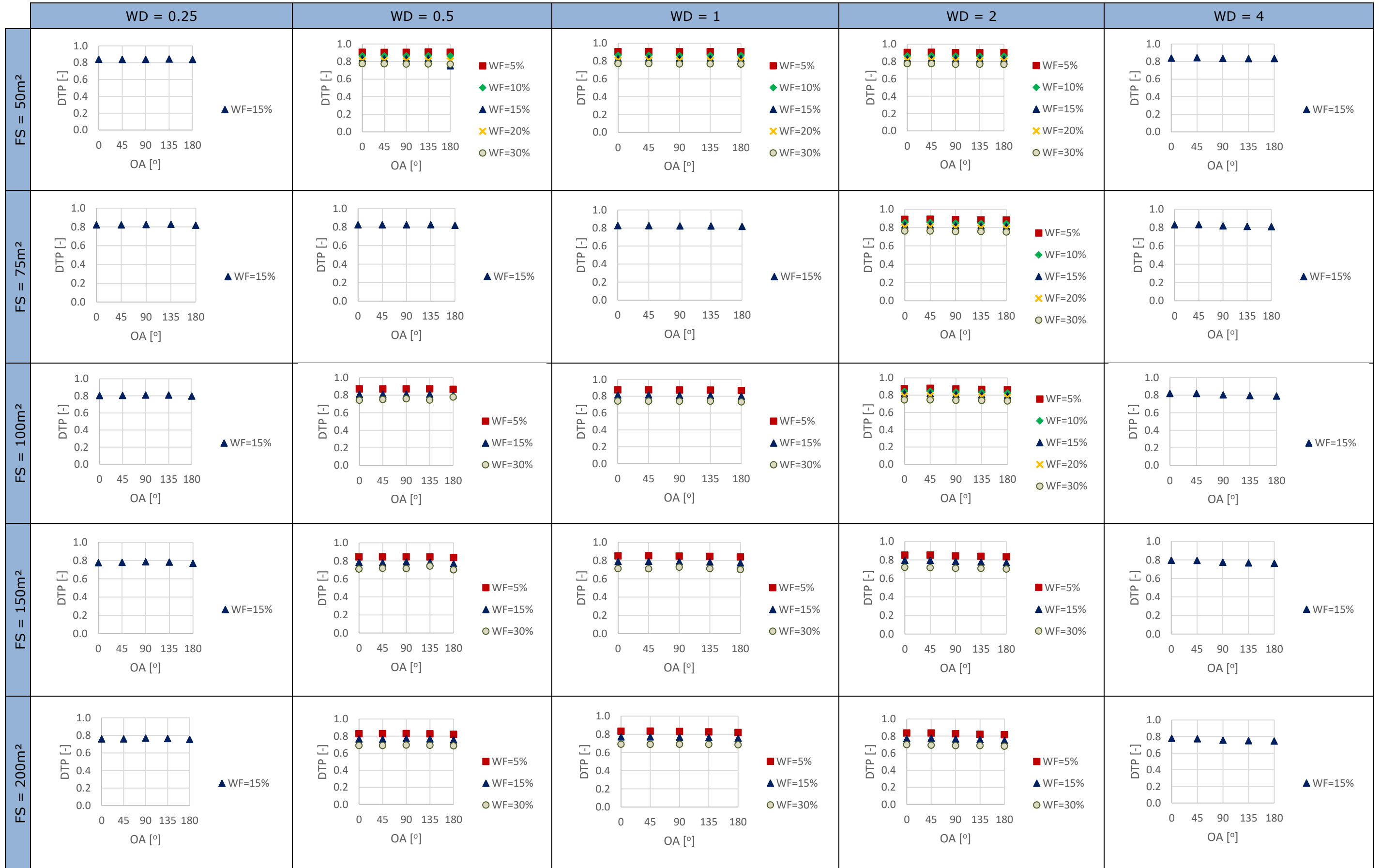
APPENDIX G - EVOLUTION OF CI'S DTP IN LIGHT STRUCTURED BUILDINGS FOR DIFFERENT FS, WD, WF AND OA



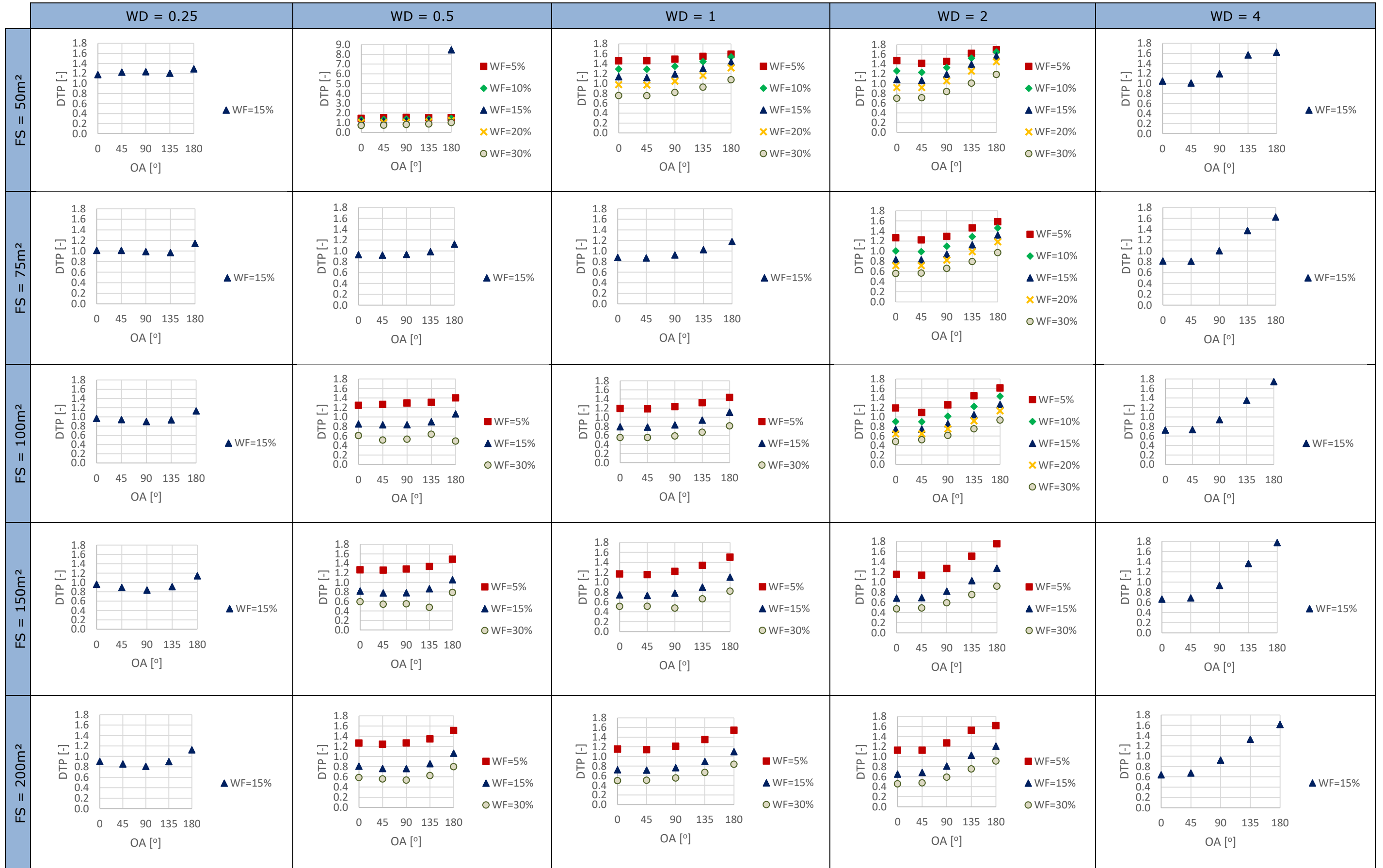
APPENDIX H - EVOLUTION OF Cf'S DTP IN LIGHT STRUCTURED BUILDINGS FOR DIFFERENT FS, WD, WF AND OA



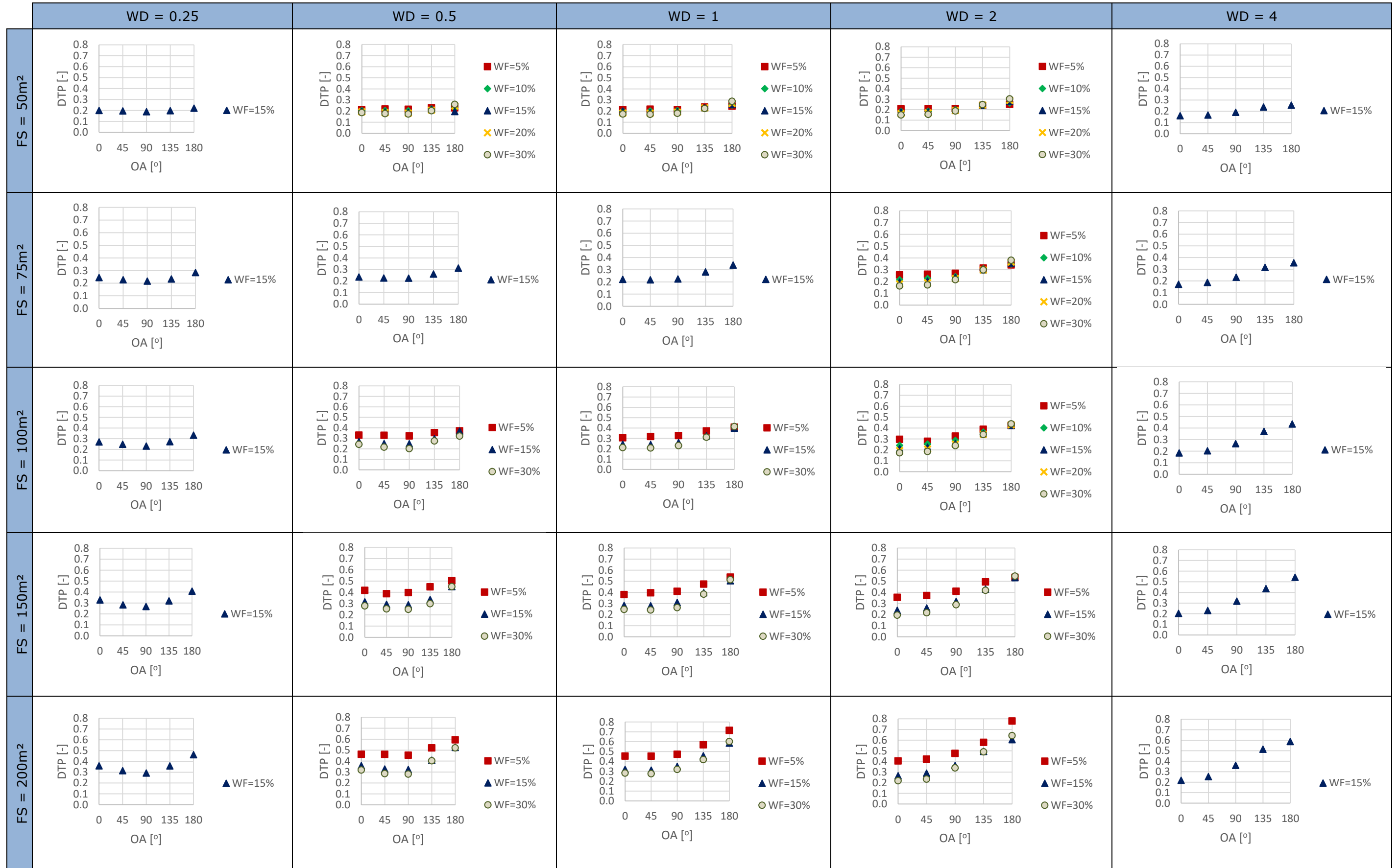
APPENDIX I - EVOLUTION OF ROOTSIDE'S DTP IN HEAVY STRUCTURED BUILDINGS FOR DIFFERENT FS, WD, WF AND OA



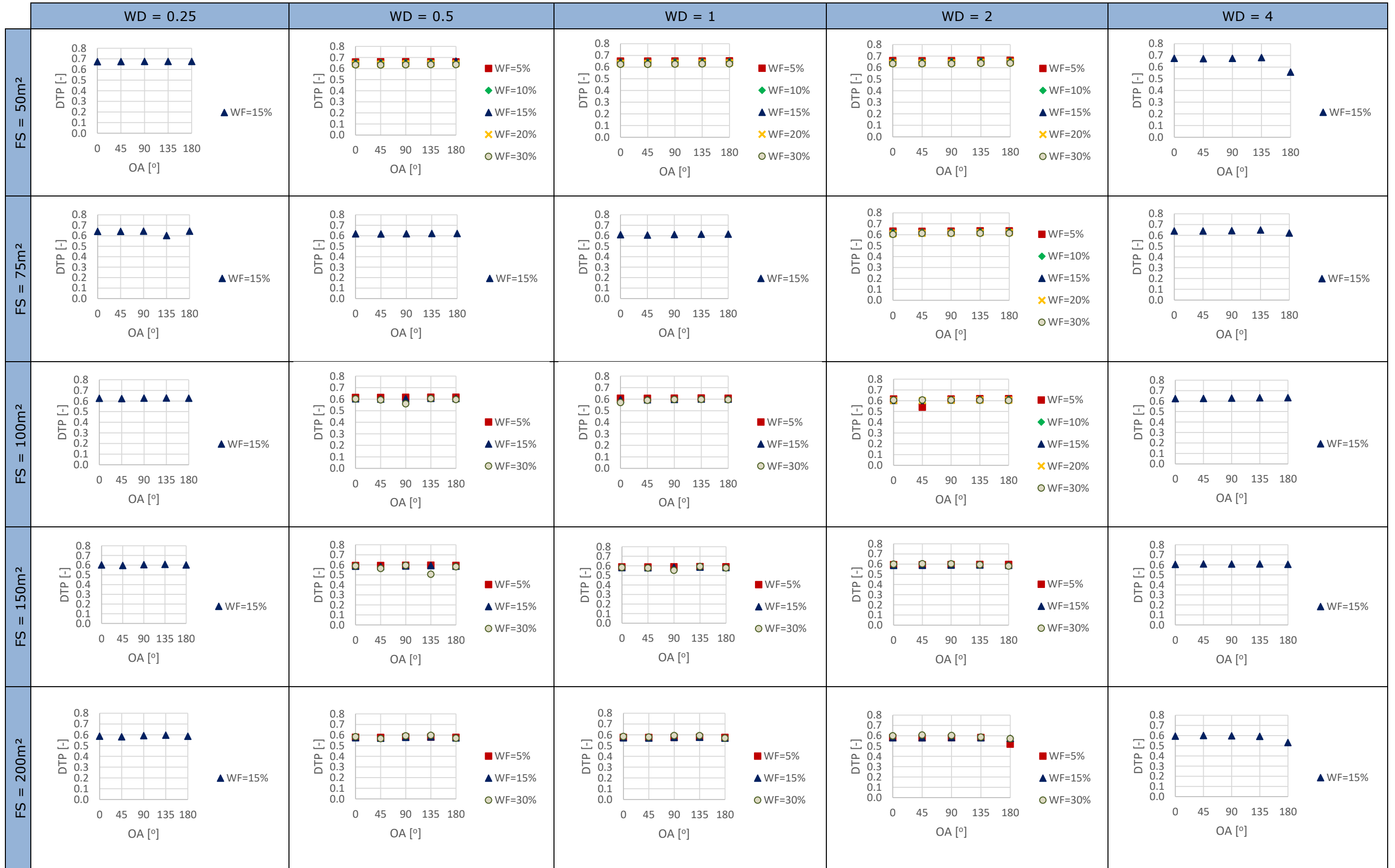
APPENDIX J - EVOLUTION OF R_{FLOOR}'S DTP IN HEAVY STRUCTURED BUILDINGS FOR DIFFERENT FS, WD, WF AND OA



APPENDIX K - EVOLUTION OF CO'S DTP IN HEAVY STRUCTURED BUILDINGS FOR DIFFERENT FS, WD, WF AND OA



APPENDIX L - EVOLUTION OF CI'S DTP IN HEAVY STRUCTURED BUILDINGS FOR DIFFERENT FS, WD, WF AND OA



APPENDIX M - EVOLUTION OF Cf'S DTP IN HEAVY STRUCTURED BUILDINGS FOR DIFFERENT FS, WD, WF AND OA

